ORTA DOĞU TEKNİK ÜNİVERSİTESİ
FEN BİLİMLERİ ENSTİTÜSÜ MÜDÜRLÜĞÜ

TEZ ŞABLONU ONAY FORMU
THESIS TEMPLATE CONFIRMATION FORM

1. Şablonda verilen yerleşim ve boşluklar değiştirilmemelidir.
2. **Jüri tarihi** Başlık Sayfası, İmza Sayfası, Abstract ve Öz'de ilgili yerlere yazılmalıdır.
3. İmza sayfasında jüri üyelerinin unvanları doğru olarak yazılmalıdır. Tüm imzalar **mavi pilot kalemle** atılmalıdır.
4. **Disiplinlerarası** programlarda görevlendirilen öğretim üyeleri için jüri üyeleri kısmında tam zamanlı olarak çalıştıkları anabilim dalı başkanlığının ismi yazılmalıdır. Örneğin: bir öğretim üyesi Biyoteknoloji programında görev yapıyor ve biyoloji bölümünde tam zamanlı çalışıyorsa, İmza sayfasına biyoloji bölümü yazılmalıdır. İstisnai olarak, disiplinler arası program başkanı ve tez danışmanı için disiplinlerarası program adı yazılmalıdır.
5. Tezin **son sayfasının sayfa** numarası Abstract ve Öz'de ilgili yerlere yazılmalıdır.
6. Bütün chapterlar, referanslar, ekler ve CV sağ sayfada başlamalıdır. Bunun için **kesmeler** kullanılmıştır. **Kesmelerin kayması** fazladan boş sayfaların oluşmasına sebep olabilir. Bu gibi durumlarda paragraf (¶) işaretine tıklayarak kesmeleri görünür hale getirin ve yerlerini **kontrol edin**.
7. Figürler ve tablolar kenar boşluklarına taşmamalıdır.
8. Şablonda yorum olarak eklenen uyarılar dikkatle okunmalı ve uygulanmalıdır.
9. Tez yazdırılmadan önce PDF olarak kaydedilmelidir. Şablonda yorum olarak eklenen uyarılar PDF dokümanında yer almamalıdır.
10. Tez taslaklarının kontrol işlemleri tamamlandığında, bu durum öğrencilere METU uzantılı öğrenci e-posta adresleri aracılığıyla duyurulacaktır.
11. Tez yazım süreci ile ilgili herhangi bir sıkıntı yaşarsanız, Sıkça Sorulan Sorular (SSS) sayfamızı ziyaret ederek yaşadığınız sıkıntıyla ilgili bir çözüm bulabilirsiniz.

1. Do not change the spacing and placement in the template.
2. Write **defense date** to the related places given on Title page, Approval page, Abstract and Öz.
3. Write the titles of the examining committee members correctly on Approval Page. **Blue ink** must be used for all signatures.
4. For faculty members working in **interdisciplinary programs**, the name of the department that they work full-time should be written on the Approval page. For example, if a faculty member staffs in the biotechnology program and works full-time in the biology department, the department of biology should be written on the approval page. Exceptionally, for the interdisciplinary program chair and your thesis supervisor, the interdisciplinary program name should be written.
5. Write **the page number of the last page** in the related places given on Abstract and Öz pages.
6. All chapters, references, appendices and CV must be started on the right page. **Section Breaks** were used for this. **Change in the placement** of section breaks can result in extra blank pages. In such cases, make the section breaks visible by clicking paragraph (¶) mark and **check their position.**
7. All figures and tables must be given inside the page. Nothing must appear in the margins.
8. All the warnings given on the comments section through the thesis template must be read and applied.
9. Save your thesis as pdf and Disable all the comments before taking the printout.
10. This will be announced to the students via their METU students e-mail addresses when the control of the thesis drafts has been completed.
11. If you have any problems with the thesis writing process, you may visit our Frequently Asked Questions (FAQ) page and find a solution to your problem.

☒ **Yukarıda bulunan tüm maddeleri okudum, anladım ve kabul ediyorum. / I have read, understand and accept all of the items above.**

Name : **Nazlı Şevval**
Surname : **Menemenli**
E-Mail : **nazli.menemenli@metu.edu.tr**
Date : **29.03.24**
Signature : _____

EFFECTS OF NUTRIENT DEPLETION ON TRANSLATIONAL REGULATION IN HCT-116 COLORECTAL CANCER CELLS

A THESIS SUBMITTED TO
THE GRADUATE SCHOOL OF NATURAL AND APPLIED SCIENCES
OF
MIDDLE EAST TECHNICAL UNIVERSITY

BY

NAZLI ŞEVVAL MENEMENLİ

IN PARTIAL FULFILLMENT OF THE REQUIREMENTS
FOR
THE DEGREE OF MASTER OF SCIENCE
IN
BIOCHEMISTRY

MARCH 2024

Approval of the thesis:

EFFECTS OF NUTRIENT DEPLETION ON TRANSLATIONAL REGULATION IN HCT-116 COLORECTAL CANCER CELLS

submitted by **NAZLI ŞEVVAL MENEMENLI** in partial fulfillment of the requirements for the degree of **Master of Science** i**n Biochemistry, Middle East Technical University** by,

Prof. Dr. Naci Emre Altun
Dean, **Graduate School of Natural and Applied Sciences** _____

Assoc. Prof. Dr. Özgül Persil Çetinkol
Head of the Department, **Biochemistry** _____

Prof. Dr. Sreeparna Banerjee
Supervisor, **Biological Sciences, METU** _____

Prof. Dr. İrem Erel Göktepe
Co-Supervisor, **Chemistry, METU** _____

Examining Committee Members:

Assoc. Prof. Dr. Çağdaş Devrim Son
Biological Sciences, METU _____

Prof. Dr. Sreeparna Banerjee
Biological Sciences, METU _____

Asst. Prof. Dr. Ahmet Acar
Biological Sciences, METU _____

Asst. Prof. Dr. Aslı Sade Memişoğlu
Mathematics and Science Education, Dokuz Eylül University _____

Prof. Dr. İrem Erel Göktepe
Chemistry, METU _____

Date: 29.03.2024

I hereby declare that all information in this document has been obtained and presented in accordance with academic rules and ethical conduct. I also declare that, as required by these rules and conduct, I have fully cited and referenced all material and results that are not original to this work.

Name Last name : Nazlı Şevval Menemenli

Signature :

ABSTRACT

EFFECTS OF NUTRIENT DEPLETION ON TRANSLATIONAL REGULATION IN HCT-116 COLORECTAL CANCER CELLS

Menemenli, Nazlı Şevval
Master of Science, Biochemistry
Supervisor : Prof. Dr. Sreeparna Banerjee
Co-Supervisor: Prof. Dr. İrem Erel Göktepe

March 2024, 102 pages

Limited nutrient supply in the tumor microenvironment can activate numerous stress response pathways in order to ensure survival. Our research demonstrated that exposing HCT-116 cells to a nutrient-depleted medium containing low glucose, glutamine, and serum for 24 hours led to the inhibition of nutrient sensing pathways such as mTOR, as expected. However, the activation of Ribosomal protein S6 (RPS6), a known target of the mTOR pathway and a component of the small ribosomal subunit was observed. In the absence of an active mTOR pathway, RPS6 was phosphorylated via the MAPK pathway since U0126, a MEK inhibitor could abrogate RPS6 phosphorylation. Analysis of reverse phase protein array (RPPA) data from colorectal tumors showed that the phosphorylation of RPS6 was positively correlated with ERK1/2 phosphorylation. In addition, polysome profiling data demonstrated that nutrient restriction and inhibition of MAPK with U0126 could alter the distribution of ribosomes from polysomes to 80S monosomes, suggesting a role in translational regulation. Overall, our findings suggest that the depletion of nutrients may lead to the simultaneous activation of RPS6 and MAPK pathway as a survival mechanism in HCT-116 colorectal cancer cells.

Keywords: Colorectal Cancer, MAPK Pathway, mTOR pathway, Nutrient Depletion, Translation

ÖZ

KISITLI BESİYERİNİN HCT-116 KOLOREKTAL KANSER HÜCRELERİNİN TRANSLASYONEL KONTROLÜ ÜZERİNE ETKİLERİ

Menemenli, Nazlı Şevval
Yüksek Lisans, Biyokimya
Tez Yöneticisi: Prof. Dr. Sreeparna Banerjee
Ortak Tez Yöneticisi: Prof. Dr. İrem Erel Göktepe

Mart 2024, 102 sayfa

Tümör mikroçevresindeki kısıtlı besin kaynağı, hayatta kalmayı sağlamak için çok sayıda stres tepkisine bağlı yolakları aktive edebilir. Araştırmamız, HCT-116 hücrelerinin 24 saat boyunca düşük glikoz, glutamin ve serum içeren, besin açısından kısıtlı bir ortama maruz bırakılmasıyla, beklenildiği üzere mTOR yolağının inhibasyonuna yol açtığını göstermiştir. Ancak, mTOR yolağının bilinen bir hedefi ve bileşeni olan Ribozomal protein S6'nın (RPS6)'nın aktivasyonu da gözlemlenmiştir. mTOR yolağının inaktif olduğu durumlarda, bir MEK inhibitörü olan U0126'nın RPS6 fosforilasyonunu azaltması sonucuyla RPS6'nın MAPK yolu yoluyla fosforile edildiği gözlemlenmiştir. Kolorektal tümörlerden elde edilen ters faz protein dizisi (RPPA) veri analizi, RPS6 fosforilasyonunun ERK1/2 fosforilasyonu ile pozitif korelasyon içinde olduğunu göstermiştir. Ek olarak, polizom profili verileri, MAPK'nin U0126 ile inhibisyonunun, RPS6'nın aktivitesinin yanı sıra translasyonel düzenlemede katkısı olduğunu göstermiştir. Genel olarak bulgularımız, kısıtlı besiyerine bağlı olarak, HCT-116 kolorektal kanser hücrelerinde bir hayatta kalma mekanizması olarak RPS6 ve MAPK yolaklarının eşzamanlı aktivasyonuna yol açabileceğini göstermektedir.

Anahtar Kelimeler: Besin Açlığı, Kolon Kanseri, MAPK Sinyal Yolağı, mTOR Sinyal Yolağı, Translasyon

To my beloved family and women in science

For always encouraging me to do my best

ACKNOWLEDGMENTS

I would like to express my deepest gratitude and thanks to my supervisor Prof. Dr. Sreeparna Banerjee for her encouragement, guidance, scientific advice, and educating me in critical evaluation of data. With her patience and understanding personality, I always felt to have a chance to do it again when I needed. I would like to thank my co-supervisor Prof. Dr. İrem Erel Göktepe for her insight throughout the research.

I would like to thank my jury members Assoc. Prof. Dr. Çağdaş Devrim Son, Asst. Prof. Dr. Ahmet Acar for their suggestions and comments. I would also like to thank my jury member Asst. Prof. Dr. Aslı Sade Memişoğlu for her endless support, guidance, and contributions.

I would like to thank Prof. Dr. Encarna Martinez Salas and Prof. Dr. Bünyamin Akgül, who provided me with every opportunity and facility to carry out polysome profiling experiments. I would like to thank them very much for all their help, support, and interest. I am also grateful to Azime Akçaöz and Rosario Francisco-Velilla, who concern me with during the experiments with great patience and helped me from the beginning during this process.

I would also like to express how grateful I am to the B59 Lab members. First of all, I would like to thank the Starvation-miRNA team very much. I would like to thank Asst. Prof. Dr. Aliye Ezgi Güleç Taşkıran and Hepşen Hazal Hüsnigil for all their support as well as their contribution to my academic life. I am so grateful to know that they will support me when I need them in every aspect of my life. I am very lucky that my lab partner, Göksu Oral Tüzün, has been a very good friend from the moment I met her and has accompanied me even in my first steps in my academic life.

I would also like to thank Aydan Torun for being there for me whenever I needed her and for making me feel safe. Her ideas and advice will have a valuable place in every aspect of my life. I would like to thank Esin Gülce Seza and İsmail Güderer for their patience and help with the lab techniques I learned for the first time. I am very happy to know Hoşnaz Tuğral and Çağdaş Ermiş, with whom I always enjoy spending time with their cheerfulness and positive attitudes.

I would like to thank İrem Yücel, with whom I had so much fun spending time together and often made my muscles hurt from laughing. I will always be grateful to Nisan Korkmaz for her never-failing smile and to Özün Özcan for her support and being a very kind desk mate. I would like to thank Berna Kocaman, whom I just had the opportunity to meet, for her sweetness and understanding. I am very lucky to have such lab members who I can always consult on any subject without hesitation because they are knowledgeable not only in the field of academia but also on fashion, movies, books, entertainment, and all kinds of subjects. I will never forget their understanding and this precious time I spent with them.

I would like to thank Zehra Tavşan for helping me gain experience during my internship and for being not only an instructor but also for being there for me when I needed her opinions on every subject. I would like to thank Zeynep Aleyna Şahin for always being so kind-hearted and for the fun times we spent together.

I am also grateful to my best friend, İrem Taşdemir, for being with me at every moment since our undergraduate years and for being someone with whom I can share my good and bad days. Feeling that she was with me even in my worst times always gave me confidence.

I would like to thank my family, who have always been my support until now, for always being there for me and being selfless. I am very lucky that they always respect my decisions and thoughts in my life and value me. I am grateful to my sister, who was my first teacher, for her incredible patience in guiding and teaching me. It is impossible for my life to be meaningful without them.

Additionally, many thanks to TÜBİTAK for the financial support from BİDEB 2210-A Domestic M.S. scholarship.

Short Term Scientific Mission was funded by "Translational control in Cancer European Network" (TRANSLACORE) CA21154 in the context of COST (European Cooperation in Science and Technology) action.

This work is partially funded by Scientific and Technological Research Council of Turkey under grant number TUBİTAK 122Z320 and GAP-108-2022-10893.

TABLE OF CONTENTS

LIST OF TABLES

TABLES

LIST OF FIGURES

FIGURES

LIST OF ABBREVIATIONS

ABBREVIATIONS

CRC	Colorectal Cancer Cell
FBS	Fetal Bovine Serum
DPBS	Dulbecco's Phosphate-Buffered Saline
NEAA	Non-Essential Amino Acids
PCR	Polymerase Chain Reaction
PAGE	Polyacrylamide Gel Electrophoresis
SDS	Sodium dodecyl sulfate
5-FU	5-Fluorouracil
3-MA	3-Methyladenine
CHX	Cycloheximide
mTOR	Mechanistic target of rapamycin
mTORC1	mTOR Complex 1
mTORC2	mTOR Complex 2
RPS6	Ribosomal Protein S6
CAM	Chorioallantoic Membrane
MAPK	Mitogen-Activated Protein Kinase
FA	Fatty Acid

CHAPTER 1

INTRODUCTION

1.1 Metabolism in Cancer Cells

Metabolic rewiring of cancer can be characterized by the activation of aerobic glycolysis, a phenomenon known as the Warburg effect, elevated glutamine and fatty acid anabolism. In addition, metabolic signaling pathways can be modulated by aberrant expression of both oncogenes and tumor- suppressor genes (Jang et al., 2013). Such metabolic rewiring and activation of abnormal signaling pathways provide cancer cells with advantages such as cell proliferation and metastasis (Park et al., 2020).

Nutrient availability and cancer-driver mutations regulate the flow of energy. Additionally, abnormal metabolite accumulation can encourage the growth of tumors (Martínez-Reyes & Chandel, 2021). After uptake of glucose into the cytoplasm by transporters, it can be utilized via several pathways such as glycolysis, serine biosynthesis, the pentose phosphate pathway (PPP), or the hexosamine synthesis pathway (HSP) (Park et al., 2020).

The most prevalent amino acid in plasma is glutamine which is crucial for the proliferation of cancer cells and forms the primary source of carbon and nitrogen. Nitrogen is a necessary metabolite for nucleotide biosynthesis and glutamine is a precursor for the synthesis of other non-essential amino acids (NEAAs) and fatty acids (FA) (Pavlova & Thompson, 2016). Both exogenous uptake and de novo biosynthesis of FA by using carbons from glucose or glutamine are vital for cellular proliferation.

Increased generation of reactive oxygen species (ROS) during oxidative stress can deplete cytosolic NADPH via the regeneration of the endogenous antioxidant glutathione (GSH), FAS and other anabolic processes requiring NADPH are halted (Mikalayeva et al., 2019). Lipidomic remodeling in cancer comprises modifications in FA transport, storage as lipid droplets (LDs), de novo lipogenesis, and β-oxidation for energy generation and thereby can contribute to tumorigenesis (Koundouros & Poulogiannis, 2020).

1.1.1 Glucose Metabolism

Cancer cells maintain reservoirs of numerous carbon intermediates from glucose and glutamine that are imported from the microenvironment and can be used as building blocks for the synthesis of macromolecules. The oxidation of the carbon skeletons of glucose and glutamine can capture their reducing electrons in the form of either NADH or FADH2 (Pavlova & Thompson, 2016).

Transfer of these electrons to the electron transport chain (ETC) can be facilitated to provide ATP or NADPH cofactor that offers reducing power for an array of biosynthetic reactions. Pathways such as the tricarboxylic acid (TCA) cycle where NADH is generated, support mitochondrial electron transport by transferring electrons from NADH to oxygen. These pathways, however, are distinct from that of NADPH generation from $NADP^+$, which is facilitated by the oxidation of carbon sources (Pavlova & Thompson, 2016).

ATP is the primary source of energy in the cell. A limited amount of ATP is generated with the conversion of glucose to pyruvate via glycolysis, while majority of the ATP is produced via the TCA cycle followed by oxidative phosphorylation (OXPHOS) when oxygen is available. In the absence of oxygen, cells undergo glycolysis followed by fermentation and convert pyruvate to lactate. A phenomenon observed by Warburg in 1927 revealed that even in the presence of oxygen, tumor cells exhibited increased glucose uptake and lactic acid production, which was later

named as the **Warburg effect** (X. Lin et al., 2020). Warburg hypothesized that lactate generation was driven by mitochondrial damage due to impaired oxidative phosphorylation in cancer cells. This theory was contradicted by Sidney Weinhouse, one of Warburg's colleagues. Weinhouse's research using isotope tracing revealed that the rates of oxidative phosphorylation in normal cells and tumor cells are identical, implying that tumor cells' mitochondria are intact. To maintain their high proliferation rate, tumor cells in oxygen-rich environments use aerobic glycolysis and oxidative phosphorylation. Anaerobic glycolysis rates exceed oxidative phosphorylation as the predominant energy source only in hypoxic conditions (Le, 2021).

Although the amount of ATP generated by aerobic glycolysis is low compared to mitochondrial respiration, the highly proliferative tumor cells do display this phenotype even when they have intact mitochondria, providing some benefits. One of the benefits of preferring anaerobic glycolysis is that the rate of glucose metabolism to produce ATP is higher than that of pyruvate oxidation in the mitochondria. In this way, the tumor cells, having high ATP demand in a highly competitive and restricted environment in the context of nutrient availability, get an edge over the stromal cells. The other and more relevant explanation for gaining this phenotype might be that glucose usage is required as a carbon source for anabolic synthesis of several non-essential amino acids such as Serine, reducing equivalents such as NADPH or nucleotides from the pentose phosphate shunt and metabolite production from the intermediates of glycolysis (Liberti & Locasale, 2016).

1.1.2 Amino Acid Metabolism

Rewired metabolism of amino acids in highly proliferative cancer cells plays an important role in cell survival as well biosynthesis of metabolic intermediates needed for protein synthesis, anaplerotic supplementation for the TCA cycle, and OXPHOS for ATP production (Wei et al., 2021). Amino acids and their metabolic derivatives may promote the growth of cancer cells, modify the overall chromatin structure and

gene expression, and also play a variety of roles from post-transcriptional regulation to immunosuppression (Lieu et al., 2020).

1.1.2.1 Glutamine Metabolism

The nonessential amino acid glutamine acts as an anaplerotic carbon source to sustain the TCA cycle and lipid biosynthesis pathways and serves as a nitrogen source for amino acids and nucleotide biosynthesis. Glutamine metabolism-related proteins such as glutamine transporters, aminotransferases, glutaminase along with the essential role of glutamine in the synthesis of glutathione and redox homeostasis play a significant role in the survival and proliferation of cancer cells (Jin et al., 2023; Yoo et al., 2020).

Glutamine, which is transported into cells by glutamine transporters (e.g. SLC1A5, SLC38A1/2) on the plasma membrane, participates in diverse pathways such as the biosynthesis of other nonessential amino acids, and in the TCA cycle upon conversion to glutamate and then to alpha-ketoglutarate (α-KG) (Yoo et al., 2020). Glutamine synthetase (GS) on the other hand, catalyzes the reaction that generates glutamine from $NH4^+$ and glutamate with the consumption of ATP (Cruzat et al., 2018). Apart from the role of glutamine in biosynthesis pathways, it is also involved in oxidative stress regulation of cancer cells that characteristically show increased ROS production. The effect of enhanced ROS levels in cells is alleviated by the synthesis of glutathione, providing deactivation of peroxide free radicals. In addition, glutaminolysis generates α-KG-derived metabolites, especially citrate, which can contribute to lipid synthesis under hypoxic conditions (Yoo et al., 2020).

1.1.3 Cytokines and Growth Factors

Cytokines are generated in the tumor microenvironment by macrophages and neutrophils or by the cancer cells themselves and can play a critical role in regulating

the development and spread of malignancies (Lan et al., 2021). By creating an environment favorable for cancer growth, cytokines may either operate directly on cancer cells in an autocrine manner or indirectly on the tissues that support malignancy, such as fibroblasts and blood vessels (Morris et al., 2022).

Apart from cytokines, growth factors (such as transforming growth factor-beta 1 (TGF-β1), insulin-like growth factor 1 (IGF-1), vascular endothelial growth factor-A (VEGF-A), etc.) can contribute towards tumor growth, uncontrolled cell proliferation, changes in gene expression and avoidance of apoptosis (Elias et al., 2010).

The primary source of growth factors and cytokines in the *in vitro* culture of cancer cells is fetal bovine serum (FBS). Serum plays a vital role in the regulation of many signaling pathways, including cell cycle progression, transformation to a quiescent state, and stress response. Serum starvation is known to lead to autophagy induction, migration, and cell survival. Therefore, a better understanding of underlying mechanisms and contributions of the components of serum may provide essential information for cancer cell behavior (Ahmadiankia, 2020).

1.2 Signaling Pathways Involved in Nutrient Sensing

Rapidly dividing cancer cells show alterations in the availability of exogenous nutrients in the microenvironment, availability of endogenous metabolites and demand for ATP (Robles-Flores et al., 2021). Metabolite availability is closely monitored by nutrient sensing pathways that activate a cascade of successive reactions (You et al., 2023).

1.2.1 AMPK Pathway

The hydrolysis of ATP to ADP can drive many biological functions in living cells. Energy homeostasis is maintained by sensors and metabolism regulators. Among

them, AMP-activated protein kinase (AMPK) is a crucial cellular energy sensor (H. X. Yuan et al., 2013). When cellular energy levels are decreased due to circumstances like hypoxia and nutrient deprivation, AMPK is activated, along with catabolic reactions that can generate ATP to keep cellular energy in balance (Keerthana et al., 2023). At the same time, crucial anabolic enzymes such as acetyl-CoA carboxylase (ACC1 and ACC2) and HMG-CoA reductase (3-hydroxy-3-methyl-glutaryl-CoA reductase), which carry out rate-limiting steps for fatty-acid and sterol biosynthesis undergo inhibitory phosphorylation by AMPK (Mihaylova & Shaw, 2011).

A high AMP/ADP ratio in the cell leads to its binding to the γ-regulatory subunit of AMPK and enables the phosphorylation of Threonine 172 (Thr172) within the activation loop of the AMPK catalytic subunit. Upstream kinases, such as calcium/calmodulin-dependent protein kinase kinase (CaMKKβ) and liver kinase B1 (LKB1), are crucial regulators for mediating the phosphorylation of AMPK at Thr172 (Li et al., 2015). When nutrients are low, AMPK acts as a metabolic checkpoint that prevents cell growth and proliferation by inhibiting the mechanistic target of rapamycin complex 1 (mTORC1). This inhibition is mediated by the direct phosphorylation of the tumor suppressor tuberous sclerosis complex 2 (TSC2) on Ser1387, which in turn inhibits mTORC1 (Mihaylova & Shaw, 2011). As seen in Figure 1.1, AMPK can also phosphorylate Raptor, a member of the mTORC1 that regulates mTOR directly on two conserved serine residues (serine 722 and serine 792), leading to inactivation of mTORC1 kinase activity by the changing the protein levels of 14-3-3 and PRAS40 (Gwinn et al., 2008; van Nostrand et al., 2020).

1.2.2 mTOR Pathway

Building blocks of cells such as amino acids, glucose, nucleic acids as well as ATP are needed for cell growth and proliferation. mTOR forms two different complexes (mTORC1 and mTORC2). mTORC1 is known to be tightly regulated by the availability of amino acids and glucose (H. X. Yuan et al., 2013) (Figure 1.1). The

configuration of the Rag GTPases (GTP versus GDP bound) in the presence of amino acids facilitates the binding and localization of mTORC1 to the cytosolic face of the lysosome (Torrence & Manning, 2018). Leucine, arginine, and glutamine play a critical role in mTORC1 activation. Cytoplasmic proteins SESTRIN2 and CASTOR can sense the levels of leucine and arginine, respectively. When leucine and arginine levels are low, SESTRIN2 and CASTOR1 bind to GATOR2 upstream of mTORC1 and lead to inhibition of mTORC1 (González et al., 2020).

Apart from amino acids, the energy status of the cells, glucose availability, stress factors, and growth factors can also regulate mTORC1 activity. The TSC complex acts as a node of convergence for mTORC1 regulation. Inhibition of TSC2 by upstream signals such as p90 ribosomal S6 kinase 1 (RSK1), AKT, phosphatidyl inositol 3 kinase (PI3K), extracellular signal-regulated kinase (ERK), and MAPKAPK2 (MK2) lead the activation of the mTORC1 pathway. Low nutrient and energy availability can inhibit the mTORC1 complex through the activation of AMPK, which can phosphorylate either Raptor or TSC2 (Melick & Jewell, 2020).

The cytoplasmic side of the lysosomal membrane provides a scaffold for the regulation of mTORC1 and its targets. Furthermore, lysosome location and abundance play a significant role in regulating mTORC1 and mTORC2 activity, as well as autophagy. Autophagy is also tightly regulated by the mTORC1 targets ULK1, ATG13, and TFEB that are permanently or transiently associated with lysosomes (Deleyto-Seldas & Efeyan, 2021).

Sufficient availability of nutrients favors the fine balance between anabolism and catabolism towards biosynthesis and suppresses catabolic pathways like autophagy. mTORC1 can directly activate the two key downstream effectors: p70S6 Kinase 1/2 (S6K1/2) and eIF4E Binding Protein (4EBP), both of which contribute towards cell growth and protein synthesis. Activation of S6K1 and the phosphorylation of its downstream target, the 40S ribosomal protein S6 (RPS6) enables the initiation of 5'-cap-dependent translation by the interaction with eIF3-preinitiation complex (PIC) complex (Holz et al., 2005; Saxton & Sabatini, 2017).

The canonical activation of S6K1 is initiated by the phosphorylation of its C-terminal domain, providing a conformation for the linker domain to be phosphorylated at Thr389 by mTORC1 to regulate cellular growth (Magnuson et al., 2012). 5'- cap-dependent translation initiation requires mTORC1-dependent phosphorylation of 4E-BP on multiple sites, inhibiting the assembly of eIF4E-eIF4F. Phosphorylated 4E-BP1 then can dissociate from eIF4E bound to the mRNA 7-methylguanosine cap structure. This allows eIF4G, eIF4A to be recruited; the ternary complex (eIF2/Met-tRNA/GTP), eIF3 and 40S ribosomal subunits are also recruited to the cap, culminating in the formation of the translation preinitiation complex (PIC) (Holz et al., 2005; Qin et al., 2016).

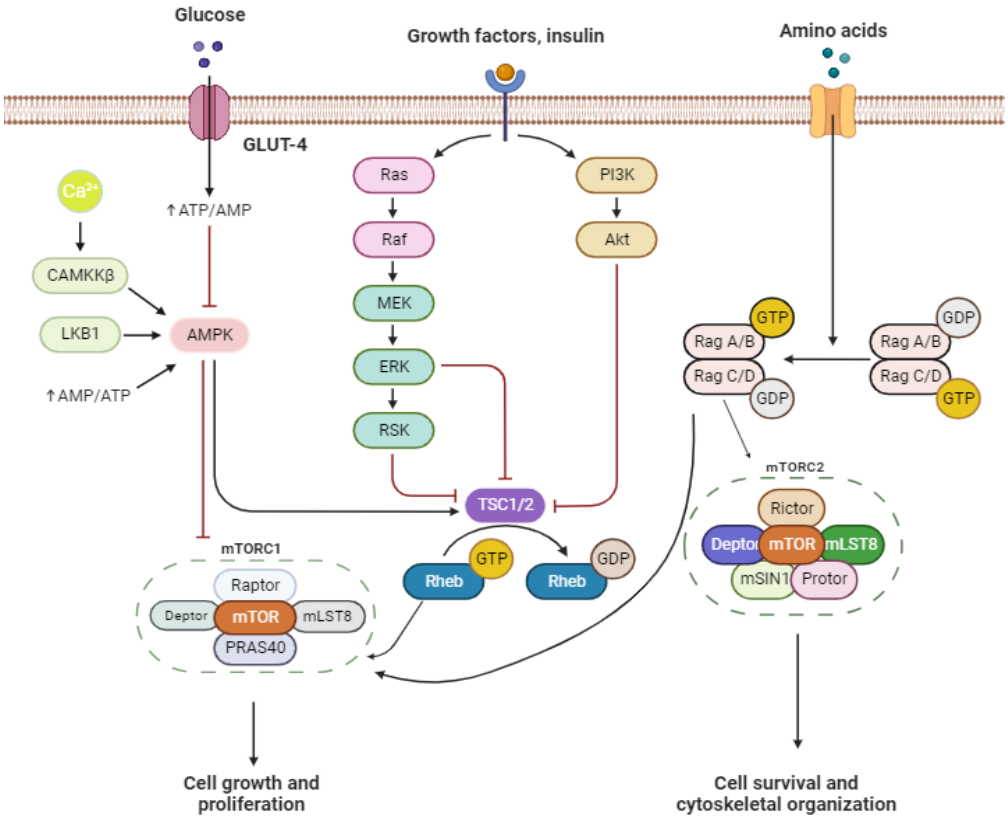

Figure 1.1. The energy sensing mechanisms in cell

The mechanistic target of rapamycin complex 1 and 2 (mTORC1 and mTORC2) are two physically and functionally different complexes that are formed by mTOR.

Figure 1.1. (cont'd) *mTORC1 combines signals from various growth factors, nutrients, and energy sources to enhance cell growth according to energy availability. While mTORC2 primarily regulates cell survival and proliferation, mTORC1 primarily regulates cell growth and metabolism. Numerous signaling pathways such as phosphoinositide-3-kinase (PI3K)/AKT, tuberous sclerosis complex subunits 1 (TSC1) and 2 (TSC2)/Rheb, LKBL/adenosine 5'-monophosphate-activated protein kinase (AMPK), VAM6/Rag GTPases, and others, have been linked to the activation of mTOR* (H. X. Yuan et al., 2013). *(Created with BioRender.com)*

1.3 Effect of Nutrient Depletion on Cancer Cell Behavior

Extracellular nutrients, including glucose, amino acids, and lipids are essential for cell growth. When these sources are restricted, cancer cells can reprogram their metabolism in order to enhance survival and adaptation to nutrient stress. Tumor cells can exhibit dependency on a particular nutrient; therefore, nutrient-limiting strategies could be therapeutically targeted for cancer treatment. In this case, depletion of a specific nutrient may highlight a vulnerability in the cells and induce growth arrest or even cell death (Fan et al., 2022).

1.3.1 Effect of Nutrient Depletion on Cell Cycle and Proliferation

Nutrients play a pivotal role in regulating the rate of cell proliferation, and they specifically alter the expression and activity of proteins that are linked to the cell cycle. Nutrient availability triggers DNA synthesis and stimulates the growth of cancer cells mainly via the regulation of expression of p21, p27 and cyclin-dependent kinases (Bohnsack & Hirschi, 2004). Starvation or nutrient depletion may induce cells to undergo a state where energy consumption decreases, and the maintenance of homeostasis is prioritized. Therefore, the cells shift to a non-dividing or quiescent state that is accompanied by the inhibition of mitogenic signaling pathways via low

levels of growth factors such as IGF-1 and cell cycle arrest via the activation of p53 and p21 (Buono & Longo, 2018).

Serum withdrawal commonly leads to an arrest of cells at the G0/G1 phase without any toxic effects, leading to a state of quiescence. Cell-cycle arrest is accompanied by the regulation of p27, p53, and Bcl-2 genes involved in the PI3K/Akt pathway (Tong et al., 2016). PI3K-activated Akt through PDK1 further leads to the activation of several downstream substrates including Bad, procaspase-9, I-κB kinase (IKK), glycogen synthase kinase-3 (GSK-3), p21Cip1, p27Kip1, CREB, the forkhead family of transcription factors (FKHR/AFX/FOX) and Raf modulating cell cycle progression or cell survival by regulating the apoptotic gene expression (Chang et al., 2003). The pathway may also interact with the p53 tumor suppressor by enabling the phosphorylation of MDM2 at Ser166 and Ser186 residues, which leads to MDM2 translocation to the nucleus to promote p53 ubiquitination. The PI3K/Akt pathways have been implicated in the regulation of p53 activity via mTOR1 (Abraham & O'Neill, 2014).

1.3.2 Effect of Nutrient Depletion on Drug Response

Oncogenes and tumor suppressor genes acquire mutations in their DNA, which can sustain cancer cell proliferation by evading cell death and altering metabolic pathways (Buono & Longo, 2018). Nutrition depletion may drive subsets of cells to undergo accelerated autophagy and enter a dormant state to enable survival (L. Wang et al., 2018). Several mechanisms have been described to explain how cancer cells support their survival, prevent apoptosis, and develop chemoresistance in response to routinely used chemotherapeutics (Yeldag et al., 2018). Cytotoxic chemotherapies mainly target rapid DNA replication and cell division in cancer cells. As a result, delayed division or entering a dormant state is an efficient approach to avoid the effects of chemotherapy, resulting in drug resistance and tumor recurrence (L. Wang et al., 2018).

Differential stress resistance (DSR) is a phenomenon that refers to the differential response of normal and cancer cells under stress conditions such as oxidative stress, nutrient depletion, or chemotherapeutic drugs. Dietary-restricted (DR) mice were shown to be more resistant to stress. Fasting for 48 to 60 hours was shown to improve protection from oxidative stress generated by the chemotherapy drug etoposide in three different strains of mice (Naveed et al., 2014). On the contrary, differential activation of signaling pathways, whether by mutation or altered metabolism, may lead to enhanced sensitivity to chemotherapy drugs via the activation of survival-related pathways (Yeldag et al., 2018). Autophagy was shown to activate chemoresistance by increasing quiescence and survival in glioblastoma cell lines, suggesting that autophagy may enhance drug resistance (L. Wang et al., 2018).

Short Term Starvation (STS) may lead to the sensitization of cancer cells to specific chemotherapy drugs (Raffaghello et al., 2008). In particular, cycles of nutrient depletion could slow the development of melanoma, glioma, and breast cancer and was shown to improve the efficacy of drugs such as cyclophosphamide and doxorubicin by activating stress pathways that increase drug sensitivity (Buono & Longo, 2018).

1.4 Effect of Nutrient Depletion on Translational Regulation in Cancer Cells

As tumors have limited resources, they respond remarkably efficiently to augmenting availability and diminishing demand for nutrients. The mTORC1 complex, which phosphorylates ribosomal protein S6 kinase (S6K) and the eukaryotic translation initiation factor 4E (elF4E)-binding protein (4E-BP1), stimulates translation initiation in the regulation of global protein synthesis. Since signaling via the mTORC1 complex is inhibited by amino acid and nutrient constraints, limited energy levels and activation of AMPK, global translation decreases under these circumstances (García-Jiménez & Goding, 2019).

With prolonged starvation, the cytosolic amino acid amount decreases, leading to an inhibition of mTORC1 signaling. Restoration of amino acid pools can be initiated by the activation of autophagy and protein degradation in the lysosome. Reactivation of the mTORC1 complex is crucial for the translation of mRNAs related to cell survival (Condon & Sabatini, 2019). The downstream effectors of the mTORC1 pathway such as S6K, and 4E-BP, can participate in translational regulation through various ways. Activated S6K1 initiates translation by stimulating the dissociation of eukaryotic Initiation Factor 3 (eIF3) from the mRNA. S6K also phosphorylates its substrates such as Ribosomal Protein S6 (RPS6), Eukaryotic Translation Initiation Factor 4B (eIF4B), Programmed Cell Death Protein 4 (PDCD4), and Eukaryotic Elongation Factor 2 Kinase (eEF2K) (M. Yang et al., 2022) (Figure 1.2).

A remarkable characteristic shared by all mRNAs that encode ribosomal proteins in higher vertebrates is the presence of an array of pyrimidine nucleotides at the 5′-UTR (5′ terminal oligopyrimidine tract or 5'TOP sequences). These mRNAs are translated upon stimulation of cells with serum or amino acids. Thus, the synthesis of both ribosomal proteins and global proteins is tightly regulated by the availability of amino acids and serum in the cell (Damgaard & Lykke-Andersen, 2011).

RPS6, a part of the 40S ribosomal subunit, plays a role in the regulation of protein translation leading to ribosome biogenesis, cell growth, proliferation and differentiation, apoptosis, glucose metabolism, and DNA repair in mammalian cells (Yi et al., 2022). The activation of RPS6 is primarily mediated by the PI3K/Akt/mTORC1/S6K pathways but can also be regulated by Ribosomal Protein S6 Kinases (RSKs) that are the downstream effectors of (RAF)/MAPK-ERK kinase (MEK)/extracellular signal-regulated kinase (ERK) cascade.

The five evolutionarily conserved C-terminal serine domains of RPS6 (S235, S236, S240, S244, and S247) are sequentially phosphorylated by S6K1 starting from the S236, while RSKs can phosphorylate S235/236 residues (Ruvinsky & Meyuhas, 2006). The phosphorylation of RPS6 has been reported to be positively correlated with the translation of mRNAs having 5' TOP motifs (Mok et al., 2013). These

mRNAs encode ribosomal proteins along with several non-ribosomal proteins involved in translation such as translation elongation factors whose elevated expression is required for cellular function (Cockman et al., 2020). In several human malignancies, an increase in the total RPS6 or phosphorylated RPS6 levels are associated with enhanced pathological grade and course of the disease. This suggests that positive and negative feedback and feedforward processes in the RPS6 pathway may offer alternative therapeutic strategies beyond the current strategies available for cancer treatment (Yi et al., 2022).

mTORC1 also regulates translation by phosphorylating its downstream target 4E-BP. Nutrient-rich conditions enable the recruitment of a subset of mRNAs (Tsukumo et al., 2016). The hyperphosphorylation of 4E-BPs by mTORC1 leads to the dissociation of 4E-BPs from eIF4E, the 5′-cap-binding subunits of the eIF4F complex, allowing the initiation of cap-dependent translation. However, when cells are treated with mTORC1 inhibitors or when cells are under nutrient depletion, 4E-BPs are hypo-phosphorylated and remain bound to eIF4E with high affinity. This prevents the assembly of the eIF4F complex and represses translation (Gingras et al., 1999). Overexpression and hyperphosphorylation of 4EBPs have been investigated in various carcinomas, which may be related to their differential activation by other kinases and expression. Of note, oncogenes such as Vascular Endothelial Growth Factor (VEGF), HIF1-α, and B-cell lymphoma 2 (BCL-2) may also undergo cap-independent translation in advanced cancer, resulting in increased translation of mRNAs containing an internal ribosome entry site (IRES) (Qin et al., 2016). mRNAs cannot be translated via cap-dependent translation under conditions such as cellular stress and viral infection. In such instances, cap-independent translation is frequently employed to initiate mRNA translation via the IRES in the absence of a 5′ cap structure (Godet et al., 2019; López et al., 2001). IRESs are RNA elements that were first discovered in *Picornaviridae* viruses and recruit ribosomes to the internal region of mRNAs to commence translation via a cap-independent mechanism. According to the recruitment types of ribosomes, IRESs in the eukaryotic genome can be classified as type I and type II IRESs. Type I IRESs interact through RNA binding

motifs and N-6-methyladenosine (m6A) modification, while type II IRESs interact through 18SrRNA with ribosomes (Y. Yang & Wang, 2019).

1.5 Effect of Integrated Stress Response on Translational Regulation

In addition to the mTOR pathway, the availability of the amino acids can be sensed by the metabolic sensor general control nonderepressible-2 kinase (GCN2 kinase). Amino acid depletion in cells results in the accumulation of uncharged tRNA, which can inhibit global translation. The binding of amino acid-free tRNAs to GCN2 kinase leads to a conformational change in the kinase and its autophosphorylation, in turn, activates downstream signaling pathways (Battu et al., 2017). GCN2 is a serine/threonine kinase that leads to phosphorylation of the alpha subunit of eukaryotic translation initiation factor 2 (eIF2a) on serine 51. This phosphorylation can also be driven by other kinases via the activation of the Integrated Stress Response (ISR) pathway (Castilho et al., 2014).

ISR is a complex signaling mechanism that is activated in response to several physiological and pathological stressors such as hypoxia, amino acid or glucose deprivation, and viral infection. ISR refers to the fact that a wide range of stimuli can be integrated into common downstream signaling pathway and cause the phosphorylation of eIF2a. The ISR pathway employs both translational inhibition and transcriptional activation of stress response genes (Pakos-Zebrucka et al., 2016; Ryoo & Vasudevan, 2017). Three other kinases: PKR-like ER kinase (PERK), heme-regulated eIF2a kinase (HRI), double-stranded RNA-dependent protein kinase (PKR), can be activated with different stressors, mediate the phosphorylation of eIF2a at S51 and the activation of an ISR. Each kinase becomes fully active via autophosphorylation and conformational change by dimerization (Pakos-Zebrucka et al., 2016).

Regulation eIF2α, a core component of the eIF2 translation initiation complex, can affect translational output. Phosphorylation of eIF2α on S51 changes eIF2α from a

substrate of the guanine exchange factor eIF2B to a competitive inhibitor. As a result, eIF2α phosphorylation inhibits the global protein synthesis by inhibiting GDP: GTP exchange reaction while increasing the translation of a particular subset of proteins, such as activating transcription factor 4 (ATF4) (Figure 1.2) (Cockman et al., 2020; Ryoo & Vasudevan, 2017). In response to unfolded protein response, low glucose, or a limited supply of amino acids, ATF4 can enhance the expression of C/EBP homologous protein (CHOP), which then cooperates with ATF4 to increase the activity of amino acid transport and autophagy-related genes. In addition, the p-eIF2α/ATF4/CHOP axis restores protein synthesis and decreases BCL-2 (anti apoptotic protein) activity to drive apoptosis under prolonged stress conditions such as oxidative stress and nutrient limitation (García-Jiménez & Goding, 2019).

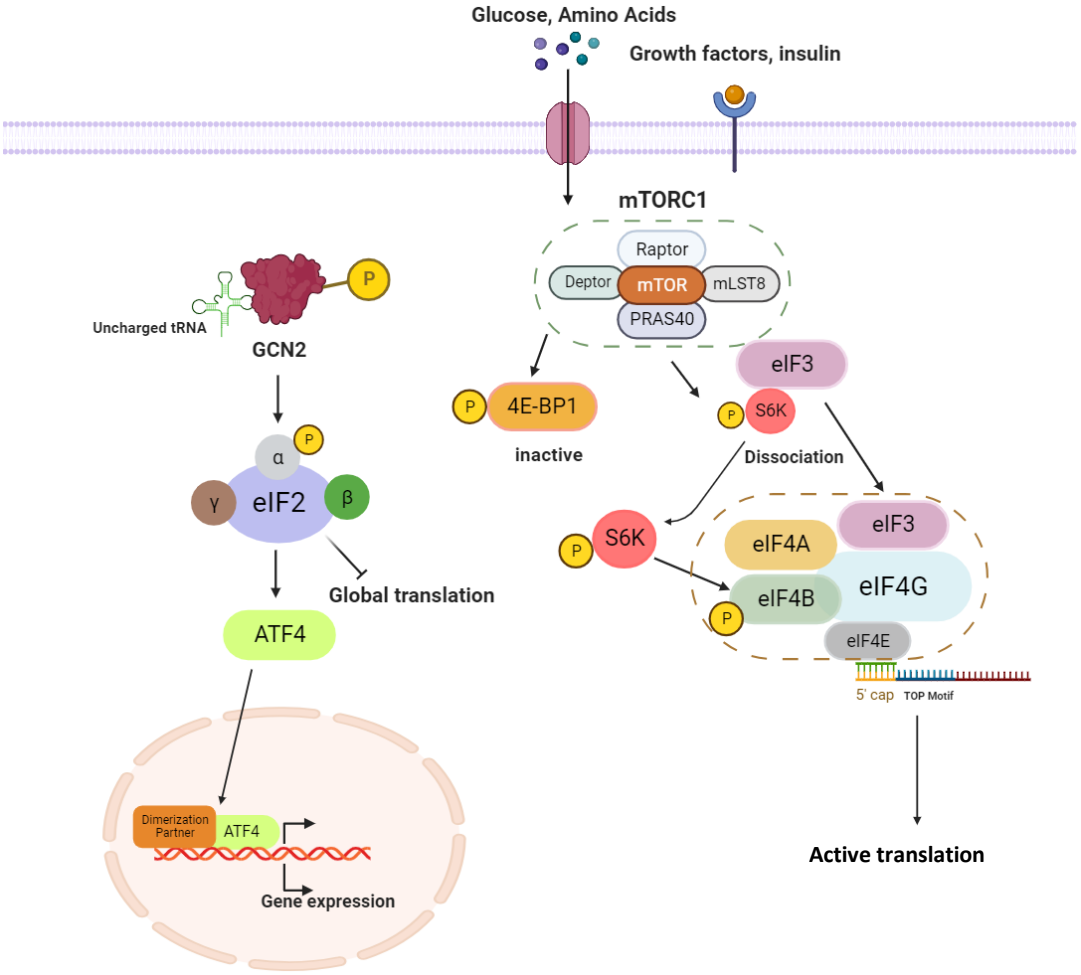

Figure 1.2. General translational control by S6K, 4E-BP1 and GCN2

Several factors (glucose, amino acids, growth factors, etc.) activate mTORC1, which can phosphorylate of 4E-BP1. Phosphorylated 4E-BP1 cannot bind to eIF4E, and the recruitment of eIF4E to the translational initiation complex is enabled. In addition, activation of S6K by mTORC1 induces dissociation from eIF3. As a result, the translation can be initiated. GCN2 is responsible for the phosphorylation of eIF2α subunit at Serine 51 to inhibit global translation, but allow the selective translation of ATF4, while ATF4 enhances the transcription of several stress response genes (M. Yang et al., 2022). *(Created with Biorender.com)*

1.6 Scope, Aim, and Novelty of This Study

Although tumors are often subjected to environmental constraints for the availability of nutrients, an excess demand over supply of any essential nutrient is not feasible in the long-term. As a result, cancer cells increase the supply and decrease the demand for nutrients. Increasing supply strategies include metabolic adaptation by using alternate resources (metabolic plasticity) or by reducing protein synthesis (García-Jiménez & Goding, 2019).

Nutrient depletion can lead to metabolic rewiring. To better understand this, several colorectal cancer cell lines were incubated in a nutrient-depleted medium optimized in the capacity of a TÜBİTAK 1001 project (118Z116) in our lab. This nutrient-depleted medium contains 1% FBS, 0.1g/L glucose, and 0.2mM L-glutamine, corresponding to 10% of the nutrients available in the complete medium. Upon incubation of HCT-116 colorectal cancer cells in this nutrient-depleted medium, the mTORC1 complex was inhibited, as expected; however, increased phosphorylation of the ribosomal protein and mTORC1 target RPS6 on both Serine 235/236 and Serine 240/244 were observed, with a stronger activation on Serine 235/236.

The ongoing activation of RPS6 may indicate the remodeling of nutrient-sensing pathways and alterations in translational regulation under nutrient-depletion. Therefore, I hypothesized that the activation of RPS6 under nutrient-depletion may provide survival advantages by rewiring the demand for protein synthesis.

To address my hypothesis, I examined the followings:

1. Upstream activators of RPS6 in nutrient-depleted HCT-116 cells,

2. The effects of nutrient depletion on translational regulation, and

3. Sensitivity of nutrient-depleted HCT-116 cells to chemotherapy drugs.

This study revealed for the first time that exposing HCT-116 cells to a physiologically relevant nutrient depleted medium stimulates the activation of RPS6, which could be abrogated by the MEK1/2 inhibitor U0126, but not the mTOR inhibitor AZD8055. These results provide an insight into the compensatory signaling mechanisms governing RPS6 activation during nutrient depletion and its activity on maintaining the translational machinery. Furthermore, these findings may provide an opportunity to identify pathways that enable cell survival despite nutrient depletion as future targets.

CHAPTER 2

MATERIALS AND METHODS

2.1 Cell Culture

HCT-116 (colorectal cancer cell line) used in this study was purchased from DKFZ (Heidelberg, Germany), Caco-2 (colorectal cancer cell line) were purchased from ŞAP Institute (Ankara, Turkey), HCT-116 cells were grown in an incubator supplemented with 5% CO_2 at 37^{o}C. RPMI 1640 growth medium (without phenol red) for HCT-116 cells was prepared by the supplementation of 2 mM L-Glutamine, 10% fetal bovine serum (FBS; Capricorn), and 100 U/mL penicillin - 100µg/mL streptomycin. Caco-2 cells were grown in Eagle's minimum essential medium (EMEM) containing 1 g/L glucose, supplemented with 2 mM L-Glutamine, 20% FBS, 100 U/mL penicillin - 100µg/mL streptomycin, 0.1 mM non-essential amino acids (NEAA), and 1mM sodium pyruvate. All cell culture supplementation materials are shown as percentages according to their final concentration. FBS was purchased from Capricorn. All other cell culture materials were purchased from Biological Industries. In order to eliminate mycoplasma contamination, Plasmocin® (Invivogen, France) at 2.5 µg/mL concentration was added routinely to the culturing media of cells and mycoplasma control was performed continuously. Cells were frozen for long-term storage by resuspending the pellets in complete media (without Plasmocin) containing 5% DMSO (dimethyl sulfoxide) (Sigma, cat#: 154938). All sterile plastic consumables for cell culture were purchased from Sarstedt (Germany) or Jet Biofil (China).

2.2 Cell Line Characteristics

HCT-116 cells were isolated from the colon of an adult male and can be classified as fast growing with a doubling time of around 20-24 hours. This microsatellite unstable cell line has epithelial morphology and is classified as adherent. It has a mutation in *KRAS* proto-oncogene (G13D) and *PIK3CA* gene (H1047R) and it has wild type *BRAF*, *PTEN*, and *TP53* (Ahmed et al., 2013).

Caco-2 cells, isolated from colon tissue of an aged male patient with colorectal adenocarcinoma, can be classified as rapidly growing cell line with a doubling time as around 20-24 hours. This microsatellite stable cell line has epithelial-like morphology and has a mutation in *TP53* (E204X), wild type *BRAF*, *KRAS*, *PIK3CA*, and *PTEN* (Ahmed et al., 2013).

Both cell lines were authenticated by STR analysis (Genoks, Ankara) in the course of the study.

2.3 Genomic DNA Isolation for STR Analysis of the HCT-116 Cells

Approximately $2x10^6$ HCT-116 cells were precipitated at 3000 rpm for 5 min at cold centrifuge (4 °C) and the pellet was washed with DPBS. For the genomic DNA isolation cell pellet was resuspended in 500 µL Lysis Buffer containing 10 mM Tris-HCl (pH: 8.5), 5mM EDTA, 200 mM NaCl and 0.2% SDS. The resuspended cells were incubated with the lysis buffer at 60°C for 5 minutes. 2.5 µL Proteinase K (20 mg/mL stock) and 1µL RNAase A (10 mg/mL stock) for 500 µL volume were introduced into the resuspension buffer and lysate was incubated at 60°C for 60 minutes. Next, 50 µL 3M Na-acetate was added into the cell lysate. 2.5 volumes of cold 100% EtOH were introduced into the cells and the cell lysis was incubated at -20°C overnight. The next day, cell lysate was centrifuged at 10,000 rpm for 10 minutes. The supernatant was discarded, and the pellet washed with 1mL or 70% EtOH pre-cooled at -20°C. The lysate was centrifuged at 10,000 rpm for 10 minutes again. Discarding the supernatant, Eppendorf tube containing pellet was inverted for

air drying, and incubated at room temperature until liquid was completely dried. The pellet was resuspended in 100 µL nuclease-free water and incubated at 65°C for 60 minutes. After centrifugation of cells at 500 x *g* for 5 minutes, supernatant was transferred to fresh Eppendorf. The supernatant was chilled on ice and genomic DNA concentration measurement was carried out using a Nanodrop. The suspension was stored at -20°C until sent for STR analysis (Genoks LifeScience Company) in a cold chain. The STR report is given in the Appendix. The same genomic DNA isolation protocol was also used for routine mycoplasma testing by PCR.

2.4 Nutrient Depletion Protocol

The nutrient depleted medium for HCT-116 cells was prepared from RPMI-1640 medium (without glucose and L-glutamine) and supplemented with 0.1 g/L glucose, 0.2 mM L-glutamine, 1% FBS and 100 U/mL penicillin - 100µg/mL streptomycin. The nutrient depleted medium for Caco-2 cells was prepared by DMEM medium (without glucose and L-glutamine) and supplemented with 0.1 g/L glucose, 0.2 mM L-glutamine, 1% FBS and 100 U/mL penicillin - 100µg/mL streptomycin.

Cells for nutrient depletion treatment were seeded to 6-well plates (300,000 to 500,000 cells/well) or T25 flask (about 1,000,000 cells)and allowed to attach overnight. The next day the medium was discarded, and cells were washed with Dulbecco's Phosphate-Buffered Saline (DPBS; Biological Industries) prior to incubation in the nutrient depleted medium. The optimized nutrient depletion duration was 48 hours for Caco-2 cells and 24 hours for HCT-116. Beyond these durations we observed extensive cell death. At the end of nutrient depletion, the cells were processed for protein isolation. The duration for replenishment with complete medium was 24 hours following the nutrient depletion treatment. Before adding the complete medium, the cells were washed with DPBS.

2.5 Chemical Perturbation Experiments

Chemical treatments carried out with HCT-116 cells are provided in Table 2.1 showing the mode of action of chemicals, treatment concentration and duration along with their solvents used as a vehicle. The treatment duration did not exceed the duration of nutrient depletion and the incubation with the chemical was carried out in the nutrient depleted medium or complete medium (used as control).

Table 2.1 Chemicals used in the study

Chemical Name	Mode of Action	Concentration & Duration	Solvent (Vehicle)
U0126 (MEK1/2 inhibitor)	Inhibition of Ras/Raf/MEK/ERK signaling pathway by selectively inhibiting MEK1/2 kinases	0.5 μM; 24 hours (co-treatment)	DMSO (0.01%)
AZD8055 (mTORC1/2 inhibitor)	Competitive inhibition of mTOR kinase activity by acting against PI3K	5 μM; 24 hours or 48 hours (co-treatment)	DMSO (0.01%)
ISRIB (Integrated Stress Response inhibitor)	Reversion of the p-eIF2A effects by activation of eIF2B	100 nM; 2 hours for WB & co-treatment for MTT Assay	DMSO (0.01%)

Table 2.1 (cont'd) Chemicals used in the study

Chemical Name	Mode of Action	Concentration & Duration	Solvent (Vehicle)
Cisplatin (anti-cancer agent)	Induction of DNA damage by cross-linking with purine bases	5 μg/ml; 24 hours or 48 hours (co-treatment)	DPBS (0.24%)
5-Fluorourasil (anti-cancer and anti-metabolite agent)	Inhibition of thymidylate synthase	20 μM; 24 hours or 48 hours (co-treatment)	DMSO (0.05%)

2.6 Protein Isolation and Quantification

Total protein isolation was carried out by using a lysis buffer prepared with Mammalian Protein Extraction Reagent M-PER (Thermo Fisher Scientific, USA), 1X PhosSTOP Phosphatase Inhibitor (Roche, Germany) and 1X complete Mini EDTA-free Protease Inhibitor Cocktail (Roche, Germany). The collected cell pellets were washed with DPBS and precipitated at 1500 x *g* for 5 min at 4 °C. Next, the cell pellets were lysed in MPER lysis buffer according to the pellet volume. The physical lysis was done by vortexing for 30 seconds and incubation for 10 minutes on ice; this process was repeated three times. After lysis, the tubes were centrifuged 14000 x *g* for 10 min at 4 °C. The supernatants were collected into the fresh Eppendorf tubes to be stored at -80 ^{o}C until use for western blotting.

After protein isolation, 1 μL of the protein solution (1:5 dilution) was mixed with 250 μL of Coomassie Protein Assay Reagent (Thermo Fisher Scientific) as three replicates in 96-well microplates. MultiSkan GO Microplate Spectrophotometer (Thermo Scientific) was used to measure protein absorbance at 595 nm. The protein

quantification was carried out by using an equation obtained from the standard curve. The standard curve was generated with absorbance measurements of bovine serum albumin (BSA) at concentrations from 25 to 2000 μg/mL mixed with Coomassie Protein Assay Reagent.

2.7 Western blot

Protein isolates (10-30 μg) were incubated with 6X Laemmli Buffer and boiled for 7 minutes at 95 °C before loading into the wells of 12% SDS-polyacrylamide gel in calculated amounts. PageRuler Plus Prestained Protein Ladder (Thermo Fisher Scientific, USA) was used as a ladder with molecular weights between 10 to 250 kDa. The running process was carried out first at 60V until all the proteins moved towards the separating gel, then the protein separation was continued at 90V for approximately 2 hours. A wet transfer of proteins to a Polyvinylidene Fluoride (PVDF) membrane was carried out by using the sandwich model at 115V for 90 minutes with continuous cooling. The membranes were blocked in 5% skimmed milk prepared with TBS-T buffer at room temperature for 1 hour on an orbital shaker. Next, the membrane was incubated overnight on an orbital shaker at 4 ^{o}C with the primary antibody diluted in 5% skim milk or BSA (AppliChem) in 0.1% TBS-T according to the manufacturer's instructions. The next day, the membranes were washed three times with TBS-T for 10 minutes each on a rocker. The membranes were then incubated in the secondary antibody for 1 hour at room temperature on an orbital shaker. After washing the membranes three times with TBS-T for 10 minutes each, the membranes were incubated with Clarity ECL Substrate (Bio-Rad) in the dark and at room temperature for approximately one minute followed by imaging.

The protein band intensities were visualized in ChemiDoc MP Imaging System (Bio-Rad) with an exposure time until the most saturated intensity was obtained. The adjusted band intensities for protein of interests were obtained with ImageLab software and adjusted band intensities were normalized to that of housekeeping proteins for the densitometric analysis to eliminate any differences in loading

volume. When further incubations with primary antibody was required, the membranes were incubated for 4-5 minutes at 80 ^{o}C in a pre-heated mild stripping buffer. Before adding a new primary antibody, the membranes were washed three times with TBS-T for 10 minutes each. Table 2.2 shows all the antibodies used in this study.

Table 2.2 The list of antibodies used in this study

Antibody Name	Origin	Brand	Catalog Number	Size (kDa)
ATF4	Rabbit	St John's Laboratory	STJ92467	49
eIF2α (S51)	Rabbit	St John's Laboratory	STJ11102562	38
Total RPS6	Rabbit	Cell Signaling Technology	2217S	32
RPS6 (S235/236)	Rabbit	Cell Signaling Technology	2211S	32
RPS6 (S240/244)	Rabbit	St John's Laboratory	STJ113488	36
Total 4E-BP1	Rabbit	Cell Signaling Technology	9644T	15/20
4E-BP1 (S65)	Rabbit	Cell Signaling Technology	9451S	15/20
Histone Deacetylase 1 (HDAC1)	Rabbit	Cell Signaling Technology	2062S	62
ß-actin (C4)	Mouse	Santa Cruz Biotechnology	sc-47778	45
α-Tubulin (11H10)	Rabbit	Cell Signaling Technology	9099S	55

Table 2.2 (cont'd) The list of antibodies used in this study

ERK 1/2 (T202/Y204)	Rabbit	Santa Cruz Biotechnology	sc-16982	42/44
p90RSK (T573)	Rabbit	Cell Signaling Technology	9346	90
p70S6K (T389)	Rabbit	Cell Signaling Technology	9234S	70/85
Total p70S6K (49DS7)	Rabbit	Cell Signaling Technology	2708P	70/85
GAPDH (FL-335)	Rabbit	Santa Cruz Biotechnology	Sc-25778	37
Goat α-Mouse		Advansta	R05072 500	
Goat α-Rabbit		Advansta	R05071 500	

2.8 Chorioallantoic Membrane (CAM) Assay

Fertilized Leghorn eggs (from Tavukçuluk Research Institute, Ankara) were used for Chorioallantoic Membrane Assay. The eggs were delivered at an ambient temperature of 12 ºC and wiped with distilled water upon receipt. Then, eggs were put on a holder with the more rounded part facing upwards. They were incubated for 7 days in a pre-decontaminated incubator at 37 ºC and 60-70% humidity with autoclaved water. On the 7th day, the face of the eggs where the hole will be opened was wiped with ethanol and small piece of first-aid silk tape was placed to that area. Then the eggshell was pierced with the help of sterilized fine tweezers so that a 1 mm hole was introduced. On day 8, a window with a diameter of nearly 1 cm was opened with a sterilized curved scissor starting from the hole where eggshell was pierced the day before. One or two drops of sterile DPBS was introduced onto the eggshell membrane, which was pierced so that it can absorb the DPBS through the

space between eggshell membrane and the CAM. Later, the eggshell membrane was carefully removed without any harm to the CAM or the blood vessels of the embryo. The eggshell opening was covered with a piece of first-aid silk tape before placing back into the incubator.

Preparation and inoculation of the CAM xenograft was carried out on Day 9. 20 µL of viable 1×10^6 cell suspension in cold medium was mixed with 20 µL thawed cold Matrigel (Corning, USA) at a 1:1 ratio. 40 µL of Matrigel/cell suspension mixture was placed onto the petri dish as droplets and the droplets was left at room temperature for 10 minutes before incubation in a 37°C humidified incubator for 1 hour. This process provided the solidification of Matrigel prior to inoculation. After incubation, a few drops of DPBS were placed to the edge of each Matrigel spheroid so that it could be easily scraped from the petri dish without deteriorating its structure. The Matrigel droplets were placed through the eggshell opening onto the CAM where the vessels are denser. The tumor inoculated openings were closed with a tape tightly and the eggs were kept in the incubator for another 5 days. Any eggs showing signs of death of the embryo were immediately removed. Next, the microtumours were harvested for ongoing experiments. The embryos were sacrificed by quickly cutting the neck with sharp scissors to cause minimum distress and disposed in the medical waste for incineration. The microtumours were measured for the calculation of tumor volume and stored at -80 °C in sterile eppendorf tubes until use.

Tumor volume was calculated with the formula below.

Tumor volume = pellet length × width × height × 0.52 (Böhm et al., 2019)

2.9 Proliferation Assay – MTT

MTT [3-(4, 5-dimethylthiazol-2-yl)-2,5-diphenyltetrazolium bromide] assay was performed to assess the metabolic activity change or to examine cell proliferation capability of cells in response to chemotherapeutic reagents or chemicals used in this

study. On the first day of assay, the cells were seeded on a 96-well plate at 10,000 cells/well in a 100 µl complete medium. The cells were incubated overnight for attachment. The next day, the cells were either treated with relevant chemicals individually or in combination at the pre-optimized concentrations and durations shown in Table 2.1. At the end of the treatment, 12 mM MTT solution was prepared by dissolving 5mg MTT in 1 mL of DPBS (Biological Industries). This stock MTT solution was diluted with fresh complete medium as being 1.2 mM MTT solution was obtained. The treatment medium of cells was discarded and 100 µL of prepared 1.2 mM MTT solution was added to each well. Following 4 hours of incubation, 10 µL 1 % SDS (dissolved in autoclaved distilled water)- 0.01M HCl solution was introduced directly into the MTT-added wells. After 18 hours of incubation at 37 ^{o}C, absorbance measurement was done at 570 nm by using Multiskan-GO spectrophotometer.

2.10 Cell Viability Assay – Trypan Blue Exclusion Assay

The effect of nutrient depletion on cell viability was assessed by Trypan Blue Exclusion Assay. The adequate number of cells were seeded, and the next day nutrient depletion was carried out as described above. The treatment hours for Trypan Blue counting were chosen as 24, 48 and 72 hours to examine the effect of nutrient depletion at different time points. At the end of the treatment, the medium of the cells was collected in a 15 mL falcon tube so as to not eliminate detached or dead cells. Then, the attached cells were washed with DPBS and adequate amount of Trypsin (0.05%)-EDTA (0.02%) solution was introduced onto the cells. After 3-4 minutes incubation in an incubator, the detached cells were mixed with the collected suspended cells. Then the cells were centrifuged for 4 minutes at 350 x *g*. The supernatant was discarded, and the remaining cell pellet was dissolved in fresh 1 mL of complete medium. 0.5% Trypan Blue solution was mixed with cell suspension in a 1:1 (v/v) ratio and incubated at room temperature for 5 minutes. 10 µl of the stained cell mixture was placed on a hemocytometer for counting. The cells

were counted separately as unstained (viable) and stained (nonviable) under a binocular light microscope.

The viable cell percentage was determined as below:

Viable cells (%) = (total number of viable cells/total number of cells) x 100

2.11 Colony Formation Assay

6-well plates were initially seeded with 1000 cells per well and allowed to attach overnight. Subsequently, the cells were washed once with PBS. The next day, the designated depletion treatment was initiated. The cells were then cultured in a humidified incubator at 37ºC with 5% CO2, and their medium was refreshed every 48 hours. For replenishment, after the designated depletion treatments for 24 or 48 hours, the medium was replaced with the complete medium. Once the colonies were large enough to be visible to the naked eye, the treatment was terminated, the wells were washed once with PBS and the colonies were fixed and stained.

For cell fixation, 4% paraformaldehyde (PFA) (diluted from 16% PFA with PBS) was applied to the cells and incubated for 15 minutes at room temperature. Next, the PFA was removed, and the cells were washed with PBS. Following this, 1 ml of 0.5% crystal violet solution prepared in methanol (Sigma Aldrich, USA) was added to the wells and incubated for 20 minutes at room temperature on an orbital shaker. Subsequent to incubation, the cells underwent a gentle wash with tap water until all excess crystal violet solution was removed. The wells were left to air-dry overnight. Manual imaging and counting of colonies were carried using the white tray of the ChemiDoc Imaging system and Image Lab software (BioRad, USA).

2.12 Polysome Profiling

2.12.1 Sucrose Gradient Preparation

Buffer A (1X) containing 15 mM Tris-HCl (pH: 7.4), 80 mM KCl, 5 mM $MgCl_2$ and cycloheximide (100 µg/mL) was supplemented with sucrose to generate 10% and 50% (w/v) sucrose solutions. The sucrose gradient was prepared on ice with a gradient maker apparatus using 5.5 mL of the two different concentrations of sucrose to obtain a total of 11 mL gradient from highest concentration at the bottom through to the lowest concentration at the top. The gradient was prepared in silicone ultracentrifuge tubes. The prepared gradient was stored in a cold room until use. The tubes were moved very carefully to not disrupt the gradient.

2.12.2 Cell Lysate Preparation for Polysome Profiling

Buffer A (1X) containing 15 mM Tris-HCl (pH: 7.4), 80 mM KCl, 5 mM MgCl2 and cycloheximide (100 µg/mL) was supplemented with protease inhibitors (Roche cocktail), RNAse Out (20 U/mL) and 1% Triton-X-100 to prepare Cell Lysis Buffer A. At the end of respective treatments, the medium of the plates was removed and 4 mL of cold PBS & Cycloheximide (100 µg/mL) solution was added to the plates. The cells were incubated for 5 minutes in the cell culture hood at RT. After removing the PBS & Cycloheximide solution, 900 µL pre-prepared Cell Lysis Buffer A was added to the plates. The plates were shaken gently to spread the lysis buffer throughout the plate. The lysates were transferred into the fresh Eppendorf tubes, centrifuged for 10 minutes at 4^oC at 14,000 rpm and the supernatants were collected into fresh tubes. The RNA concentration was determined by measuring the A260 values using a Nanodrop. For fractionation, the required volumes for approximately 15-20 ODs were determined.

2.12.3 Ultracentrifugation and Fractionation of Sucrose Gradient for Polysome Profiling

The previously prepared sucrose gradient tubes were placed into the rotor buckets of SW 40 Ti (Beckman Coulter). Into each sucrose gradient, the required volume of cell lysates for the measured OD value was added each tube and balanced by adding Buffer A before carrying out ultracentrifugation. The gradients were ultracentrifuged at 39,000 rpm for 2 hours and 15 minutes at 4^{o}C by using maximum acceleration and deceleration settings. After ultracentrifugation, the buckets were removed carefully and placed on ice for fractionation. The fractions were collected by using ISCO Density Gradient Fractionator Model 185 with settings sensitivity 2, A260 and noise filter 4. The glycerol motor was activated in the forward direction to collect 12 fractions of 1 mL each into fresh Eppendorf tubes. Meanwhile, the absorbance values were automatically recorded at A260 to generate the polysome profile. The tubes were placed on ice and then at -80°C until use.

2.12.4 Western Blot Analysis from Polysome Profiling Fractions

Equal volumes from each fraction (1 through 12) were mixed with the loading buffer in a fresh tube. The selected volume was the maximum that can fit into wells of a 12% gel of 1.5 mm width generated with a 15-well comb. Subsequently, the protein mixture was boiled for 7 minutes at 95 °C. Following this, the standard gel electrophoresis and transfer process were carried out for Western blot analysis.

2.13 Statistical Analysis

Each experiment included a minimum of two biological replicates unless otherwise specified, each of which comprised at least two technical replicates. GraphPad Prism 8 (GraphPad Software Inc., USA) was employed for data analysis. Significance assessment utilized either one-way ANOVA, two-way ANOVA or Student's t-test. Statistical significance was established with a threshold of a p-value less than 0.05.

CHAPTER 3

RESULTS

3.1 The Effect of Nutrient Depletion on the Viability of HCT-116 Colorectal Cancer Cells

Nutrients such as amino acids, glucose, lipids, vitamins, and inorganic salts are required for all cell types to proliferate and maintain homeostasis in response to environmental stresses. Tumor cells are more reliant on one or more nutrients to sustain their survival and essential functions, which include macromolecule synthesis, energy production and redox control. Restriction in extracellular nutrient availability may affect the viability of cancer cells upon the activation of a number of regulatory pathways such as apoptosis (Fan et al., 2022). Therefore, several *in vitro* and *in vivo* assays were applied to determine viability of the cells.

3.1.1 Evaluation of the Effect of Nutrient Depletion on the Viability of HCT-116 Colorectal Cancer Cells *in vitro*

In the capacity of a TÜBİTAK 1001 project (118Z116) a nutrient depleted medium (glucose and glutamine-free RPMI medium supplemented with 1% FBS, 0.1g/L glucose, and 0.2mM L-glutamine) was optimized which could better mimic the physiological environment of tumor cells. The activation of AMPK (phosphorylation at T172) and induction of autophagy (increased levels of LC3-II and/or decreased levels of p62, increased levels of Beclin-1) were used as markers of cells under nutrient restriction. On the basis of these markers, the optimized incubation time in the nutrient restricted medium was determined as 48 hours for Caco-2, LoVo and T84 colorectal cancer cells as these cells also showed high viability at this timepoint. To determine the nutrient stress response in HCT-116 cells, the change in viability

was first examined after incubation in the nutrient restricted medium for 24 and 48 hours with Trypan Blue Exclusion Assay. A significant decrement in the number of viable cells was observed, with nearly 50% of the cells dying after incubation with the nutrient depleted medium for 48 hours (Fig. 3.1 A). However, 24 hours of incubation did not decrease the viability of HCT-116 cells (Fig. 3.1 B). In addition, the effect of long-term nutrient depletion (up to eight days) on the proliferation and viability was evaluated with a colony formation assay (Figure 3.1 C & D). Although HCT-116 cells were highly sensitive to nutrient depletion as seen in Trypan Blue Exclusion Assay, the surviving cells were highly viable and could successfully form colonies even with prolonged starvation. However, the size of the colonies was much smaller with the nutrient depleted cells compared to the nutrient rich cells (Figure 3.1 C & D). Replenishment of the cells after 24 hours (Figure 3.1 C) or 48 hours (Figure 3.1 D) of nutrient depletion resulted in a remarkable restoration in the number of colonies. As a result, both viability and proliferative capacity of cells lowered though there are persistent cells that can tolerate even higher durations of starvation.

Next, the metabolic activity was determined with an MTT assay. This assay is based on the ability of NADPH-dependent oxidoreductase enzymes to reduce the tetrazolium dye MTT to its insoluble formazan form (Kuete et al., 2017). The metabolic activity of nutrient depleted HCT-116 cells showed a temporal decrease. Although the number of viable cells after 24 hours of nutrient depletion was nearly 100% (Figure 3.1 A), the metabolic activity of the cells decreased by half, and this activity decreased further to 41.8% upon 48 hours starvation (Figure 3.1 E).

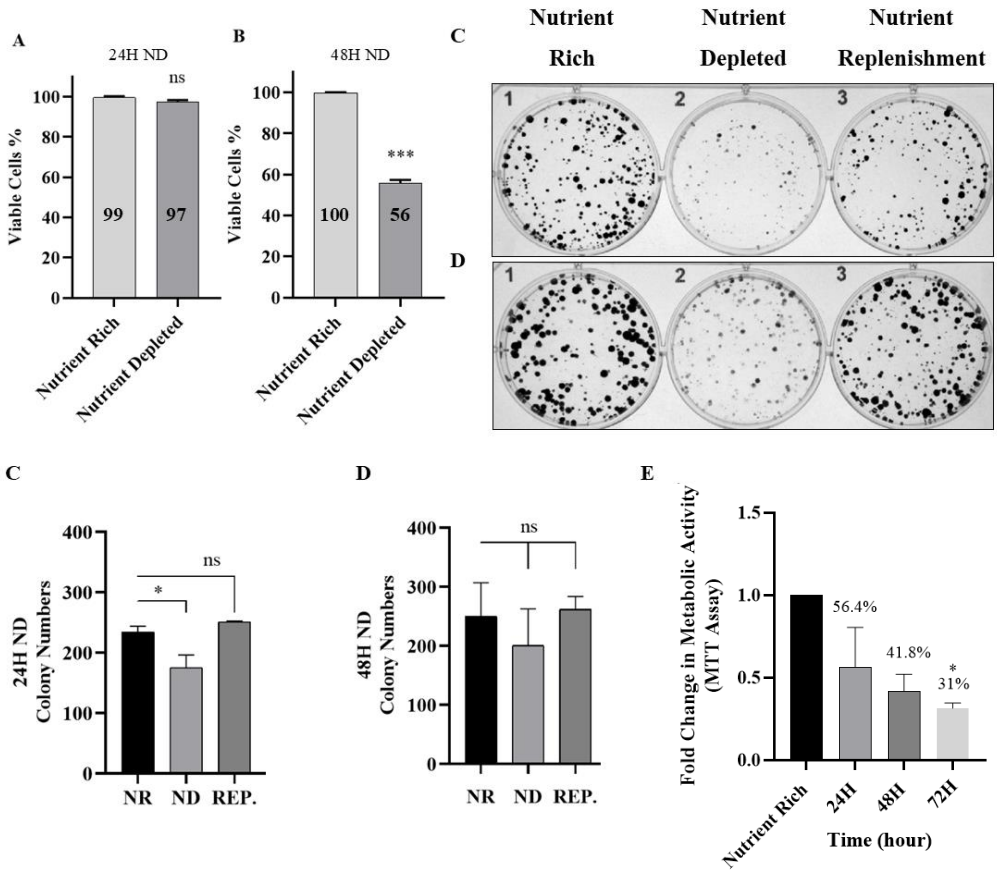

Figure 3.1. Evaluation the effect of nutrient depletion on cell viability *in vitro*

HCT-116 cells were incubated with either complete (Nutrient Rich; RPMI medium supplemented with 10% FBS, 2mM L-Glutamine, 1g/L glucose) or nutrient depleted medium (glucose and glutamine-free RPMI medium supplemented with 1% FBS, 0.1g/L glucose and 0.2mM L-glutamine) for 24 hours (A) or 48 hours (B) and then Trypan Blue Exclusion Assay was carried out. Panels C and D show the colony formation assay data upon prolonged starvation (up to eight days). Replenishment (C) was carried out by depleting the nutrients for 24 hours followed by the complete medium for seven days. Replenishment shown in D entailed nutrient depletion for 48 hours followed by complete medium for six days. The quantification of the colonies are shown in graphs C and D. The metabolic activity assay (MTT assay) is shown in E with percentages after normalization with the nutrient rich (control) cells. Data

Figure 3.1. (cont'd) *represent the two independent biological replicates of HCT-116 cells with standard error of the mean (SEM) values. Statistical analysis was carried out using an unpaired t-test (*** $p<0.05$) for the Trypan Blue Exclusion Assay and one-way ANOVA for the colony formation assay (* $p<0.05$, ns: not significant).*

3.1.2 Evaluation of the Effect of Nutrient Depletion on the Proliferation of HCT-116 Colorectal Cancer Cells *in vivo*

To meet the energy demand of highly proliferative cancer cells, interactions with the extracellular environment play a vital role. Sustained tumor growth is a result of continuing proliferation despite fluctuations in nutrient availability in the microenvironment since nutrient fluctuations may alter the proliferation rate of cells (Altea-Manzano et al., 2020). Therefore, the effects of nutrient depletion under physiological conditions *in vivo* with the chorioallantoic membrane (CAM) assay were examined.

Following 48 hours of incubation of HCT-116 cells with either complete or nutrient depleted medium, equal numbers of viable cells ($1x10^6$ cells for each egg) were inoculated on the chorioallantoic membrane (CAM) of fertilized Leghorn chicken eggs as described in the Methods section. Microtumours were excised five days after the inoculation to determine the tumor volume. The tumors generated from both nutrient rich and nutrient depleted cells were of comparable volume and not significantly different (Figure 3.2 B). The experiment was carried out with help from Hepşen Hazal Hüsnügil, Göksu Oral-Tüzün and Aliye Ezgi Güleç-Taşkıran.

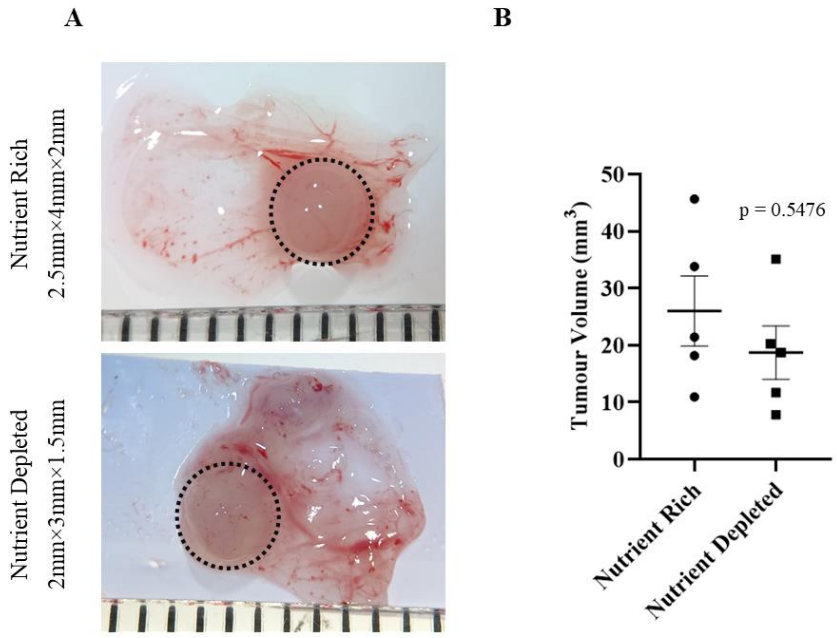

Figure 3.2. Evaluation the effect of nutrient depletion on tumor size *in vivo*

Representative microtumour images of CAM assay performed as at least two different biological replicates. (A) Microtumour volumes of pretreated nutrient rich (n=5) and nutrient depleted (n=5) groups [± standard error of the mean (SEM)]. (B) Dashed circles show the microtumour area, and the remaining part is the CAM tissue with blood vessels. Unpaired t-test (Mann-Whitney test) was used for statistical analysis.

3.2 Evaluation of the Activation of Nutrient Sensing Mechanisms in Nutrient Depleted Colorectal Cancer Cells

The mTORC1 complex regulates anabolic processes and maintains nutrient sensing to sustain cell growth and metabolic activity. The eukaryotic translation initiation factor 4E (eIF4E)-binding protein 1 (4E-BP1) and Ribosomal Protein S6 Kinase 1/2 (p70S6K1/2) are the most well-studied downstream effectors of the mTORC1 complex. 4E-BP1 is a negative regulator of translation (M. Yang et al., 2022). S6K1

phosphorylation by mTORC1 at Thr389 can activate the 40S ribosomal protein (RP) S6 via phosphorylation at Ser240/244 and Ser235/236 (Ruvinsky & Meyuhas, 2006). Western blot analysis was used to examine whether there was a temporal regulation in mTORC1 activation via the phosphorylation of p70S6K, 4EBP1 and RPS6 with nutrient depletion in a time course experiment. A decrease in phosphorylation of p70S6K and 4EBP1 was observed within 2 hours of incubation with the nutrient restricted medium, with a complete loss of phosphorylation after 2 hours, suggesting early inhibition of mTORC1. Of note, a robust increase in p-RPS6 (Ser240/244 and 235/236) was observed within 2 hours of nutrient depletion which was sustained until 24 hours of nutrient depletion (Figure 3.3 A & B).

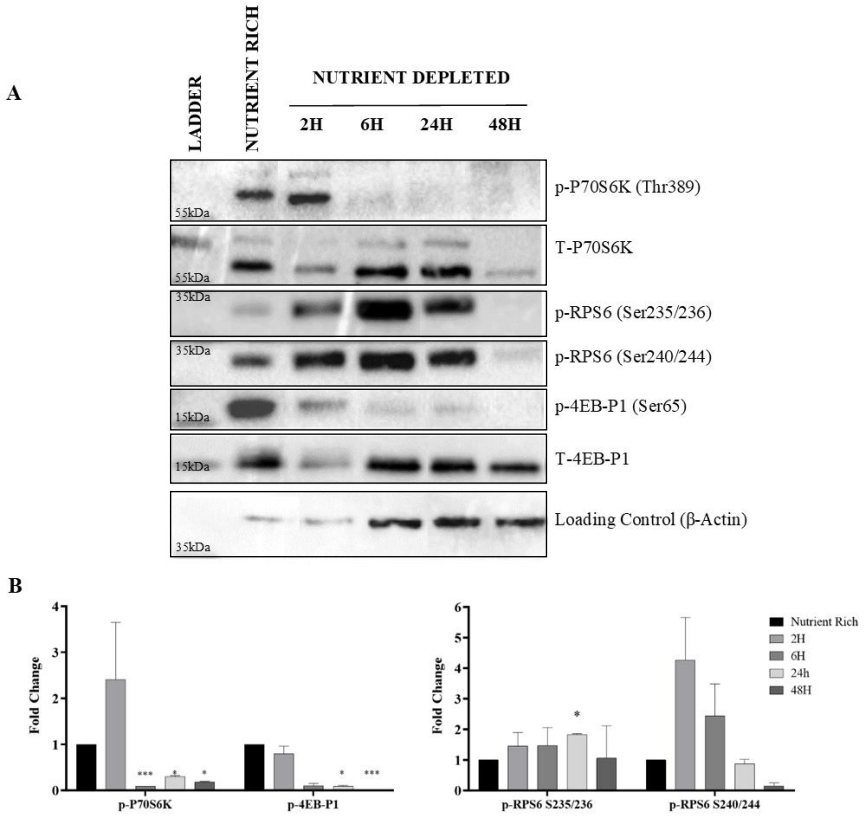

Figure 3.3. Time course evaluation of the activation of RPS6 and mTORC1 related upstream effectors

Figure 3.3. (cont'd) *HCT-116 cells were cultured with the nutrient depleted medium for the indicated time points, and with nutrient rich medium for 48 hours as a control and collected for protein isolation. 10 μg proteins were loaded on 12% SDS-PAGE gel. Representative blot from 3 independent biological replicates is indicated (A). Fold changes in protein levels with respect to controls are shown in densitometric analyses (±SEM). Statistical analyses were carried out using two-way ANOVA followed by Dunnett multiple comparison test. *p<0.05, ***p<0.001).*

Since the 48 hours of nutrient depletion led to extensive death in HCT-116 cells, and the RPS6 phosphorylation remained high until 24 hours, all following experiments were carried out after 24 hours of nutrient depletion. The activation of RPS6 while the mTORC1 activity is inhibited suggested an mTORC-1 independent activation of RPS6 with nutrient depletion. Therefore, the possible upstream activators of RPS6 other than mTORC1 was evaluated. RPS6 was shown to be activated via the p90 ribosomal S6 kinases (RSKs) which are part of the Ras/ERK pathway. ERK can activate the RSK2 through the phosphorylation of Thr577 in its C-terminal kinase domain activation loop (Doehn et al., 2004). In addition, RSKs, especially RSK1 and RSK2 selectively contribute to RPS6 activation at Ser235/236 in response to oncogenic RAS, while all other residues can be activated by S6K1 (Hutchinson et al., 2011; Roux et al., 2007). In this regard, the activity of RSK2 (p90 Ribosomal S6 Kinase2) and ERK1/2 was evaluated along with RPS6 activation in the time course nutrient depletion analysis. The gradual increment of p-p90RSK and p-ERK1/2 in a time-dependent manner was observed in nutrient depleted cells compared to the nutrient rich cells (Figure 3.4 A & B). Following RSK, ERK1/2 activation increased at 24 or 48 hours of nutrient depletion. However, only RPS6 activation at Ser235/236 was high in 24 hours of nutrient depletion compared to the other residue that is solely activated by mTORC1 (Ser240/244), which suggests ERK1/2 dependent activation of RPS6 in nutrient depleted HCT-116 cells.

To further determine the contribution of ERK1/2 activity on RPS6 activation, U0126, a selective inhibitor of MEK1/MEK2 kinases, which are the upstream activators of ERK1/2 (Ong et al., 2015), was used. The decrease in p-ERK1/2 and p-RSK levels along with RPS6 phosphorylation at both sites with U0126 was observed solely in the nutrient depleted condition, although the decrease did not reach statistical significance (Figure 3.4 C & D).

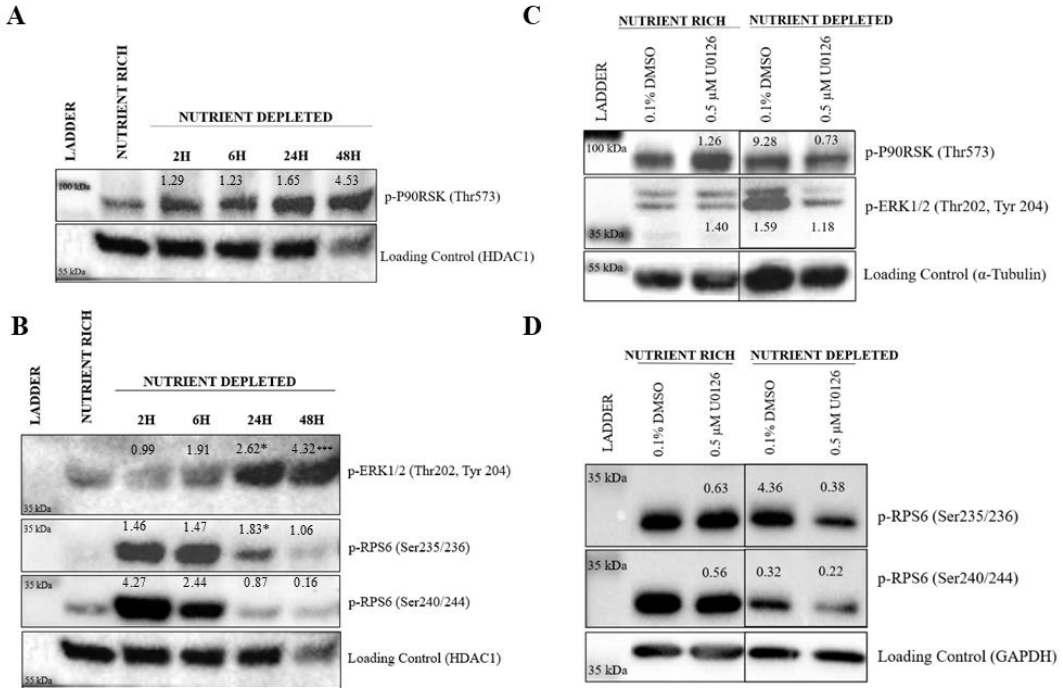

Figure 3.4. Evaluation of the temporal activation of RPS6 and its potential upstream effectors upon nutrient depletion

HCT-116 cells were cultured with nutrient depleted media (ND) for the indicated time points. The cells were incubated in the nutrient rich (NR) medium for 48 hours as a control. Where indicated, the cells were co-treated with 0.5 μM U0126 in NR or ND media for 24 hours and collected for protein isolation. 10-30 μg proteins were loaded on an 12% SDS-PAGE gel. A representative blot from one replicate is indicated (A & B). Representative blot from 3 independent biological replicates is indicated (C & D). Fold changes in proteins with respect to controls are shown

Figure 3.4. (cont'd) *shown with values. Statistical analyses were carried out using two-way ANOVA followed by Dunnett multiple comparison test (*p<0.05, ***p<0.001 and the ns: not significant).*

To further determine the intrinsic mechanisms of mTOR activity and mTOR dependency in the phosphorylation of RPS6 protein, the mTOR kinase inhibitor, AZD8055, was used (Zhao et al., 2014). As seen in Figure 3.5, the mTOR activity was inhibited as shown by the decrease in p-P70S6K and p-4EB-P1. However, the treatment with 5μM AZD8055 did not result in a noticeable decrease in the phosphorylation of RPS6 at either residue in nutrient depleted cells. On the other hand, the efficacy of AZD8055 was observable in nutrient rich cells by inhibiting of RPS6 phosphorylation at both residues examined.

Western blot densitometric analysis was employed to quantify the levels of phosphorylated RPS6 (for both Ser235/236 and Ser240/244 residues), and the results consistently showed no significant change with nutrient depletion compared to the control cells. This outcome supports the presence of alternative regulatory mechanisms for RPS6 phosphorylation triggered by nutrient depletion.

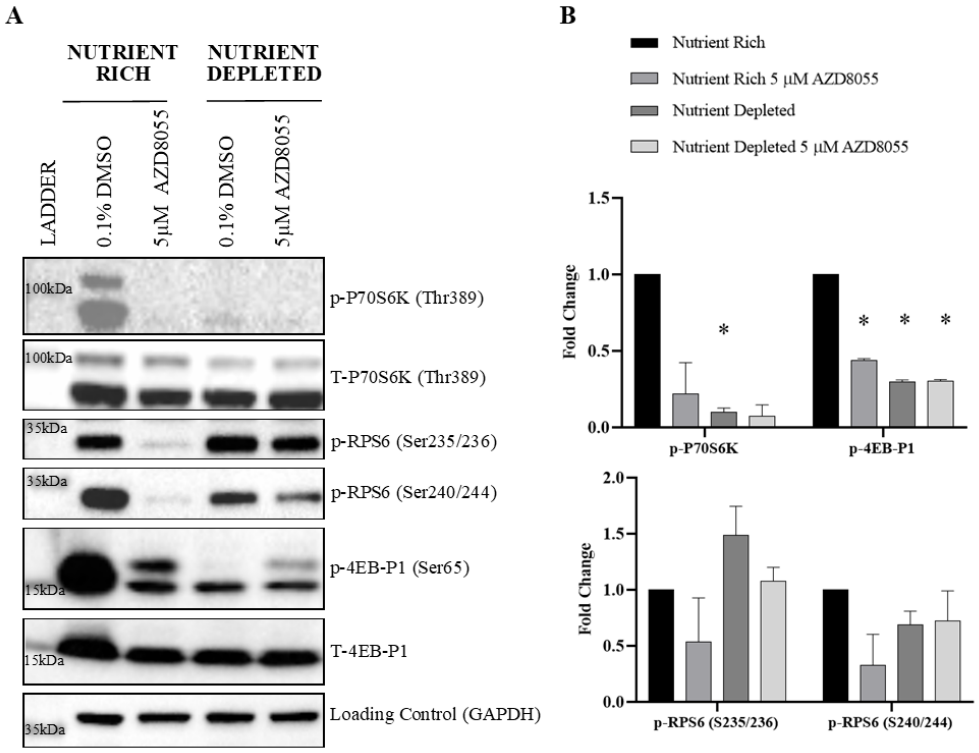

Figure 3.5. Evaluation of the effect of mTORC1 activity on downstream effectors upon treatment with AZD8055

*HCT-116 cells were cultured with nutrient depleted media (ND) for 24 hours. The cells were incubated in the nutrient rich (NR) medium for 24 hours as a control. Where indicated, the cells were co-treated with 5 µM AZD8055 in NR or ND media for 24 hours and collected for protein isolation. 10 µg proteins were loaded on an 12% SDS-PAGE gel. A representative blot from two independent replicate is indicated (A). Fold changes in proteins with respect to controls are shown in densitometric analyses graphs (±SEM) (B). Statistical analyses were carried out using two-way ANOVA followed by Dunnett multiple comparison test (*p<0.05).*

3.3 Evaluation of the RPS6 Activation in the context of Components of the Culture Medium

In addition to the identification of the upstream activators of RPS6, we also identified which components of the complete medium play a crucial role and are required for the mTORC1-related activation of RPS6. For this reason, the cells were first nutrient depleted for 24 hours. Next, these cells were replenished with the nutrient depleted medium containing each of the additional components individually for 24 hours.

As seen in Figure 3.6, neither FBS nor amino acids (L-Glutamine, NEAA and L-Alanine) were as efficient as glucose or the complete medium to re-activate both p-P70S6K and p-4EBP1. However, the phosphorylation of RPS6 at Ser235/236, but not S240/244 was increased dramatically in the presence of amino acids, which may suggest an mTORC1- independent activation of RPS6.

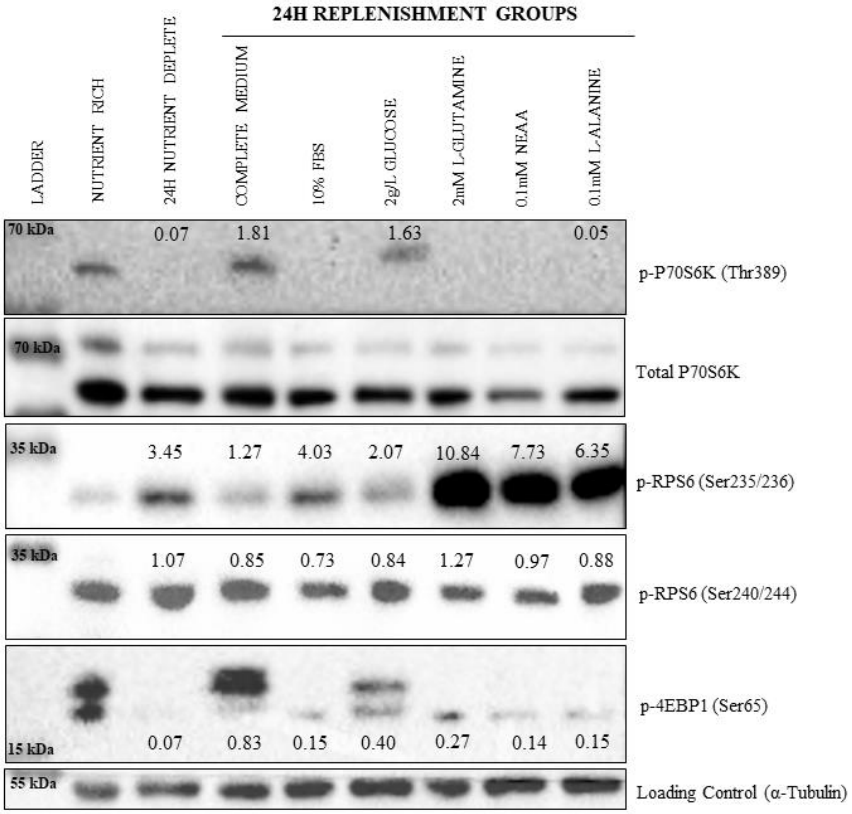

Figure 3.6. Evaluation of the activation of RPS6 and its upstream effectors in response to supplementation of components one by one

HCT-116 cells were cultured with nutrient depleted media (ND) for 24 hours, with nutrient rich (NR) medium for 48 hours as a control, and ND media for 24 hours then replenished with the specified media for 24 hours, then collected for protein isolation. 10 µg proteins were loaded on 12% SDS-PAGE gel. A representative blot from two independent biological replicates is shown. Fold changes in the phosphorylation of the proteins with respect to controls are shown. Statistical analyses were carried out using two-way ANOVA followed by Dunnett multiple comparison test. None of the protein markers showed a significant increment.

3.4 The Assessment of the Effect of Ras Mutagenesis on MAPK Dependent RPS6 Activation in Nutrient Depleted Cells

Since the HCT-116 cell line is Ras mutated, next it was determined whether hyperactive KRAS/MAPK signaling plays any role in the response to nutrient restriction. Of note, an independent thesis study in our lab showed that LoVo cells (also with a Ras mutation) behaved very similarly to HCT-116 cells upon nutrient depletion (Oral, 2023). To further determine whether this activation is mainly regulated via MAPK pathway, Caco-2 colorectal cancer cells which has wild type *BRAF* and *KRAS* (Ahmed et al., 2013) were treated with either AZD8055 or U0126 in the concentrations specified before.

In contrast to our findings with HCT-116 cells, our experiment with the Caco-2 cell line (Figure 3.7) revealed no significant increase in phospho-RPS6 levels at both residues after incubation with nutrient depleted medium for 48 hours (optimized duration for Caco-2). As seen in Figure 3.7, U0126 treatment also did not lead to any significant change in the RPS6 levels in both nutrient rich and nutrient depleted conditions. In addition, the p-ERK1/2 levels in the nutrient depleted condition were low in contrast to the HCT-116 cell line. Moreover, the AZD8055 inhibited the upstream effector of RPS6 clearly with a significant decrease seen in p-P70S6K levels, as well as with a decrease seen in p-RPS6 levels itself.

This deviation in findings between HCT-116 and Caco-2 cells may reveal heterogeneous responses in the molecular processes controlling RPS6 phosphorylation in response to nutrient depletion in these two different cell lines having different mutations.

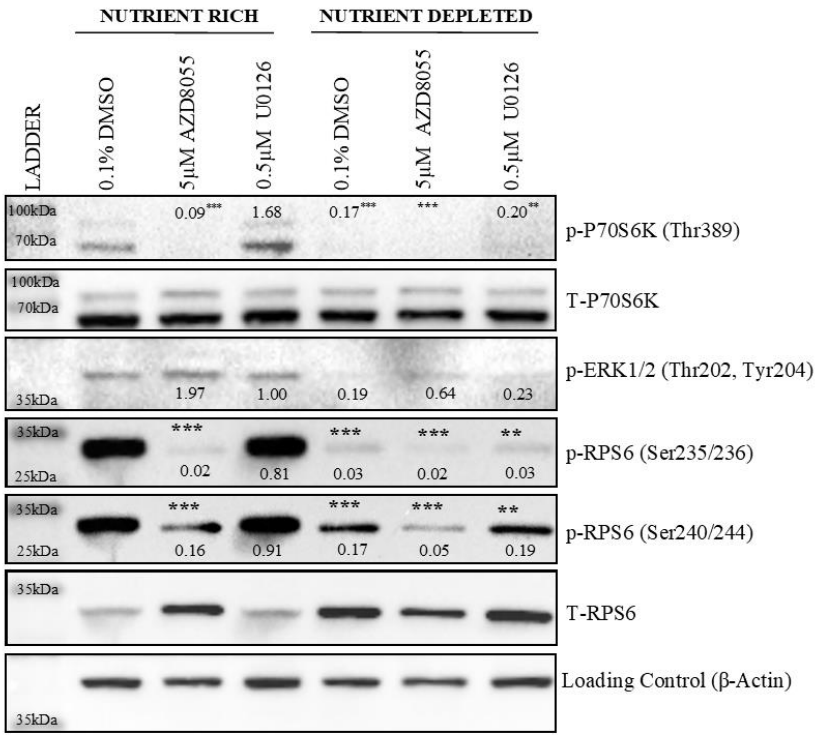

Figure 3.7. Investigation of the effect of mTORC1 and MAPK on RPS6 phosphorylation in Caco-2 colorectal cancer cells

*Caco-2 cells were cultured with nutrient depleted media (ND) for 48 hours, with nutrient rich (NR) medium for 48 hours as a control. Where indicated, the cells were co-treated with 5 μM AZD8055 in NR or ND media or treated with 24 hours nutrient depleted media prior to 0.5 μM U0126 for 24 hours. After treatments, cells were collected for protein isolation. 30 μg proteins were loaded on 12% SDS-PAGE gel. Representative blot from one biological replicate is indicated. Fold changes in proteins with respect to controls are given with values. Statistical analysis was carried out using two-way ANOVA followed by Dunnett multiple comparison test (***p<0.001, **p<0.01).*

3.5 *In Silico* Investigation of the Correlation of Co-activation of ERK1/2 and Ribosomal Protein S6

To further evaluate the relationship between ERK1/2 and RPS6 phosphorylation at S235/236 and S240/244, the Reverse Phase Protein Array analysis of the Colon Adenocarcinoma (COAD) cohort available from The Cancer Genome Atlas (TCGA) was incorporated. In addition to the *in vitro* analyses that showed a concomitant activation of RPS6 and ERK1/2, proteins of the colorectal cancer tumors currently available in RPPA showed a significant and strong positive correlation between the phosphorylation of ERK1/2 and RPS6 (Figure 3.8).

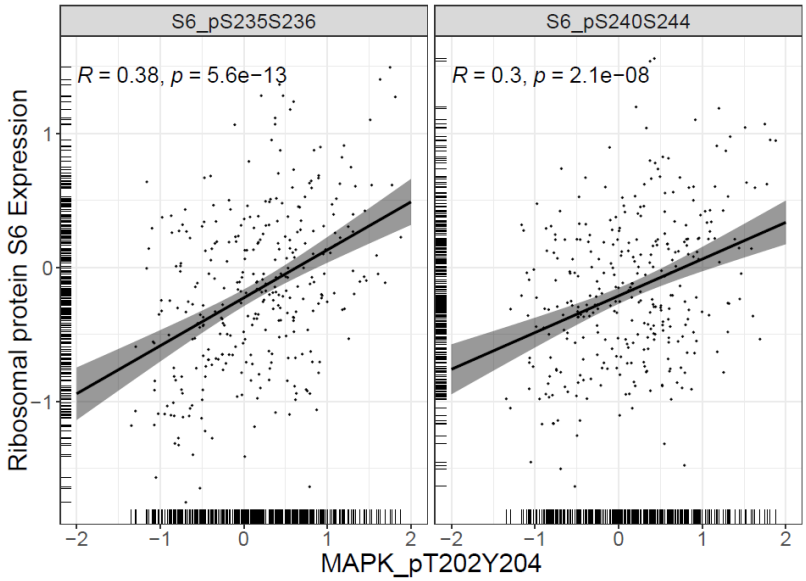

Figure 3.8. The correlation analysis to elucidate the relationship between the phosphorylation of RPS6 and ERK1/2 in colorectal cancer patients

The TCGA cohort's reverse phase protein array (RPPA) data for RPS6 (phosphorylation at Ser235/236 and Ser240/244) and ERK1/2 (T202/Y204) were analysed to elucidate the relation according to the clinical outcomes. Spearman's

Figure 3.8. (cont'd) *correlation coefficient was implied due to the non-normal distribution of the data. The data and the figure were generated by İsmail Güderer.*

3.6 Evaluation of the Global Translation with Polysome Profiling in HCT-116 Cells in Response to MEK Inhibitor U0126

Translation, which is an energy-demanding process, plays a crucial role in governing gene expression. In response to different stimuli, translation is regulated by converging signaling pathways through the mTOR and MAPK. As the downstream component in translation machinery, RPS6 is one of the most important targets that is activated via both Ras/ERK and mTORC1 pathway through RSKs and S6K, respectively, at the Ser235/236 residue (Roux & Topisirovic, 2018). In this study, based on the correlation between MAPK and RPS6 activation, the effect of nutrient depletion and ERK1/2 inhibition on global translation and translation efficiency were assessed by polysome profiling. In addition, the presence of phosphorylated RPS6 protein in different types of ribosomal particles (40S, 60S, 80S, light and heavy polysomes) was evaluated. For this purpose, HCT-116 cell lysates treated with specific chemicals or media were loaded onto a linear 10-50% sucrose gradient, and fractions were collected from the gradient. The input was used as a control to determine the success of the treatments.

As seen in Figure 3.9. A & B, Western blot analysis containing each fraction revealed that p-RPS6 in nutrient-rich and U0126 treated cells was found weakly in the supernatant and was detected all along the gradient including free subunits corresponding to the 40S and 60S, 80S (monosomes) and also polysomes (both light and heavy). In addition, as seen in Figure 3.9. C & D, p-RPS6 in nutrient-depleted and U0126 treated cells was not found in the supernatant, was found weakly in the free subunits corresponding to the 40S and 60S and was detected strongly in 80S (monosomes) and weakly all along the polysomes. The profile of the nutrient-rich cells suggest that a significant portion of ribosomes were engaged in polysomal translation compared to the nutrient-rich U0126 treated cells and nutrient-depleted

plus U0126 treated cells. A potential slowdown in the translation can be observed in the profile which indicates a shift in the translation dynamic through an increase in the 80S level. Moreover, the 80S level was augmented in response to ERK1/2 inhibition with U0126 treatment and nutrient depletion. These 80S ribosomes (but not the 40S or 60S tibosomes or polysomes) also contained high levels of total and phosphorylated RPS6.

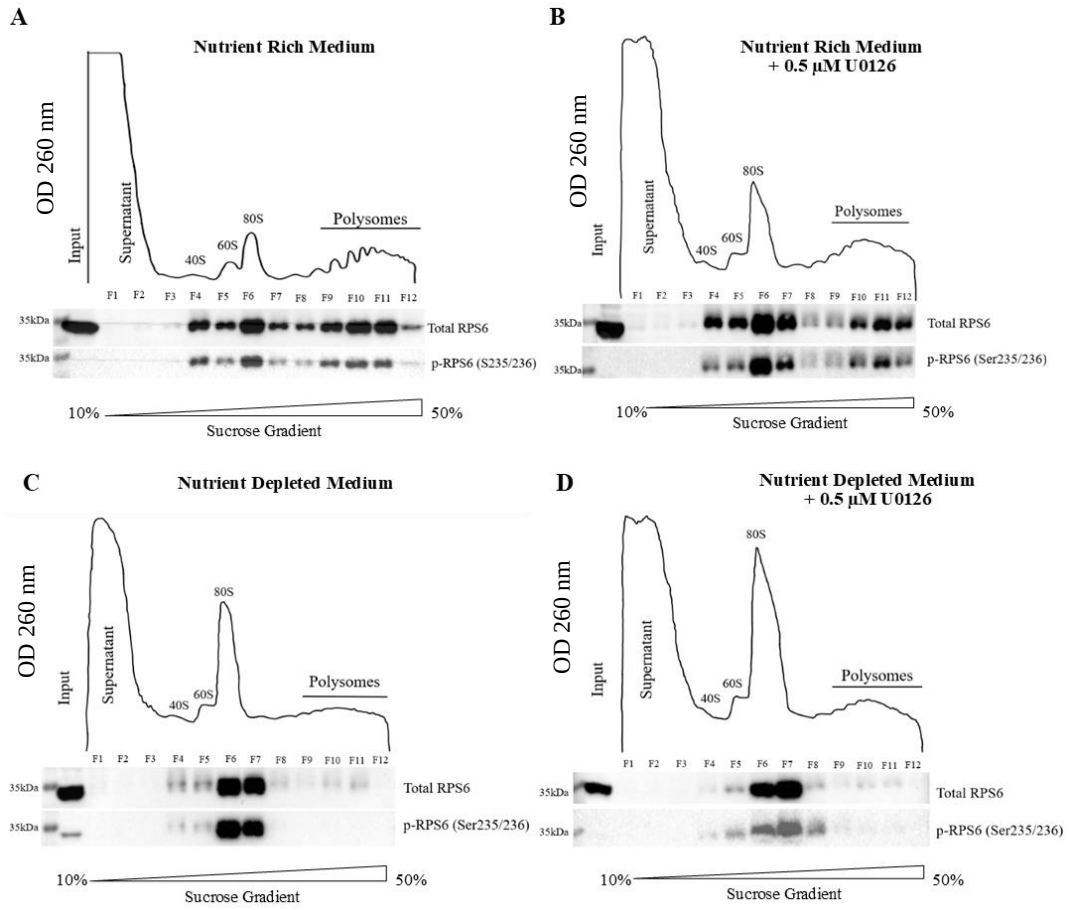

Figure 3.9. Evaluation of the polysome profile of HCT-116 cells with corresponding treatment

Polysome profile of total lysate from HCT-116 cells separated on a 10–50% sucrose gradient. In the fractions, input corresponds to the total lysate, which was not Figure

3.9. (cont'd) *fractionated, supernatant corresponds to the first two fractions obtained from sucrose gradient, 40S and 60S corresponds to the small and large ribosomal subunits respectively, the 80S corresponds to 80S ribosomes (monosomes) and the polysomes containing heavy (fraction 9) and light fractions (fraction 12) are indicated. F represents the fractions with their corresponding numbers. The expression of total RPS6 and p-RPS6 (Ser235/236) proteins were analyzed in the fractions using western blot. Equal volume of (25 µL) the fractions obtained from the gradient was loaded on 12% SDS-PAGE gel. A representative profile and blot from two independent biological replicates are indicated. (A) represents the polysome profile of the cells in nutrient rich medium, (B) represents the profile of the cells treated with 0.5 µM U0126 for 24 hours, (C) represents the polysome profile of the cells in nutrient depleted medium and (D) represents the profile of the cells treated with 0.5 µM U0126 for 24 hours in nutrient depleted medium. Ribosomal profiling was carried out in collaboration with Prof. Encarna Martinez-Salas in the context of COST Action "Translational control in Cancer European Network" (TRANSLACORE) CA21154.*

3.7 Investigation of the Integrated Stress Response Upon Nutrient Depletion in HCT-116 Cells

The integrated stress response (ISR) pathway is a stress sensing mechanism activated in response to different environmental stimuli to subsequently provide phosphorylation of eIF2α at Serine 51 to modulate the translational rate. Meanwhile, the translation of specific mRNAs such as ATF4 (a transcription factor) is enhanced to maintain the protein homeostasis (Holmes et al., 2022). We observed a high level of ATF4 in nutrient rich cells, which increased further with nutrient depletion as early as 2 hours and remained high for the entire duration of nutrient depletion. On the other hand, p-eIF2a (Ser51) was also high in nutrient rich cells. Upon nutrient-depletion, p-eIF2α remained high for the first 6h, after which a gradual decrease was observed over time.

This observation suggests that while p-eIF2α activity leads to an increase in the expression of ATF4 for the first few hours of starvation, ATF4 may remain activated via non-eIF2α mediated processes upon prolonged starvation in order to maintain survival in cells under nutrient stress. To further determine the activity of ISR upon nutrient depletion, HCT-116 cells were treated with 100 nM ISR inhibitor (ISRIB) simultaneously for the last 2 hours of 24 hours nutrient depletion. As a positive control of active ISR, nutrient rich cells were treated with 1 ug/mL Tunicamycin (ER-stress inducer). As seen in Figure 3.10 (B), ISRIB treatment decreased the ATF4 levels, suggesting the possibility of activation of ISR. Of note, no inhibition of p-eIF2α was observed with ISRIB since the drug is functional downstream of eIF2α (Anand & Walter, 2020).

Another interesting observation from this western blot is the high p-eIF2α level in the nutrient rich cells compared to the nutrient depleted cells in which amino acids and growth factors are reduced. We speculate that under nutrient rich conditions cancer cells have a high rate of protein synthesis, which may lead to an unfolded protein response and therefore ISR. Loss of nutrients can be tolerated by the cells for about 16h (other members of our lab have carried out further experiments with 16h of nutrient restriction), after which the inhibition of protein translation (please see polysome profiling data) may relieve any ER stress and therefore activation of p-eIF2α.

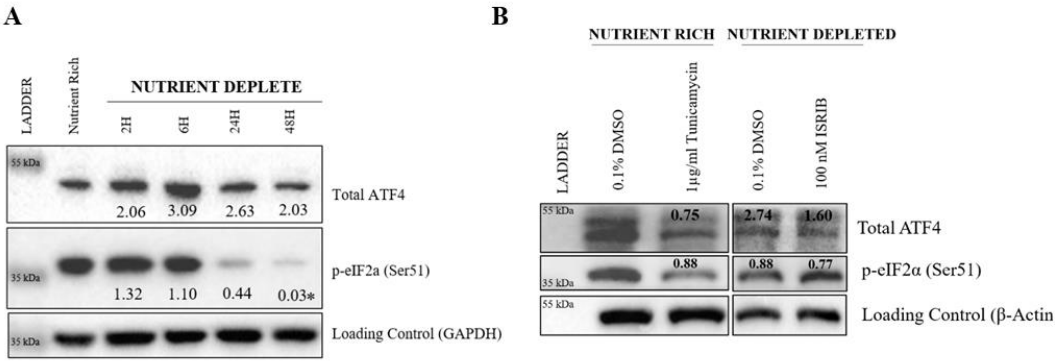

Figure 3.10. Evaluation of the ISR activation in response to nutrient depletion in HCT-116 colorectal cancer cells

*(A) HCT-116 cell treated with nutrient rich and nutrient depleted medium at determined (0-24 hours) time points showing the phosphorylation of eIF2α and the levels of ATF4. (B) HCT-116 cells were cultured with either nutrient rich or nutrient depleted medium only for 24 hours and 100nm ISRIB or vehicle (DMSO) was added in the last 2 hours of total treatment duration. 10-15 µg proteins were loaded on 12% SDS-PAGE gel. Representative blot from 2 independent biological replicates is shown. Fold changes in proteins with respect to controls are given with values. Statistical analysis was carried out using two-way ANOVA followed by Dunnett multiple comparison test (*p<0.05) values.*

Next, we determined which component of the complete medium could be implicated in the increase in the ISR markers. For this reason, the cells were first nutrient depleted for 24 hours; next, these cells were replenished with the nutrient depleted medium containing L-glutamine or FBS or glucose or NEAA that were added individually and equal to the concentration found in the complete medium. As seen in Figure 3.11, both ATF4 expression and p-eIF2α levels were particularly low in the cells replenished with NEAA or L-Alanine. Since the amino acid supply was increased in the environment, this may trigger the cells to reactivate the translational machinery with the decreased phosphorylation of eIF2α. These data suggest that the

activation of ATF4 and eIF2α (at 2-6h of nutrient depletion) may have resulted from the loss of amino acids from the culture medium. At the later stages (24 hours of nutrient depletion), an overall decrease in protein translation may have led to a relief of any ER stress and therefore a decrease in p-eIF2α .

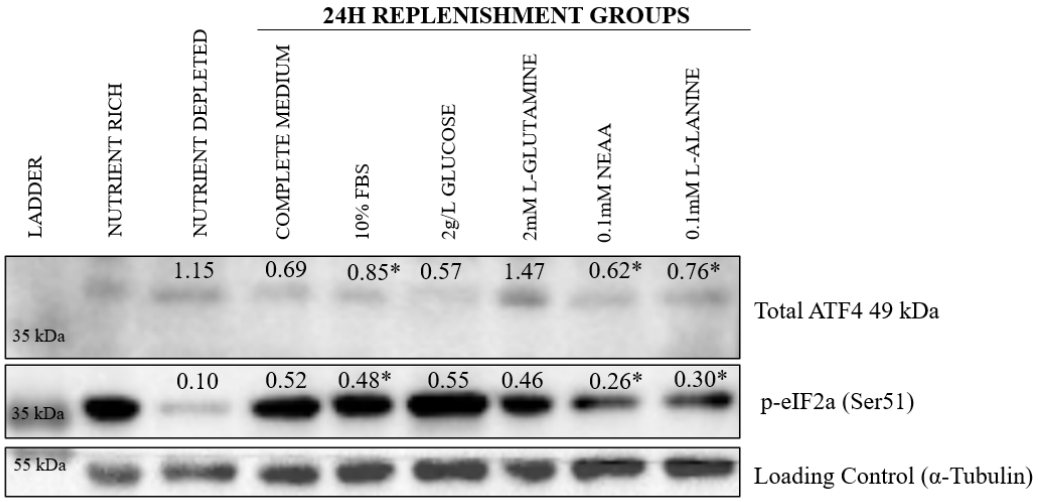

Figure 3.11. Abrogation of ISR in nutrient restricted cells replenished with amino acids

*HCT-116 cells were cultured with nutrient depleted media (ND) for 24 hours, with nutrient rich (NR) medium for 48 hours as a control, and ND media for 24 hours then replenished with the ND medium containing the specific supplements individually for 24 hours, then collected for protein isolation. 10 µg proteins were loaded on 12% SDS-PAGE gel. Representative blot from two independent biological replicates is shown. Fold changes in protein levels with respect to controls are shown. Statistical analyses were carried out using two-way ANOVA followed by Dunnett multiple comparison test (*p<0.05).*

3.8 Investigation of the Metabolic Vulnerability Upon Nutrient Depletion and in Combination with ERK Inhibition in HCT-116 Cells

In tumors, extracellular signal-related kinases (ERKs) promote cell proliferation and migration while also regulating apoptosis and differentiation when facing environmental stresses, including challenges posed by chemotherapy. Due to its pivotal role as a sensor for external signals ERKs may detect changes in the tumor microenvironment to initiate adaptive responses in cancer cells mainly via downstream effectors including RSKs. RSKs can also control cell proliferation, survival, and migration (Salaroglio et al., 2019). Therefore, to test whether MEK inhibition may lead to any change in cell viability of HCT-116 cells in nutrient rich and nutrient depleted media, HCT-116 cells were treated with U0126, and cell viability was detected with Trypan Blue exclusion assay.

As seen in Figure 3.12 (A), none of the concentrations of U0126 affected the viability of HCT-116 cells. Therefore, the activity of the ERK1/2 was assessed in the presence of the different concentrations of U1026 by western blot (Figure 3.12 B). The phosphorylation of ERK1/2 remained unchanged in nutrient rich cells at the different concentrations of U0126, while the phosphorylation levels showed a dose dependent decrease in the nutrient depleted cells. Of note, some ERK1/2 phosphorylation was retained even with the highest concentration of the inhibitor. This suggests that U0126 may not completely suppress ERK1/2 phosphorylation; any residual activity may be sufficient to ensure cell proliferation.

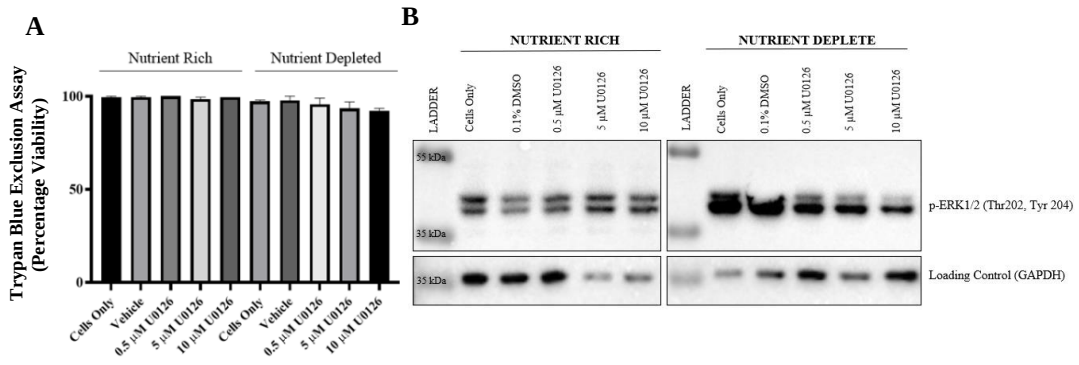

Figure 3.12. Investigation of the MEK inhibitor U0126 on the cell viability of HCT-116 cells in response to nutrient depletion.

HCT-116 cells were incubated with either nutrient rich or nutrient depleted medium for 24 hours and supplemented with MEK inhibitor U0126 at four different concentrations (0.5μM - 10μM) as well as vehicle. (A) Trypan Blue Exclusion Assay was carried out on the U0126 treated cells using a BioRad TC20 Automated Cell Counter. (B) HCT-116 cells were incubated in the nutrient rich or deficient medium and co-treated with U0126 (0.5μM - 10μM) for 24 hours. The cells were collected for protein isolation. 10-15 μg proteins were loaded on 12% SDS-PAGE gel. Data in panel A, represent the two independent biological replicates of HCT-116 cells with standard error of the mean (SEM) values. Statistical analysis was carried out using ordinary one-way ANOVA. The change of the viability between groups were not significant.

10 μM U0126 was selected as the concentration to determine whether a combination of ERK1/2 inhibition with a chemotherapy drug (5-FU and Cisplatin) can lead to increased cell death. However, the metabolic vulnerability of the nutrient depleted HCT-116 cells did not change any further even when combined with Cisplatin or 5-FU (Figure 3.13). The metabolic activity assessed by MTT Assay may indicate that the nutrient depleted cells maintain resistance to drugs via a pathway independent from the ERK1/2 pathway. Of note, a strong inhibition of metabolic activity/cell

viability with 5-FU and U0126 alone and in combination in the nutrient rich cells was observed. This suggests that nutrient depleted cells may activate adaptive pathways to maintain survival even in the presence of chemotherapy drugs. No sensitization of HCT-116 cells (which has a Ras mutation) to chemotherapeutic drugs was not observed in the presence of U0126.

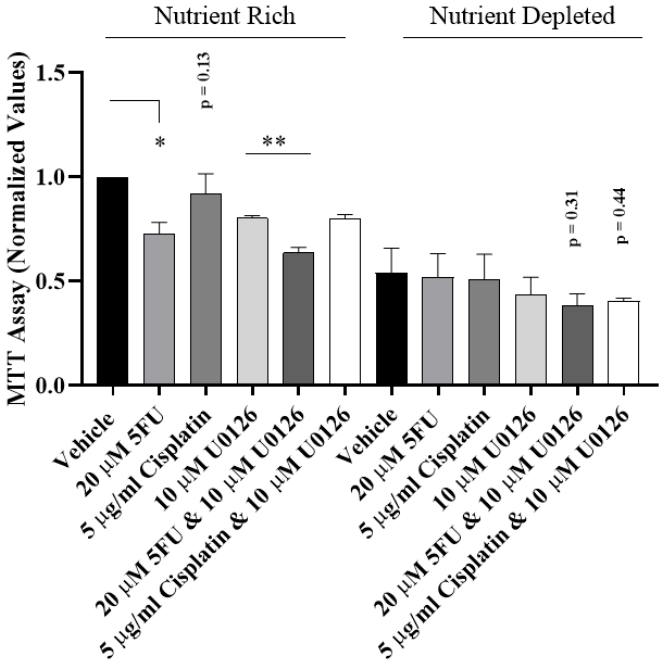

Figure 3.13. The Effect of MEK Inhibition on Metabolic Activity of HCT-116 Cells

*The change in metabolic activity of HCT-116 cells in response nutrient restriction and chemotherapeutic drugs was evaluated with an MTT Assay. The effect of MEK inhibitor U0126 was assessed in combination with 5-FU or cisplatin. Data represents 2 independent biological replicates for MTT Assay with ± SEM. The two-way ANOVA followed by Dunnett multiple comparison test (*p<0.05, **p<0.01) was performed as statistical analysis.*

3.9 Investigation of the Metabolic Vulnerability Upon Nutrient Depletion and Integrated Stress Response Inhibition in HCT-116 Cells

Activation of ATF4 via ISR can rewire cellular metabolism, enhance amino acid and antioxidant production, and counterbalance cellular stress. In cases of persistent stress, ISR might eventually lead to apoptotic cell death. Nonetheless, the processes dictating how the ISR regulates both cell survival and death in response to various types of stresses are unknown (Bilen et al., 2022). The activation of ATF4 in nutrient depleted cells was observed and reasoned that this might contribute to resistance to chemotherapy drugs. Therefore, the effect of ISR suppression on HCT-116 cell survival and metabolic activity in nutrient-rich and nutrient depleted HCT-116 cells incubated with the ISR inhibitor ISRIB in a dose dependent manner, in combination with the chemotherapeutic reagent 5-FU were evaluated.

The metabolic activity (viability) of nutrient depleted cells was not altered with different concentrations of ISRIB while 200 nM ISRIB concentration could significantly decrease the MTT signal in the nutrient rich cells (Figure 3.14 A). No significant sensitization of nutrient depleted or nutrient rich cells to 5-FU was observed when used in combination with ISRIB (Figure 3.14 B). These data suggest that the resistance mechanism elicited by the nutrient depleted medium may not be related to ISR.

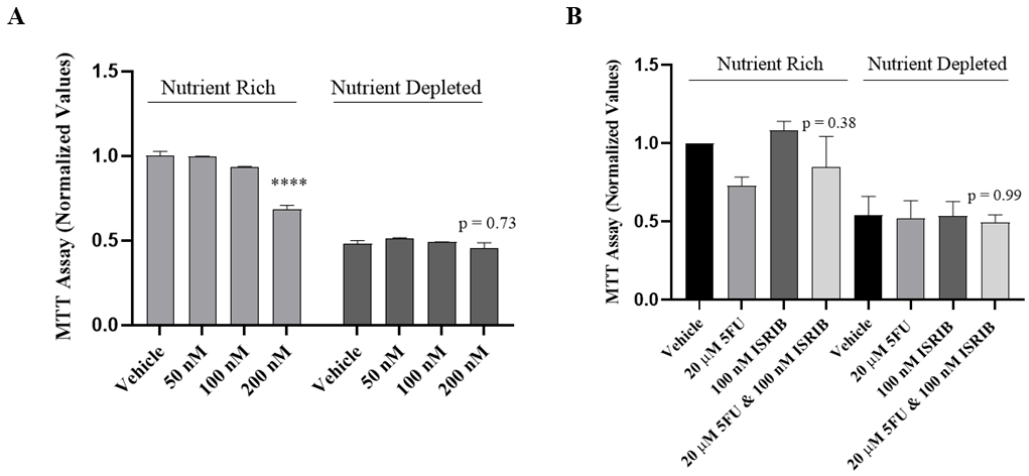

Figure 3.14. The effect of Integrated Stress Response Suppression on metabolic activity

*The change in metabolic activity of HCT-116 cells in response nutrient restriction, ISR inhibition and chemotherapeutic drugs was evaluated with an MTT Assay. (A) The dose dependent effect of ISR inhibitor ISRIB alone was assessed. Data represents 4 independent biological replicates for MTT Assay with ± SEM. The data were analyzed with two-way ANOVA followed by Tukey multiple comparison test (****p<0.0001). (B) A combination of ISRIB with 5-FU was assessed at the indicated concentrations. Data represents the average of 2 independent biological replicates with ± SEM. A two-way ANOVA followed by Dunnett multiple comparison test was performed as statistical analysis.*

CHAPTER 4

DISCUSSION

Tumors, including colorectal cancer (CRC), are known to adapt to stresses such as nutrient deficiency by rewiring their metabolism as well as oncogenic signaling to gain survival advantages (Miyo et al., 2016). Nutrient availability plays a pivotal role in the regulation of cell behavior and growth. Therefore, the abundance, activity, or both, of a multitude of transcription factors can be modulated to alter the expression of genes related to energy metabolism, survival, and proliferation (Kino et al., 2010; Y. Zhang et al., 2023).

The diminished expression or activity of key metabolic enzymes can have significant effects on the levels of metabolites and their precursors. Cancer cells exhibit increased requirement for specific nutrients or metabolic by-products even in the absence of metabolic defects. These distinct metabolic profiles of cancer cells can be potentially exploited as vulnerabilities for anti-cancer therapies (Garcia-Bermudez et al., 2020). Thus, based on their specific requirements, cancer cells can be starved of specific nutrients as a therapeutic option. Understanding the resilience of cancer cells to metabolic interventions is therefore crucial for the improvement of comprehensive and combinatorial anticancer strategies (X. Wang et al., 2022).

Several studies have explored the starvation of colorectal cancer cells with the individual, partial or total removal of nutrients (Conacci-Sorrell et al., 2014; Devenport et al., 2021; Miyo et al., 2016; Sato et al., 2007). In this thesis, the starvation response of colorectal cancer cells incubated in an optimized nutrient depleted medium (glucose and glutamine-free RPMI medium supplemented with 1% FBS, 0.1g/L glucose, and 0.2mM L-glutamine) was evaluated. Although a complete removal of nutrients by using Hank's buffered saline solution (HBSS) and/or Earle's buffered salt solution (EBSS) has been reported in the literature, the optimized

nutrient depleted medium used in the current thesis provides a more physiologically relevant environment while preventing the acute cell death due to the accumulation of reaction oxygen species (ROS) when nutrients are completely removed (Uriarte et al., 2021; Wu et al., 2013). My study demonstrated for the first time that HCT-116 colorectal cancer cells incubated in the nutrient restriction medium showed the activation of ribosomal protein S6 (RPS6) via an mTOR independent process and via the activation of extracellular signal-regulated kinases (ERK1/2). In addition, the potential upstream activators of RPS6 and the effect of this activation on general global translation in the context restricted nutrient availability were examined.

4.1 Cell Viability, Metabolic Activity and Nutrient Sensing Pathway Activation with Response to Nutrient Depletion in HCT-116 Colorectal Cancer Cells

4.1.1 The Effect of Nutrient Depletion on Cell Viability and Proliferation

Normal tissue growth is highly regulated, and very different from the regulation observed in tumors. As a hallmark of cancer, deregulated signaling pathways that can activate cell growth and cell cycle progression can cause increased and uncontrolled proliferation of cells (Uriarte et al., 2021). Cancer cells require nutrients to sustain their growth; withdrawal of nutrients can cause extensive cell death through the activation of apoptotic pathways in cancer cells (Kim, 2010; Sa-nongdej et al., 2021).

We have conducted multiple assays to provide a more comprehensive understanding of cellular responses of HCT-116 colorectal cancer cells to nutrient depletion. As a viability assay, the Trypan Blue Exclusion assay indicated that HCT-116 cells were viable at 24 hours of nutrient restriction; however, the viability decreased by nearly 50% when the nutrient depletion was extended to 48 hours. An MTT assay showed that the reductive activity displayed a robust decrease with 24-48 hours of starvation suggesting that both viability and metabolic activity of cells were decreased (Figure

3.1 A&B, E). Since HCT-116 cells are highly proliferative, cell viability and metabolic activity may decrease significantly when the required nutrients are not available in the environment (Simanurak et al., 2023). A clonogenic assay, on the other hand, showed that the ability of cancer cells to generate colonies from single cells was maintained even with prolonged starvation, although the colony sizes were smaller. This suggests a decrease in the proliferation rate of cells that retain their viability upon nutrient depletion (Figure 3.1 C&D). Of note, such viable cells may retain their aggressiveness (Yeung et al., 2010). In fact, we observed that the nutrient depleted cells were capable of formation of tumors in an *in vivo* Chorioallantoic membrane (CAM) assay with only a modest (non-significant) change in tumor volume compared to the nutrient rich control cells (Figure 3.2).

4.1.2 The Effect of Nutrient Depletion on Nutrient Sensing mTOR Pathway

The effect of nutrient depletion on the mTOR-related nutrient sensing mechanisms was assessed as a function of time. The mTOR pathway plays a key regulatory role by integrating many signal transduction pathways to activate cell cycle progression, protein translation, cellular metabolism, and cell growth and inhibit autophagy in response to energy and nutrient availability in cells (Condon & Sabatini, 2019). Therefore, the activation of the mTOR pathway through the phosphorylation and activation of p70S6K at Thr389, 4EBP1 at Ser65 and p70S6K dependent activation of 40S ribosomal protein S6 (RPS6) at both Ser235/236 and S240/244 by western blot were examined. A gradual decrease in the phosphorylation of p70S6K at Thr389, 4EBP1 at Ser65 and RPS6 at Ser 240/244 was observed over several hours of nutrient depletion, as expected. However, to our surprise, the phosphorylation of RPS6 at the Ser 235/236 site did not decrease; rather, the protein retained its phosphorylation for 24th hours of nutrient depletion (Figure 3.3).

RPS6 participates not only in ribosomal biogenesis and translational regulation, but also in cell cycle progression, proliferation, and growth regulation in addition to cell

migration, drug resistance and apoptosis (Yi et al., 2022). These multifaceted roles of RPS6 suggest its role as an indispensable target that is activated upon nutrient depletion and inhibition of mTORC1 signaling.

Although RPS6 is known to be strongly activated via mTORC1, alternative upstream activators of RPS6 phosphorylation at Ser 235/236, such as the (RAF)/MAPK-ERK kinase (MEK)/extracellular signal-regulated kinase (ERK)/Ribosomal S6 kinase (RSK) cascade have been identified (Yi et al., 2022). Therefore, whether the MAPK pathway was functional in the activation of RPS6 with nutrient depletion was examined. For this, the phosphorylation of ERK1/2 and p90RSK for the duration of nutrient depletion was examined. After 24th hours of nutrient depletion, it was observed that both ERK1/2 and p90RSK activity were high; RPS6 phosphorylation at Ser 235/236 was also high at this time point (Figure 3.4 A&B). Of note, the phosphorylation of both ERK1/2 and p90RSK remained high at 48-72 hours of nutrient depletion even when the phosphorylation of RPS6 at Ser 235/236 was decreased. Thus, ERK1/2 may contribute towards the activation of RPS6 only for a certain duration after mTOR activity was lost. At durations of starvation longer than 48 hours, extensive cell death in HCT-116 cells was observed; therefore, 24 hours of nutrient depletion was selected as the optimal time point for further analyses.

Since RPS6 is a very well-established downstream target of the mTOR pathway, we wanted to confirm whether any residual mTORC1 activity was responsible for the phosphorylation of RPS6. For this, the mTOR kinase inhibitor AZD8055 was used. The nutrient rich control cells showed a significant decrease in P70S6K, 4EBP1 and RPS6 activation upon treatment with AZD8055. This was expected since the nutrient rich cells had a functional mTORC1 pathway (Figure 3.5 A&B). The nutrient depleted cells showed minimal phosphorylation of P70S6K and 4EBP1, which could not be inhibited any further with AZD8055. Importantly, no change in the phosphorylation of RPS6 at Ser235/236 was observed in nutrient depleted cells treated with AZD8055, while a slight decrease was observed in Ser240/244. These findings demonstrated the independence of RPS6 activation from mTORC1 signaling upon nutrient depletion.

To substantiate whether ERK1/2 led to the activation of RPS6, the nutrient rich and restricted cells were treated with a low concentration (0.5μM) the MEK1/2 kinase inhibitor U0126. This concentration was selected since we wanted the MAPK pathway to be inhibited without causing extensive cell death. It was observed that treatment at this low concentration was sufficient to robustly decrease the phosphorylation of RPS6 at Ser 235/236 while modestly decreasing the phosphorylation of p-ERK1/2 and p-P90RSK in nutrient rich and depleted HCT-116 cells (Figure 3.4 C&D). The modest decrease in the phosphorylation of ERK1/2 and RSK in cells treated with the MEK inhibitor may be associated with the gain of alternative mechanisms to keep the MAPK pathway active in HCT-116 cells that have a Ras mutation (Kun et al., 2021). These data suggest that ERK1/2 may be activated in nutrient deficient cells to compensate for the activation of the mTORC1 pathway, which was almost completely inhibited. This temporal regulation of ERK1/2 activation may be related a rewiring of metabolism-related signaling close to the doubling time of approximately 20-24 hours of HCT-116 cells (Ahmed et al., 2013). The cycling time may become longer upon serum deprivation via the nutrient depleted medium. Hyperphosphorylation of RPS6 was shown to be correlated with oncogenic RAS-induced cell-cycle arrest and the extra-ribosomal functions of RPS6 in the regulation of cell-cycle progression and proliferation (Yi et al., 2022).

Next, we evaluated which component of the nutrient restricted medium was responsible for the activation of ERK1/2 and the loss of mTOR signaling. For this, 24 hours nutrient depleted cells were subjected to the replenishment of different components of the culture medium such as amino acids, glucose, serum, and growth factors (Figure 3.6). Several studies have shown that alanine on its own can promote mTORC1 activation (Dyachok et al., 2016; Takahara et al., 2020). The culture medium was replenished with a mixture of non-essential amino acids (NEAA) and L-alanine (8.9 mg/L) that also included 0.2 mM L-glutamine. Interestingly, supplementation of the nutrient deficient cells with NEAA was not sufficient to reactivate mTOR (phosphorylation of p70S6K) but was sufficient to activate RPS6. The reactivation of mTOR (phosphorylation of p70S6K and 4EBP1) was seen in

cells replenished with glucose alone but not upon replenishment with serum or amino acids. Another interesting observation was the increased phosphorylation of RPS6 at Ser235/236, but not at Ser 240/244 in response to amino acid supplementation. This observation implies that the two phosphorylation sites of RPS6 may respond to alternative kinases, particularly in response to diverse stimuli.

Since our findings are related to the MAPK pathway, we examined whether these responses to nutrition deprivation were exclusive to cell lines with a Ras mutation. Therefore, we examined whether similar responses would be observed Caco-2 cells line which has wild type *BRAF* and *KRAS* (Ahmed et al., 2013). Caco-2 cells showed a robust decrease in phosphorylation of RPS6 at both residues in response to both nutrient depletion and AZD8055 treatment. More importantly, U0126 treatment did not decrease the phosphorylation of RPS6 in both nutrient depleted and rich conditions (Figure 3.7). This suggests that unlike the Ras mutated HCT-116 cells, RPS6 in Caco-2 was primarily regulated by mTOR. This finding may provide context for future research into targeted therapeutics suited to particular mutational backgrounds in colorectal cancers.

To establish whether the co-activation of RPS6 and MAPK (ERK1/2) was also relevant to human colorectal cancer, Reverse Phase Protein Array data from The Cancer Genome Atlas (TCGA) Colon Adenocarcinoma (COAD) cohort was assessed. Specifically, the correlation between RPS6 phosphorylation at residues Ser 240/244 or Ser 235/236 and ERK1/2 at Thr 202/Tyr204 was analyzed. Our data demonstrated a high correlation (Spearman's correlation coefficient) between the phosphorylation levels of ERK1/2 and RPS6. Notably, a more substantial and robust correlation was identified for RPS6 phosphorylated at S235/236 (Figure 3.8). These data suggest that ERK1/2 mediated phosphorylation of RPS6 may be relevant to human cancers as well. Such associations highlight the compensatory activation of alternative signaling cascades in cancer cells to maintain cell growth and proliferation when a mitogenic pathway such as mTOR is inhibited. Further research into the functional implications of this link could provide important insights into the

underlying mechanisms that drive colorectal cancer growth, potentially guiding the development of targeted therapy options.

4.2 The Effect of RPS6 Activation on Global Translation in Nutrient Depleted HCT-116 Cells

Since we observed that RPS6, a protein found in the small subunit of the ribosome, was active in nutrient depleted cells, we hypothesized that the active RPS6 may affect the translational profile of HCT-116 cells. Therefore, polysomal profiling was used to assess the distribution and phosphorylation of RPS6 in the different ribosomal fractions and its effect on global translational profile in nutrient depleted cells. Since our data suggested that the sustained phosphorylation of RPS6 in nutrient depleted cells was mediated by ERK1/2, polysome profile in HCT-116 cells treated with the MEK inhibitor U0126 was also examined. Polysome profiling with a sucrose gradient is a well-established method for separating ribosomal subunits, monosomes, and polysomes. This technique determines the absorbance of mRNA (and thereby its abundance) in different fractions (monosomes, polysomes etc), providing a snapshot of the state of translation under different growth conditions or treatments. Ribosomal profiling entails deep sequencing of ribosome-protected mRNA fragments (RPFs), which enables genome-wide monitoring of ribosome position and density (Liu & Qian, 2016).

Polysome profiling (carried out in collaboration with Prof. Encarna Martinez-Salas and Prof. Dr. Bünyamin Akgül) revealed a unique footprint of free 40S and 60S subunits, 80S (monosomes) and polysome fractions in HCT-116 cells with nutrient deficiency or MEK inhibition. We observed that in both nutrient rich and restricted cells, phosphorylated RPS6 (Ser235/236) was associated more prominently with the monosome fractions, while its association with polysomes was decreased in response to nutrient depletion. Notably, the polysome fractions were decreased while the monosome fractions were increased in the nutrient depleted cells (Figure 3.9 A, B, C & D). Nutrient restriction is known to cause disintegration of the polysome and an

increase in the 80S monosomal fraction (Liu & Qian, 2016), which was observed in HCT-116 cells as well.

The MAPK pathway is a major regulatory pathway in translational regulation (Yuan et al., 2020). The constitutive mitogenic activity of ERK1/2 in Ras mutated HCT-116 cells grown in complete medium was reflected by a robust rate of translation in the polysome profile. The polysome area was slightly decreased upon the treatment with MEK inhibitor, U0126, while 80S peak was increased. This may indicate a slight decrease in translational rate when MEK was inhibited. However, the profiling approach may not provide an accurate picture of the formation of monosomes, i.e. whether they are formed from the re-association of free ribosomal subunits or whether they are localized on actively translated mRNAs. In addition, it is currently unknown whether the "empty" ribosomes that are not associated with any mRNAs are artefacts of sample preparation or have undiscovered biological importance (Liu & Qian, 2016).

We observed a remarkable decrease in the polysome peaks and increase in the monosome peaks in response to nutrient depletion. This may be indicative of decreased activity of the mTOR pathway, and its downstream effectors involved in translational regulation. mTOR signaling regulates protein translation primarily through eukaryotic translation initiation factor 4E (eIF4E)-binding protein (4E-BP), ribosomal protein S6 kinase (S6K), and their downstream targets. These components play an important role in the rapid cellular response to environmental changes (Yang et al., 2022). Therefore, an active RPS6 is not the only factor that can regulate translational efficiency via mTOR. On the other hand, the basal RPS6 dependent translational activity may increase ribosomal biogenesis and translation of specific target mRNAs with a 5'-terminal oligopyrimidine track (5'-TOP mRNAs) (Yi et al., 2022). This 5'TOP motif, which is highly conserved, enables cells to respond to changes to regulate expression of proteins involved in ribosome production and translation to maintain cellular homeostasis (Cockman et al., 2020).

The balance between initiation and total elongation time determines the relative occupancy of polysomes and monosomes across the transcriptome. More specifically, an mRNA tends to be mostly linked to polysomes if the initiation step proceeds more quickly than the elongation phase. On the other hand, an mRNA is more likely to be linked to monosomes when initiation is noticeably slower than elongation (Heyer & Moore, 2016). The length of the ORF is also a crucial factor in determining the number of ribosomes per mRNA. On the other hand, monosomes can translate crucial regulatory proteins like transcription factors, kinases, and phosphatases but also denote translational regulation with respect to the length of the open reading frame (ORF). The shortest canonical ORFs in coding sequence genes are often occupied by a single ribosome (Heyer & Moore, 2016). The shift to an increase in the monosome fraction in nutrient depleted cells could be related to alterations in the initiation of translation due to a decrease in the amino acid pool (Figure 3.9 C&D). Consequently, RPS6 activation in nutrient depleted cells can maintain a basal level of protein synthesis to preserve cell homeostasis.

4.3 The Effect of Integrated Stress Response Induction on Translational Control

Since a decrease in the global translation was observed in the nutrient depleted cells that are surviving, we hypothesized a role of a stress response pathway such as the Integrated Stress Response (ISR) pathway in these cells. The ISR pathway is triggered under a variety of stressors, including nutritional stress. Stressed cells display the phosphorylation of eukaryotic initiation factor eIF2, a key component of the ISR, at Serine 51. This phosphorylation leads to inhibition of 5'cap-dependent translation, resulting in a significant decrease in protein synthesis and serves to conserve macromolecules such as amino acids during times of scarcity. Interestingly, several mRNAs implicated in the cell's stress response, such as the transcription factor ATF4, can show increased expression in the presence of ISR (Licari et al., 2021). To evaluate whether ISR was activated in nutrient restricted HCT-116 cells,

the activation of key ISR proteins p-eIF2α (Ser 51) and ATF4 were examined by western blot.

eIF2 dependent expression of ATF4 is canonical signal transduction pathway for ISR. It was observed that ATF4 and p-eIF2α (Ser51) levels were high in nutrient rich cells, suggesting the activation of ISR even under nutrient replete conditions. eIF2α can be activated downstream of three independent kinases: PERK, reflecting endoplasmic reticulum (ER) stress; GCN2, reflecting amino acid stress and HRI, reflecting oxidative stress (Ryoo & Vasudevan, 2017). Cancer cells synthesize numerous proteins and growth factors that may lead to ER stress, which may be reflected in the high eIF2α phosphorylation (Tunçer et al., 2020), even when nutrients are not limiting (Costa-Mattioli & Walter, 2020; Lewerenz & Maher, 2009). A gradual decrease in eIF2α phosphorylation (Ser 51) was observed when the duration of nutrient restriction was increased from 2 to 24 hours, although the protein levels of ATF4 remained unchanged (Figure 3.10 A). These data hint at the p-eIF2α independent regulation of ATF4. Although both eIF2α and ATF4 serve in the ISR, the expression of the target genes differs for different cellular stressors. Thus, even when cells are confronted with equivalent conditions, such as the absence of one essential amino acid vs another, there is a large variation in the genes that are differentially regulated (Mazor & Stipanuk, 2016). ATF4 may help tumor cells to adapt to various environmental stimuli and lead to changes in gene expression that can alter metabolism enhance vascularization along with cell survival and growth (Wek & Staschke, 2010). Several studies have reported eIF2α independent activation of ATF4 (Ben-Sahra et al., 2016; Torrence et al., 2021; Zhai et al., 2021).

The decrease in p-eIF2α at the later stages of nutrient restriction is also of interest. There may be two potential mechanisms: prolonged starvation can lead to the breakdown of cellular proteins by autophagy and the release of amino acids from the lysosome, which can reactivate translation (Singh & Cuervo, 2011). However, no re-activation of the mTOR pathway at the later stages of nutrient depletion was observed, suggesting that this may not be the mechanism for the decreased phosphorylation of eIF2α. Another possibility is that the decrease of protein

translation with nutrient depletion may have led to a mitigation of ER stress, and thereby a decrease in p-eIF2α. Yet another possibility is that activation of eIF2α is necessary for cell survival, which becomes feasible only for the first 24 hours of nutrient depletion. After this duration, the cells initiate the activation of cell death pathways, which necessitates the inactivation of eIF2α. Future studies will establish whether the decrease in eIF2α phosphorylation is the trigger that is needed for loss of cell viability.

To determine if high ATF4 expression in nutrient restricted HCT-116 cells even when eIF2α phosphorylation was diminished was due to ISR, ATF4 expression was examined in cells treated with the small molecule ISR inhibitor ISRIB, which acts downstream of eIF2α phosphorylation (Pavitt, 2013). As expected, no change in the phosphorylation of eIF2α was observed, while ATF4 levels were slightly decreased in response to ISRIB treatment in both control and nutrient depleted cells (Figure 3.10 B). This modest change may be reflective of the concentration of the drug used for the specific cell line, which might not have been sufficient to lead to any major decrease in the expression of ATF4 or there might be other non-canonical activators of ATF4. A recent study has shown that oncogenic BRAF could increase the expression of ATF4 and its associated target genes in melanoma (Nagasawa et al., 2020). The MEK-ERK system may also act as an upstream regulator for sustained ATF4 expression. ERK1/2 was shown to provide a temporary signaling input from the canonical protein synthesis apparatus to the transcriptional regulation of ISR in HepG2 cells (Stone et al., 2021).

Cellular sensitivity to the availability of amino acids and the activation of ISR is critical to the cell's ability to respond to changing nutritional circumstances. Cells can adapt to amino acid stress and increase their chances of survival by regulating protein synthesis and activating gene expression that can mitigate stress. As part of the ISR, GCN2 acts as an early responder of low availability of amino acids, by sensing tRNAs that are uncharged with amino acids. Signaling via GCN2 prevents further depletion of intracellular amino acid pools by activating eIF2α, which can inhibit global protein synthesis (Jonsson et al., 2019). Although the actual activation

of GCN2 in this thesis was not shown (the antibody purchased from Cell Signaling Technology did not show adequate specificity and sensitivity and a replacement has been requested), the fact that RPS6 phosphorylation was enhanced in nutrient deficient cells supplemented with NEAA, eIF2α was phosphorylated (Ser 51) and ATF4 was activated with nutrient deficiency strongly hints at the activation of a GCN2 mediated ISR (Figure 3.11) at the early stages of nutrient depletion.

Additionally, a remarkable decrease in the rate of translation in response to nutrient depletion has been observed as seen by polysome profiling. Although the exact mechanism for the translational slowdown was not identified in this thesis, translational repression at the later stages of nutrient depletion (24 hours) when p-eIF2α is low may be due to a direct effect on the canonical translational machinery. This idea is currently being explored in our laboratory.

4.4 Nutrient Depletion Dependent Chemoresistance in HCT-116 cells

Chemoresistance is the characterized by a loss of sensitivity of cancer cells to chemotherapy, allowing the cells to survive in the presence of drugs intended to prevent their proliferation. Highly proliferative cancer cells activate signaling pathways that regulate nutrient availability and the flow of carbons and nitrogen through metabolic pathways. This adaptation is crucial to meet the increased demand for macromolecules. The availability of nutrients significantly influences both the survival of cancer cells and their response to chemotherapy (Yeldag et al., 2018; Zhu & Thompson, 2019). Our observation of ERK1/2 related activation of RPS6, ATF4 activity and translational regulation in the nutrient depletion suggested the activation of survival mechanisms. We hypothesized that inhibition of ERK1/2 using the MEK inhibitor U1026 may decrease cell viability. However, it was observed that treatment of HCT-116 cells with UO126 did not decrease the phosphorylation of ERK1/2 or the viability of nutrient depleted HCT-116 cells (Figure 3.12 A&B). Of note, U0126 treatment led to a robust decrease in phosphorylation of RPS6 at Ser 235/236. This

surprising finding suggests the activation of alternative mechanisms for resistance of HCT-116 cells to U0126.

Development of resistance to MEK inhibitors via the activation of alternate receptor tyrosine kinases (RTKs) such as the PI3K/AKT pathway has been reported. Therefore, combinatorial inhibition of multiple pathways has come to the forefront (Kun et al., 2021). Therefore, it was examined whether the combination of U0126 with chemotherapeutic drugs such as Cisplatin and 5-FU may lead to enhanced cell death.

An MTT assay indicated that U0126 treatment led to a significant decrease in the metabolic activity of the nutrient rich cells alone or in combination with different doses of 5-FU; however, the change was not robust in the nutrient depleted cells. The mechanism of action of 5-FU is primarily through the inhibition of the enzyme thymidylate synthase (TS) by forming a stable complex. TS catalyzes the conversion of deoxyuridine monophosphate to deoxythymidine monophosphate in the synthesis of thymidine (Ghafouri-Fard et al., 2021). Resistance to 5-FU can be attributed to a number of different mechanisms, such as increased expression of TS and other enzymes of nucleotide biosynthesis pathways, inhibition of DNA repair pathways via the methylation of *MLH1*, or overexpression of anti-apoptotic proteins such as Bcl-2, Bcl-XL, and Mcl-1. (Untereiner et al., 2018; N. Zhang et al., 2008).

HCT-116 cells showed low sensitivity and high resistance to Cisplatin in both nutrient rich and depleted cells and no additive effect was observed with MEK inhibition (Figure 3.13). Although cisplatin is not used as a therapeutic option in colorectal cancer, its mechanism of action by forming DNA adducts can prevent cell division. One study proposed that cisplatin stimulates autophagy as a resistance strategy for the survival of human bladder cancer cells (J. F. Lin et al., 2017). In nutrient depleted HCT-116 cells the activation of autophagy, which may have led to resistance to cisplatin, can be examined to provide an insight into the mechanistic effect of autophagy on intervening in treatment efficacy.

Overall, our observations suggest that nutrient depleted HCT-116 cells were not susceptible to two different chemotherapeutic drugs. Among many other mechanisms, the prolonged activity of ERK1/2 or other components of the MAPK pathway such as p38 may lead to drug resistance. ERK1/2 has been shown to mediate resistance to chemotherapy in several cancers including colon cancer (Salaroglio et al., 2019). A previous study in our lab indicated a high expression of multidrug resistance protein MDR1 in nutrient depleted T84 colorectal cancer cells (Ezgi et al., 2023). However, whether ERK1/2 plays a role in the upregulation of multidrug resistance in nutrient depleted HCT-116 cells is currently unknown. A genetic screening approach indicated that the unfolded protein response sensor kinase IRE1 is a critical component in the survival of colorectal cancer (CRC) cells harboring mutant KRAS. JNK has been shown to influence resistance to 5-fluorouracil (5-FU) in CRC by increasing BCL2 phosphorylation and autophagy, hence protecting against 5-FU-induced apoptosis (Lee et al., 2020). The ability of cancer cells to adapt to unfavorable environmental conditions gives them a selective advantage for survival and proliferation over non-transformed cells.

Next, we examined whether the activation of the ISR could lead to the observed resistance of nutrient depleted HCT-116 cells to chemotherapy drugs. However, we observed that co-treatment of HCT-116 cells with ISRIB and 5-FU did not increase the vulnerability of nutrient depleted cells to 5-FU. Thus, although the activation of p-eIF2α and ATF4 in both nutrient rich and nutrient depleted cells may provide survival advantages to cells, their inhibition via ISRIB was not sufficient to activate cell death. A recent study suggested that ISRIB can be efficacious when p-eIF2α is robustly activated (Costa-Mattioli & Walter, 2020). Therefore, it is possible that the efficacy of ISRIB was not significant in the nutrient depleted cells where the p-eIF2α level was lower. In fact, the nutrient rich cells, which showed high activation of eIF2α, showed a modest decrease in cell death at the highest ISRIB concentration (Figure 3.14 A). In addition, since the cells were already resistant to 5-FU via mechanisms independent of ISR, treatment with ISRIB could not induce any further chemosensitivity (Figure 3.14 B).

Our MTT data indicated a nearly 50% decrease in metabolic activity of nutrient depleted HCT-116 cells, although most of the cells retained their viability. A previous study from our lab has shown hypophosphorylation of pRB in 5 different colorectal cell lines after 24 hours of nutrient deficiency (Hüsnügil et al., 2024). A concomitant decrease in BrdU incorporation in nutrient depleted cells was also observed, suggesting slower progression though the cell cycle. Thus, it is possible that the slower progression of the nutrient restricted cells through the cell cycle and slow metabolic activity may override any potential effect of chemotherapy drugs.

CHAPTER 5

CONCLUSION AND FUTURE STUDIES

In this thesis, a variety of assays were used to extensively characterize the biological responses of HCT-116 colorectal cancer cells to nutritional depletion. The nutrient depleted medium consisted of 10% of the components found in complete medium. Although cell viability was high after 24 hours of nutrient depletion, a significant decrease in viability was observed after 48 hours, indicating that the cells were highly susceptible to extended starvation. This suggested metabolic vulnerability of the cells, indicating a vital reliance on environmental supplies for survival. Interestingly, a colony-formation assay indicated that cells subjected to prolonged nutrient depletion (8 days) could retain their ability to survive, albeit with smaller colony sizes suggesting a decrease in the proliferation rate of the surviving cell population.

We observed that nutrient depleted HCT-116 cells have a dynamic interplay between the mTORC1 and MAPK pathways, with a particular emphasis on the phosphorylation of ribosomal protein S6 (RPS6). This study found that key downstream factors in the mTORC1 signaling pathway were inactivated with nutrient depletion in a temporal manner, as expected, along with RPS6 phosphorylation at Ser 240/244, while RPS6 phosphorylation at Ser 235/236 remained active until the 24th hour of nutrient depletion. The Ser 240/244 site of RPS6 is known to be exclusively phosphorylated by p70S6K through mTOR activation, while the Ser235/236 site can be phosphorylated by multiple kinases.

Pharmacological perturbation assays using the MEK inhibitor U0126 and the mTOR inhibitor AZD8055 demonstrated a key role of the MAPK pathway in regulating RPS6 phosphorylation when cells are nutrient deficient. Notably, although treatment of HCT-116 cells with U0126 did not lead to any dramatic decrease in the phosphorylation of ERK1/2 and its downstream protein p90RSK, RPS6

phosphorylation at Ser 235/236 was substantially decreased at 24 hours of nutrient depletion. The RPS6 activation remained independent of mTORC1 pathway at this time point. Of note, the activation of RPS6 potentially through the MAPK pathway was seen in HCT-116 and LoVo (experiments carried out by other members in our laboratory), both of which are Ras mutated. Caco-2 cells, which have wild type Ras and Raf proteins, did not show a similar activation of RPS6 at Ser 234/245; rather, the phosphorylation at both sites (Ser240/244 and Ser235/236) was decreased concomitant with a decrease in mTOR activation with nutrient restriction. Therefore, it is feasible to speculate that Ras mutated cells can activate RPS6 as a potential survival mechanism when nutrients are limiting. Our findings through the co-activation of the MAPK and RPS6 pathways, observed both *in vitro* and *in silico,* suggests important insights into the dynamic crosstalk between these signaling cascades in colorectal cancer, particularly in the context of nutrient deprivation.

Replenishment assays using non- essential amino acids, glucose and serum, indicated diverse responses to mTORC1 reactivation and RPS6 sensitization. It was observed that a cocktail of non-essential amino acids as well as L-Alanine alone led to a robust reactivation of RPS6 at Ser 235/236. The re-activation of p70S6K (downstream of mTOR), however, was not observed in the presence of amino acids. Thus, the activation of RPS6 (but not mTOR) in the presence of amino acids indicates specific regulation of amino acid metabolism or protein translation/breakdown.

We therefore investigated the effect of nutrient restriction on global translational profile. An increase in the monosome fraction and decrease in the polysome peaks were observed, indicating a decrease in global protein synthesis rate to maintain cell viability. The involvement of the MAPK pathway, particularly ERK1/2, in translational regulation was further investigated. The inhibition of the MAPK pathway with U0126 resulted in a modest decrease in polysome peaks and a significant increase in the 80S monosome peaks, further highlighting the importance of the MAPK pathway in regulating the rate of protein translation.

The decrease in polysome fractions indicates a potential decrease in global translation. Added to this, our observation of restoration of RPS6 phosphorylation at Ser 235/236 indicated a potential role of the Integrated Stress Response (ISR) pathway, specifically downstream of the amino acid sensor GCN2. We were unable to determine the specific activation of GCN2, but did observe high phosphorylation of eIF2α and ATF4 in the control nutrient rich cells. The phosphorylation of eIF2α decreased after 24 hours of nutrient restriction, while the levels of ATF4 continued to remain high.

The observation of ERK1/2-induced RPS6 activation, persistent ATF4 activity, and translational regulation under nutritional deficiency revealed insights into putative survival mechanisms. However, it was observed that HCT-116 cells were highly resistant to the MEK inhibitor U0126, which is critical for the inhibition of ERK1/2 signaling. We also evaluated whether a combination of U0126 and chemotherapy drugs such as Cisplatin and 5-FU could lead to an additive effect on cell death. Interestingly, HCT-116 cells were resistant to both Cisplatin and 5-FU, and their combination with U0126 did not have any additive effect under nutrient depletion. This suggests that HCT-116 cells can activate distinct mechanisms of chemoresistance with nutrient depletion and emphasizes the necessity of looking into new pathways and combinatorial techniques to improve treatment efficacy.

Overall, the thesis study data highlights the interplay between mTORC1-MAPK-ISR pathways in regulating protein translational in a nutrient depleted environment (Figure 5.1). Our data suggest substantial crosstalk between these pathways for the survival and/or chemoresistance pathways in HCT-116 cells when nutrients are limiting.

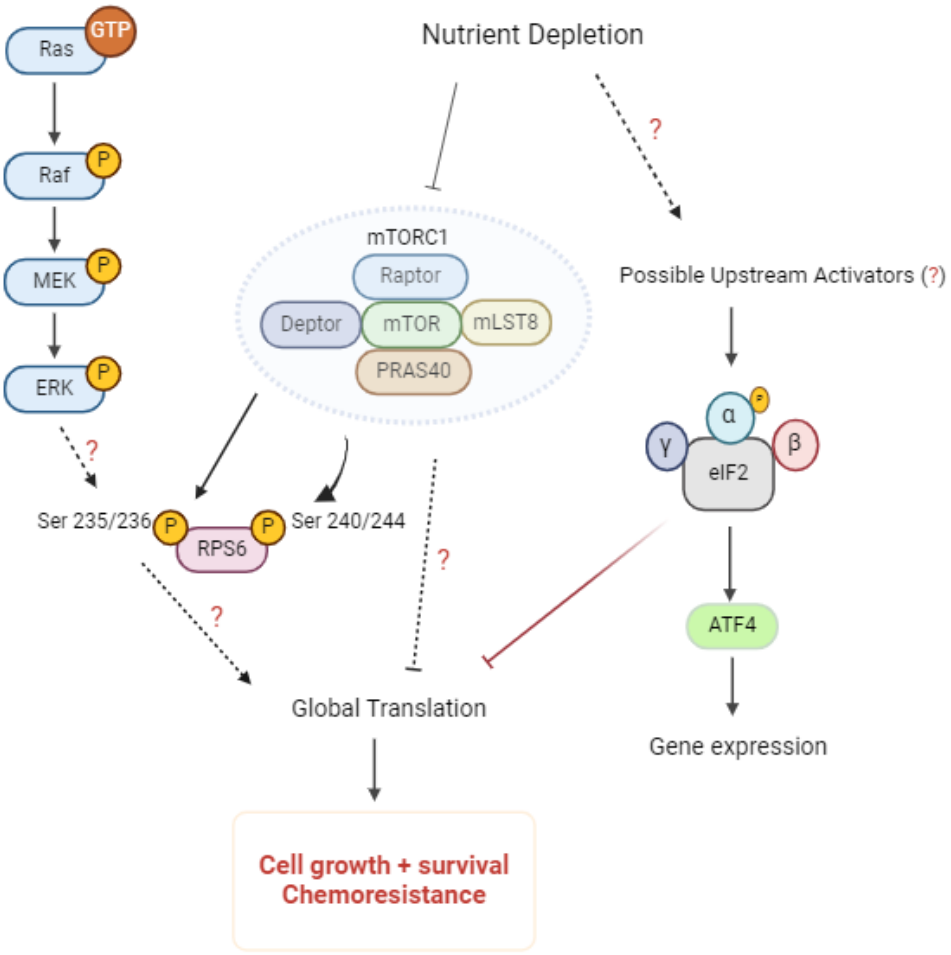

Figure 5.1. Proposed converging mechanisms of mTORC1, MAPK and ISR in the regulation of RPS6 activation and translational regulation upon nutrient depletion

Our data suggest that the activation of RPS6 via MAPK pathway in the absence of mTORC1 activity in the 24th hours of nutrient depletion may provide insights into the effect on global translation regulation. The ISR pathway on the other hand, may regulate the global translation indirectly by keeping it at basal level while ATF4 activity is retained. Overall, these converging mechanisms contribute mainly to attain survival and chemoresistance mechanisms. (Created with Biorender.com)

Although our data suggest multifaceted rewired mechanisms upon the nutrient depletion treatment, many questions remain unanswered. Further assays can be carried out to address the dependence and the role of the interconnected pathways. The future experiments that can be conducted are as follows:

1. Although the proliferation of HCT-116 cells under nutrient depletion was decreased, a colony formation assay revealed high clonogenicity of these cells. The effect of inhibition of MAPK by U0126, in both nutrient depleted and control HCT-116 cells on clonogenicity and tumor formation can be examined by the colony formation (*in vitro*) and CAM assay (*in vivo*) respectively.
2. Since the RPS6 levels were decreased with U0126 treatment while ERK1/2 activity still remained high, it is possible that other members of the MAPK family may contribute to the activation of RPS6. Other conventional MAPKs such as p38 isoforms (α, β, γ, and δ), c-Jun amino (N)-terminal kinases 1/2/3 (JNK1/2/3), and ERK5 can be assessed to correlate the MAPK dependency for RPS6 activation in Ras mutagenic HCT-116 cells.
3. We were unable to determine why the phosphorylation of eIF2α was decreased after 24 hours of nutrient restriction; at the same time, it was observed that ERK1/2 phosphorylation was increased from 24-48 hours of nutrient depletion. One possibility is that eIF2α activation provides survival signals up to a certain time point, after which the cells cannot survive any further. Thus, whether ERK1/2 can activate cell death pathways is not clear. An evaluation of cell death pathways can be carried out to determine whether eIF2α and EKR1/2 can orchestrate cell death in response to nutrient depletion.
4. The downstream targets of ERK1/2 that can potentially regulate RPS6, such as RSK or the MNK, can be examined further using specific inhibitors.
5. The polysome profiling assay can be performed in RPS6 silenced cells to assess the role of RPS6 in the regulation of protein translation in nutrient depleted cells.

6. A transcriptome profile of nutrient depleted, U0126 treated and RPS6 silenced cells may provide possible common enriched candidates and/or pathways that are activated.
7. The upstream activator of p-eIF2α, GCN2, can be examined in nutrient depleted cells, to provide insights into the amino acid dependent activity change. In addition, the ongoing ATF4 activity even when eIF2α is inhibited under nutrient stress can be further examined to investigate non canonical activation pathways for ATF4.
8. Resistance mechanisms to pharmacological treatments can be identified by examining the expression of drug efflux pumps or multidrug resistance proteins.
9. The role of converged MAPK, ISR and mTORC1 signaling pathways in survival of nutrient depleted HCT-116 cells can be further examined. These pathways can be simultaneously inhibited to investigate any increase in chemosensitivity.
10. Cancer stem-cell characteristics of the clonogenic HCT-116 cells under prolonged nutrient depletion can be assessed to provide an understanding of the activation of survival-related mechanisms.

REFERENCES

Abraham, A. G., & O'Neill, E. (2014). PI3K/Akt-mediated regulation of p53 in cancer. *Biochemical Society Transactions*, *42*(4), 798–803. https://doi.org/10.1042/BST20140070

Ahmadiankia, N. (2020). In vitro and in vivo studies of cancer cell behavior under nutrient deprivation. In *Cell Biology International* (Vol. 44, Issue 8, pp. 1588–1597). Wiley-Blackwell Publishing Ltd. https://doi.org/10.1002/cbin.11368

Ahmed, D., Eide, P. W., Eilertsen, I. A., Danielsen, S. A., Eknæs, M., Hektoen, M., Lind, G. E., & Lothe, R. A. (2013). Epigenetic and genetic features of 24 colon cancer cell lines. *Oncogenesis*, *2*. https://doi.org/10.1038/oncsis.2013.35

Altea-Manzano, P., Cuadros, A. M., Broadfield, L. A., & Fendt, S. (2020). Nutrient metabolism and cancer in the in vivo context: a metabolic game of give and take. *EMBO Reports*, *21*(10). https://doi.org/10.15252/embr.202050635

Anand, A. A., & Walter, P. (2020). Structural insights into ISRIB, a memory-enhancing inhibitor of the integrated stress response. In *FEBS Journal* (Vol. 287, Issue 2, pp. 239–245). Blackwell Publishing Ltd. https://doi.org/10.1111/febs.15073

Ben-Sahra, I., Hoxhaj, G., Ricoult, S. J. H., Asara, J. M., & Manning, B. D. (2016). mTORC1 induces purine synthesis through control of the mitochondrial tetrahydrofolate cycle. *Science*, *351*(6274), 728–733. https://doi.org/10.1126/science.aad0489

Bilen, M., Benhammouda, S., Slack, R. S., & Germain, M. (2022). The integrated stress response as a key pathway downstream of mitochondrial dysfunction. In *Current Opinion in Physiology* (Vol. 27). Elsevier Ltd. https://doi.org/10.1016/j.cophys.2022.100555

Böhm, J., Muenzner, J. K., Caliskan, A., Ndreshkjana, B., Erlenbach-Wünsch, K., Merkel, S., Croner, R., Rau, T. T., Geppert, C. I., Hartmann, A., Roehe, A. V., & Schneider-Stock, R. (2019). Loss of enhancer of zeste homologue 2 (EZH2) at tumor invasion front is correlated with higher aggressiveness in colorectal cancer cells. *Journal of Cancer Research and Clinical Oncology*, *145*(9), 2227–2240. https://doi.org/10.1007/s00432-019-02977-1

Bohnsack, B. L., & Hirschi, K. K. (2004). Nutrient regulation of cell cycle progression. In *Annual Review of Nutrition* (Vol. 24, pp. 433–453). https://doi.org/10.1146/annurev.nutr.23.011702.073203

Buono, R., & Longo, V. D. (2018). Starvation, Stress Resistance, and Cancer. In *Trends in Endocrinology and Metabolism* (Vol. 29, Issue 4, pp. 271–280). Elsevier Inc. https://doi.org/10.1016/j.tem.2018.01.008

Chang, F., Lee, J. T., Navolanic, P. M., Steelman, L. S., Shelton, J. G., Blalock, W. L., Franklin, R. A., & McCubrey, J. A. (2003). Involvement of PI3K/Akt pathway in cell cycle progression, apoptosis, and neoplastic transformation: A target for cancer chemotherapy. In *Leukemia* (Vol. 17, Issue 3, pp. 590–603). Nature Publishing Group. https://doi.org/10.1038/sj.leu.2402824

Cockman, E., Anderson, P., & Ivanov, P. (2020). Top mrnps: Molecular mechanisms and principles of regulation. In *Biomolecules* (Vol. 10, Issue 7, pp. 1–18). MDPI AG. https://doi.org/10.3390/biom10070969

Conacci-Sorrell, M., Ngouenet, C., Anderson, S., Brabletz, T., & Eisenman, R. N. (2014). Stress-induced cleavage of Myc promotes cancer cell survival. *Genes and Development*, *28*(7), 689–707. https://doi.org/10.1101/gad.231894.113

Condon, K. J., & Sabatini, D. M. (2019). Nutrient regulation of mTORC1 at a glance. *Journal of Cell Science*, *132*(21). https://doi.org/10.1242/JCS.222570

Costa-Mattioli, M., & Walter, P. (2020). The integrated stress response: From mechanism to disease. In *Science (New York, N.Y.)* (Vol. 368, Issue 6489). NLM (Medline). https://doi.org/10.1126/science.aat5314

Cruzat, V., Rogero, M. M., Keane, K. N., Curi, R., & Newsholme, P. (2018). Glutamine: Metabolism and immune function, supplementation and clinical translation. In *Nutrients* (Vol. 10, Issue 11). MDPI AG. https://doi.org/10.3390/nu10111564

Damgaard, C. K., & Lykke-Andersen, J. (2011). Translational coregulation of 5'TOP mRNAs by TIA-1 and TIAR. *Genes and Development*, *25*(19), 2057–2068. https://doi.org/10.1101/gad.17355911

Deleyto-Seldas, N., & Efeyan, A. (2021). The mTOR–Autophagy Axis and the Control of Metabolism. In *Frontiers in Cell and Developmental Biology* (Vol. 9). Frontiers Media S.A. https://doi.org/10.3389/fcell.2021.655731

Devenport, S. N., Singhal, R., Radyk, M. D., Taranto, J. G., Kerk, S. A., Chen, B., Goyert, J. W., Jain, C., Das, N. K., Oravecz-Wilson, K., Zhang, L., Greenson, J. K., Eugene Chen, Y., Soleimanpour, S. A., Reddy, P., Lyssiotis, C. A., & Shah, Y. M. (2021). Colorectal cancer cells utilize autophagy to maintain mitochondrial metabolism for cell proliferation under nutrient stress. *JCI Insight*, *6*(14). https://doi.org/10.1172/jci.insight.138835

Doehn, U., Gammeltoft, S., Shen, S.-H., & Jensen, C. J. (2004). p90 ribosomal S6 kinase 2 is associated with and dephosphorylated by protein phosphatase 2Cδ. In *Biochem. J* (Vol. 382).

Dyachok, J., Earnest, S., Iturraran, E. N., Cobb, M. H., & Ross, E. M. (2016). Amino acids regulate mTORC1 by an obligate two-step mechanism. *Journal of Biological Chemistry*, *291*(43), 22414–22426. https://doi.org/10.1074/jbc.M116.732511

Elias, E. G., Hasskamp, J. H., & Sharma, B. K. (2010). Cytokines and growth factors expressed by human cutaneous melanoma. *Cancers*, *2*(2), 794–808. https://doi.org/10.3390/cancers2020794

Ezgi, A., Taşkıran, G., Hüsnügil, H. H., Menemenli, N. S., Hampel, C., Huebner, K., Erlenbach, K., Friedrich, W., University, A., Sheraj, E.-N. I., Schneider-Stock,

R., & Banerjee, S. (2023). *Rewiring of Endolysosomal Signaling with Nutrient Depletion in Cancer Cells*. https://doi.org/10.21203/rs.3.rs-3331567/v1

Fan, K., Liu, Z., Gao, M., Tu, K., Xu, Q., & Zhang, Y. (2022). Targeting Nutrient Dependency in Cancer Treatment. In *Frontiers in Oncology* (Vol. 12). Frontiers Media S.A. https://doi.org/10.3389/fonc.2022.820173

Garcia-Bermudez, J., Williams, R. T., Guarecuco, R., & Birsoy, K. (2020). Targeting extracellular nutrient dependencies of cancer cells. In *Molecular Metabolism* (Vol. 33, pp. 67–82). Elsevier GmbH. https://doi.org/10.1016/j.molmet.2019.11.011

García-Jiménez, C., & Goding, C. R. (2019). Starvation and Pseudo-Starvation as Drivers of Cancer Metastasis through Translation Reprogramming. In *Cell Metabolism* (Vol. 29, Issue 2, pp. 254–267). Cell Press. https://doi.org/10.1016/j.cmet.2018.11.018

Ghafouri-Fard, S., Abak, A., Tondro Anamag, F., Shoorei, H., Fattahi, F., Javadinia, S. A., Basiri, A., & Taheri, M. (2021). 5-Fluorouracil: A Narrative Review on the Role of Regulatory Mechanisms in Driving Resistance to This Chemotherapeutic Agent. In *Frontiers in Oncology* (Vol. 11). Frontiers Media S.A. https://doi.org/10.3389/fonc.2021.658636

Gingras, A.-C., Gygi, S. P., Raught, B., Polakiewicz, R. D., Abraham, R. T., Hoekstra, M. F., Aebersold, R., & Sonenberg, N. (1999). *Regulation of 4E-BP1 phosphorylation: a novel two-step mechanism*. www.genesdev.org

Godet, A. C., David, F., Hantelys, F., Tatin, F., Lacazette, E., Garmy-Susini, B., & Prats, A. C. (2019). IRES trans-acting factors, key actors of the stress response. In *International Journal of Molecular Sciences* (Vol. 20, Issue 4). MDPI AG. https://doi.org/10.3390/ijms20040924

González, A., Hall, M. N., Lin, S. C., & Hardie, D. G. (2020). AMPK and TOR: The Yin and Yang of Cellular Nutrient Sensing and Growth Control. In *Cell*

Metabolism (Vol. 31, Issue 3, pp. 472–492). Cell Press. https://doi.org/10.1016/j.cmet.2020.01.015

Gwinn, D. M., Shackelford, D. B., Egan, D. F., Mihaylova, M. M., Mery, A., Vasquez, D. S., Turk, B. E., & Shaw, R. J. (2008). AMPK Phosphorylation of Raptor Mediates a Metabolic Checkpoint. *Molecular Cell*, *30*(2), 214–226. https://doi.org/10.1016/j.molcel.2008.03.003

Heyer, E. E., & Moore, M. J. (2016). Redefining the Translational Status of 80S Monosomes. *Cell*, *164*(4), 757–769. https://doi.org/10.1016/j.cell.2016.01.003

Holmes, M. J., Misra, J., & Wek, R. C. (2022). Analysis of Translational Control in the Integrated Stress Response by Polysome Profiling. In *Methods in Molecular Biology* (Vol. 2428, pp. 157–171). Humana Press Inc. https://doi.org/10.1007/978-1-0716-1975-9_10

Holz, M. K., Ballif, B. A., Gygi, S. P., & Blenis, J. (2005). mTOR and S6K1 mediate assembly of the translation preinitiation complex through dynamic protein interchange and ordered phosphorylation events. *Cell*, *123*(4), 569–580. https://doi.org/10.1016/j.cell.2005.10.024

Hüsnügil, H. H., Güleç Taşkıran, A. E., Güderer, I., Nehri, L. N., Oral, G., Menemenli, N. Ş., Özcan, Ö., Noghreh, A., Akyol, A., & Banerjee, S. (2024). Lysosomal alkalinization in nutrient restricted cancer cells activates cytoskeletal rearrangement to enhance partial epithelial to mesenchymal transition. *Translational Oncology*, *41*. https://doi.org/10.1016/j.tranon.2023.101860

Hutchinson, J. A., Shanware, N. P., Chang, H., & Tibbetts, R. S. (2011). Regulation of ribosomal protein S6 phosphorylation by casein kinase 1 and protein phosphatase 1. *Journal of Biological Chemistry*, *286*(10), 8688–8696. https://doi.org/10.1074/jbc.M110.141754

Jang, M., Kim, S. S., & Lee, J. (2013). Cancer cell metabolism: Implications for therapeutic targets. In *Experimental and Molecular Medicine* (Vol. 45, Issue 10). Nature Publishing Group. https://doi.org/10.1038/emm.2013.85

Jin, J., Byun, J. K., Choi, Y. K., & Park, K. G. (2023). Targeting glutamine metabolism as a therapeutic strategy for cancer. In *Experimental and Molecular Medicine* (Vol. 55, Issue 4, pp. 706–715). Springer Nature. https://doi.org/10.1038/s12276-023-00971-9

Jonsson, W. O., Margolies, N. S., & Anthony, T. G. (2019). Dietary sulfur amino acid restriction and the integrated stress response: Mechanistic insights. *Nutrients*, *11*(6). https://doi.org/10.3390/nu11061349

Keerthana, C. K., Rayginia, T. P., Shifana, S. C., Anto, N. P., Kalimuthu, K., Isakov, N., & Anto, R. J. (2023). The role of AMPK in cancer metabolism and its impact on the immunomodulation of the tumor microenvironment. In *Frontiers in Immunology* (Vol. 14). Frontiers Media S.A. https://doi.org/10.3389/fimmu.2023.1114582

Kim, Y. (2010). The effects of nutrient depleted microenvironments and delta-like 1 homologue (DLK1) on apoptosis in neuroblastoma. *Nutrition Research and Practice*, *4*(6), 455–461. https://doi.org/10.4162/nrp.2010.4.6.455

Kino, T., Hurt, D. E., Ichijo, T., Nader, N., & Chrousos, G. P. (2010). Noncoding RNA Gas5 is a growth arrest- and starvation-associated repressor of the glucocorticoid receptor. *Science Signaling*, *3*(107). https://doi.org/10.1126/scisignal.2000568

Koundouros, N., & Poulogiannis, G. (2020). Reprogramming of fatty acid metabolism in cancer. In *British Journal of Cancer* (Vol. 122, Issue 1, pp. 4–22). Springer Nature. https://doi.org/10.1038/s41416-019-0650-z

Kuete, V., Karaosmanoğlu, O., & Sivas, H. (2017). Anticancer Activities of African Medicinal Spices and Vegetables. In *Medicinal Spices and Vegetables from Africa: Therapeutic Potential Against Metabolic, Inflammatory, Infectious and*

Systemic Diseases (pp. 271–297). Elsevier Inc. https://doi.org/10.1016/B978-0-12-809286-6.00010-8

Kun, E., Tsang, Y. T. M., Ng, C. W., Gershenson, D. M., & Wong, K. K. (2021). MEK inhibitor resistance mechanisms and recent developments in combination trials. In *Cancer Treatment Reviews* (Vol. 92). W.B. Saunders Ltd. https://doi.org/10.1016/j.ctrv.2020.102137

Lan, T., Chen, L., & Wei, X. (2021). Inflammatory cytokines in cancer: Comprehensive understanding and clinical progress in gene therapy. In *Cells* (Vol. 10, Issue 1, pp. 1–16). MDPI. https://doi.org/10.3390/cells10010100

Le, A. (2021). Erratum: Correction to: The Heterogeneity of Cancer Metabolism (Advances in experimental medicine and biology). In *Advances in experimental medicine and biology* (Vol. 1311). NLM (Medline). https://doi.org/10.1007/978-3-030-65768-0_19

Lee, S., Rauch, J., & Kolch, W. (2020). Targeting MAPK signaling in cancer: Mechanisms of drug resistance and sensitivity. In *International Journal of Molecular Sciences* (Vol. 21, Issue 3). MDPI AG. https://doi.org/10.3390/ijms21031102

Lewerenz, J., & Maher, P. (2009). Basal levels of eIF2α phosphorylation determine cellular antioxidant status by regulating ATF4 and xCT expression. *Journal of Biological Chemistry*, *284*(2), 1106–1115. https://doi.org/10.1074/jbc.M807325200

Li, W., Saud, S. M., Young, M. R., Chen, G., & Hua, B. (2015). *Targeting AMPK for cancer prevention and treatment* (Vol. 6, Issue 10). www.impactjournals.com/oncotarget

Liberti, M. V., & Locasale, J. W. (2016). The Warburg Effect: How Does it Benefit Cancer Cells? In *Trends in Biochemical Sciences* (Vol. 41, Issue 3, pp. 211–218). Elsevier Ltd. https://doi.org/10.1016/j.tibs.2015.12.001

Licari, E., Sánchez-del-Campo, L., & Falletta, P. (2021). The two faces of the Integrated Stress Response in cancer progression and therapeutic strategies. In *International Journal of Biochemistry and Cell Biology* (Vol. 139). Elsevier Ltd. https://doi.org/10.1016/j.biocel.2021.106059

Lieu, E. L., Nguyen, T., Rhyne, S., & Kim, J. (2020). Amino acids in cancer. In *Experimental and Molecular Medicine* (Vol. 52, Issue 1, pp. 15–30). Springer Nature. https://doi.org/10.1038/s12276-020-0375-3

Lin, J. F., Lin, Y. C., Tsai, T. F., Chen, H. E., Chou, K. Y., & Hwang, T. I. S. (2017). Cisplatin induces protective autophagy through activation of BECN1 in human bladder cancer cells. *Drug Design, Development and Therapy*, *11*, 1517–1533. https://doi.org/10.2147/DDDT.S126464

Lin, X., Xiao, Z., Chen, T., Liang, S. H., & Guo, H. (2020). Glucose Metabolism on Tumor Plasticity, Diagnosis, and Treatment. In *Frontiers in Oncology* (Vol. 10). Frontiers Media S.A. https://doi.org/10.3389/fonc.2020.00317

Liu, B., & Qian, S. B. (2016). Characterizing inactive ribosomes in translational profiling. *Translation*, *4*(1). https://doi.org/10.1080/21690731.2015.1138018

López, S., Quinto, D. E., Lafuente, E., & Martínez-Salas, E. (2001). *IRES interaction with translation initiation factors: Functional characterization of novel RNA contacts with eIF3, eIF4B, and eIF4GII*.

Magnuson, B., Ekim, B., & Fingar, D. C. (2012). Regulation and function of ribosomal protein S6 kinase (S6K) within mTOR signalling networks. In *Biochemical Journal* (Vol. 441, Issue 1, pp. 1–21). https://doi.org/10.1042/BJ20110892

Martínez-Reyes, I., & Chandel, N. S. (2021). Cancer metabolism: looking forward. In *Nature Reviews Cancer* (Vol. 21, Issue 10, pp. 669–680). Nature Research. https://doi.org/10.1038/s41568-021-00378-6

Mazor, K. M., & Stipanuk, M. H. (2016). GCN2- and eIF2α-phosphorylation-independent, but ATF4-dependent, induction of CARE-containing genes in methionine-deficient cells. *Amino Acids*, *48*(12), 2831–2842. https://doi.org/10.1007/s00726-016-2318-9

Melick, C. H., & Jewell, J. L. (2020). Regulation of mtorc1 by upstream stimuli. In *Genes* (Vol. 11, Issue 9, pp. 1–28). MDPI AG. https://doi.org/10.3390/genes11090989

Mihaylova, M. M., & Shaw, R. J. (2011). The AMPK signalling pathway coordinates cell growth, autophagy and metabolism. In *Nature Cell Biology* (Vol. 13, Issue 9, pp. 1016–1023). https://doi.org/10.1038/ncb2329

Mikalayeva, V., Ceslevičienė, I., Sarapinienė, I., Žvikas, V., Skeberdis, V. A., Jakštas, V., & Bordel, S. (2019). Fatty acid synthesis and degradation interplay to regulate the oxidative stress in cancer cells. *International Journal of Molecular Sciences*, *20*(6). https://doi.org/10.3390/ijms20061348

Miyo, M., Konno, M., Nishida, N., Sueda, T., Noguchi, K., Matsui, H., Colvin, H., Kawamoto, K., Koseki, J., Haraguchi, N., Nishimura, J., Hata, T., Gotoh, N., Matsuda, F., Satoh, T., Mizushima, T., Shimizu, H., Doki, Y., Mori, M., & Ishii, H. (2016). Metabolic Adaptation to Nutritional Stress in Human Colorectal Cancer. *Scientific Reports*, *6*. https://doi.org/10.1038/srep38415

Mok, K. W., Mruk, D. D., & Cheng, C. Y. (2013). Regulation of Blood-Testis Barrier (BTB) Dynamics during Spermatogenesis via the "Yin" and "Yang" Effects of Mammalian Target of Rapamycin Complex 1 (mTORC1) and mTORC2. In *International Review of Cell and Molecular Biology* (Vol. 301, pp. 291–358). Elsevier Inc. https://doi.org/10.1016/B978-0-12-407704-1.00006-3

Morris, R. M., Mortimer, T. O., & O'Neill, K. L. (2022). Cytokines: Can Cancer Get the Message? In *Cancers* (Vol. 14, Issue 9). MDPI. https://doi.org/10.3390/cancers14092178

Nagasawa, I., Koido, M., Tani, Y., Tsukahara, S., Kunimasa, K., & Tomida, A. (2020). Disrupting ATF4 Expression Mechanisms Provides an Effective Strategy for BRAF-Targeted Melanoma Therapy. *IScience*, *23*(4). https://doi.org/10.1016/j.isci.2020.101028

Naveed, S., Aslam, M., & Ahmad, A. (2014). Starvation based differential chemotherapy: A novel approach for cancer treatment. *Oman Medical Journal*, *29*(6), 391–398. https://doi.org/10.5001/omj.2014.107

Ong, Q., Guo, S., Zhang, K., & Cui, B. (2015). U0126 protects cells against oxidative stress independent of its function as a MEK inhibitor. *ACS Chemical Neuroscience*, *6*(1), 130–137. https://doi.org/10.1021/cn500288n

Oral, G. (2023). *Activation of Survival Pathways in Nutrient Restricted Colorectal Cancer Cells.* A Thesis Submitted to The Graduate School of Natural And Applied Sciences Of Middle East Technical University.

Pakos-Zebrucka, K., Koryga, I., Mnich, K., Ljujic, M., Samali, A., & Gorman, A. M. (2016). The integrated stress response. *EMBO Reports*, *17*(10), 1374–1395. https://doi.org/10.15252/embr.201642195

Park, J. H., Pyun, W. Y., & Park, H. W. (2020). Cancer Metabolism: Phenotype, Signaling and Therapeutic Targets. In *Cells* (Vol. 9, Issue 10). NLM (Medline). https://doi.org/10.3390/cells9102308

Pavitt, G. D. (2013). Less translational control, more memory. *ELife*, *2013*(2). https://doi.org/10.7554/eLife.00895

Pavlova, N. N., & Thompson, C. B. (2016). The Emerging Hallmarks of Cancer Metabolism. In *Cell Metabolism* (Vol. 23, Issue 1, pp. 27–47). Cell Press. https://doi.org/10.1016/j.cmet.2015.12.006

Qin, X., Jiang, B., & Zhang, Y. (2016). 4E-BP1, a multifactor regulated multifunctional protein. In *Cell Cycle* (Vol. 15, Issue 6, pp. 781–786). Taylor and Francis Inc. https://doi.org/10.1080/15384101.2016.1151581

Raffaghello, L., Lee, C., Safdie, F. M., Wei, M., Madia, F., Bianchi, G., & Longo, V. D. (2008). *Starvation-dependent differential stress resistance protects normal but not cancer cells against high-dose chemotherapy*. www.pnas.org/cgi/content/full/

Robles-Flores, M., Moreno-Londoño, A. P., & Castañeda-Patlán, M. C. (2021). Signaling Pathways Involved in Nutrient Sensing Control in Cancer Stem Cells: An Overview. In *Frontiers in Endocrinology* (Vol. 12). Frontiers Media S.A. https://doi.org/10.3389/fendo.2021.627745

Roux, P. P., Shahbazian, D., Vu, H., Holz, M. K., Cohen, M. S., Taunton, J., Sonenberg, N., & Blenis, J. (2007). RAS/ERK signaling promotes site-specific ribosomal protein S6 phosphorylation via RSK and stimulates cap-dependent translation. *Journal of Biological Chemistry*, *282*(19), 14056–14064. https://doi.org/10.1074/jbc.M700906200

Roux, P. P., & Topisirovic, I. (2018). Signaling Pathways Involved in the Regulation of mRNA Translation. *Molecular and Cellular Biology*, *38*(12). https://doi.org/10.1128/mcb.00070-18

Ruvinsky, I., & Meyuhas, O. (2006). Ribosomal protein S6 phosphorylation: from protein synthesis to cell size. In *Trends in Biochemical Sciences* (Vol. 31, Issue 6, pp. 342–348). https://doi.org/10.1016/j.tibs.2006.04.003

Ryoo, H. D., & Vasudevan, D. (2017). Two distinct nodes of translational inhibition in the Integrated Stress Response. In *BMB Reports* (Vol. 50, Issue 11, pp. 539–545). The Biochemical Society of the Republic of Korea. https://doi.org/10.5483/BMBRep.2017.50.11.157

Salaroglio, I. C., Mungo, E., Gazzano, E., Kopecka, J., & Riganti, C. (2019). ERK is a pivotal player of chemo-immune-resistance in cancer. In *International Journal of Molecular Sciences* (Vol. 20, Issue 10). MDPI AG. https://doi.org/10.3390/ijms20102505

Sa-nongdej, W., Chongthammakun, S., & Songthaveesin, C. (2021). Nutrient starvation induces apoptosis and autophagy in C6 glioma stem-like cells. *Heliyon*, *7*(2). https://doi.org/10.1016/j.heliyon.2021.e06352

Sato, K., Tsuchihara, K., Fujii, S., Sugiyama, M., Goya, T., Atomi, Y., Ueno, T., Ochiai, A., & Esumi, H. (2007). Autophagy is activated in colorectal cancer cells and contributes to the tolerance to nutrient deprivation. *Cancer Research*, *67*(20), 9677–9684. https://doi.org/10.1158/0008-5472.CAN-07-1462

Saxton, R. A., & Sabatini, D. M. (2017). mTOR Signaling in Growth, Metabolism, and Disease. In *Cell* (Vol. 168, Issue 6, pp. 960–976). Cell Press. https://doi.org/10.1016/j.cell.2017.02.004

Simanurak, O., Pekthong, D., Somran, J., Wangteeraprasert, A., Srikummool, M., Kaewpaeng, N., Parhira, S., & Srisawang, P. (2023). Enhanced apoptosis of HCT116 colon cancer cells treated with extracts from Calotropis gigantea stem bark by starvation. *Heliyon*, *9*(7). https://doi.org/10.1016/j.heliyon.2023.e18013

Singh, R., & Cuervo, A. M. (2011). Autophagy in the cellular energetic balance. In *Cell Metabolism* (Vol. 13, Issue 5, pp. 495–504). https://doi.org/10.1016/j.cmet.2011.04.004

Stone, K. P., Ghosh, S., Kovalik, J. P., Orgeron, M., Wanders, D., Sims, L. C., & Gettys, T. W. (2021). The acute transcriptional responses to dietary methionine restriction are triggered by inhibition of ternary complex formation and linked to Erk1/2, mTOR, and ATF4. *Scientific Reports*, *11*(1). https://doi.org/10.1038/s41598-021-83380-0

Takahara, T., Amemiya, Y., Sugiyama, R., Maki, M., & Shibata, H. (2020). Amino acid-dependent control of mTORC1 signaling: A variety of regulatory modes. In *Journal of Biomedical Science* (Vol. 27, Issue 1). BioMed Central Ltd. https://doi.org/10.1186/s12929-020-00679-2

Tong, J., Sun, D., Yang, C., Wang, Y., Sun, S., Li, Q., Bao, J., & Liu, Y. (2016). Serum starvation and thymidine double blocking achieved efficient cell cycle synchronization and altered the expression of p27, p53, bcl-2 in canine breast cancer cells. *Research in Veterinary Science*, *105*, 10–14. https://doi.org/10.1016/j.rvsc.2016.01.008

Torrence, M. E., Macarthur, M. R., Hosios, A. M., Valvezan, A. J., Asara, J. M., Mitchell, J. R., & Manning, B. D. (2021). The mtorc1-mediated activation of atf4 promotes protein and glutathione synthesis downstream of growth signals. *ELife*, *10*. https://doi.org/10.7554/eLife.63326

Torrence, M. E., & Manning, B. D. (2018). Nutrient Sensing in Cancer. *Annu. Rev. Cancer Biol*, *2*, 251–269. https://doi.org/10.1146/annurev-cancerbio

Tsukumo, Y., Alain, T., Fonseca, B. D., Nadon, R., & Sonenberg, N. (2016). Translation control during prolonged mTORC1 inhibition mediated by 4E-BP3. *Nature Communications*, *7*. https://doi.org/10.1038/ncomms11776

Tunçer, S., Sade-Memişoğlu, A., Keşküş, A. G., Sheraj, I., Güner, G., Akyol, A., & Banerjee, S. (2020). Enhanced expression of HNF4α during intestinal epithelial differentiation is involved in the activation of ER stress. *FEBS Journal*, *287*(12), 2504–2523. https://doi.org/10.1111/febs.15152

Untereiner, A. A., Pavlidou, A., Druzhyna, N., Papapetropoulos, A., Hellmich, M. R., & Szabo, C. (2018). Drug resistance induces the upregulation of H2S-producing enzymes in HCT116 colon cancer cells. *Biochemical Pharmacology*, *149*, 174–185. https://doi.org/10.1016/j.bcp.2017.10.007

Uriarte, M., Sen Nkwe, N., Tremblay, R., Ahmed, O., Messmer, C., Mashtalir, N., Barbour, H., Masclef, L., Voide, M., Viallard, C., Daou, S., Abdelhadi, D., Ronato, D., Paydar, M., Darracq, A., Boulay, K., Desjardins-Lecavalier, N., Sapieha, P., Masson, J. Y., … Affar, E. B. (2021). Starvation-induced proteasome assemblies in the nucleus link amino acid supply to apoptosis. *Nature Communications*, *12*(1). https://doi.org/10.1038/s41467-021-27306-4

van Nostrand, J. L., Hellberg, K., Luo, E. C., van Nostrand, E. L., Dayn, A., Yu, J., Shokhirev, M. N., Dayn, Y., Yeo, G. W., & Shaw, R. J. (2020). AMPK regulation of Raptor and TSC2 mediate metformin effects on transcriptional control of anabolism and inflammation. *Genes and Development*, *34*(19–20), 1330–1344. https://doi.org/10.1101/gad.339895.120

Wang, L., Shang, Z., Zhou, Y., Hu, X., Chen, Y., Fan, Y., Wei, X., Wu, L., Liang, Q., Zhang, J., & Gao, Z. (2018). Autophagy mediates glucose starvation-induced glioblastoma cell quiescence and chemoresistance through coordinating cell metabolism, cell cycle, and survival. *Cell Death and Disease*, *9*(2). https://doi.org/10.1038/s41419-017-0242-x

Wang, X., Li, Y., Jia, F., Cui, X., Pan, Z., & Wu, Y. (2022). Boosting nutrient starvation-dominated cancer therapy through curcumin-augmented mitochondrial Ca2+ overload and obatoclax-mediated autophagy inhibition as supported by a novel nano-modulator GO-Alg@CaP/CO. *Journal of Nanobiotechnology*, *20*(1). https://doi.org/10.1186/s12951-022-01439-0

Wei, Z., Liu, X., Cheng, C., Yu, W., & Yi, P. (2021). Metabolism of Amino Acids in Cancer. In *Frontiers in Cell and Developmental Biology* (Vol. 8). Frontiers Media S.A. https://doi.org/10.3389/fcell.2020.603837

Wek, R. C., & Staschke, K. A. (2010). How do tumours adapt to nutrient stress. In *EMBO Journal* (Vol. 29, Issue 12, pp. 1946–1947). https://doi.org/10.1038/emboj.2010.110

Wu, C. A., Chao, Y., Shiah, S. G., & Lin, W. W. (2013). Nutrient deprivation induces the Warburg effect through ROS/AMPK-dependent activation of pyruvate dehydrogenase kinase. *Biochimica et Biophysica Acta - Molecular Cell Research*, *1833*(5), 1147–1156. https://doi.org/10.1016/j.bbamcr.2013.01.025

Yang, M., Lu, Y., Piao, W., & Jin, H. (2022). The Translational Regulation in mTOR Pathway. In *Biomolecules* (Vol. 12, Issue 6). MDPI. https://doi.org/10.3390/biom12060802

Yang, Y., & Wang, Z. (2019). IRES-mediated cap-independent translation, a path leading to hidden proteome. In *Journal of Molecular Cell Biology* (Vol. 11, Issue 10, pp. 911–919). Oxford University Press. https://doi.org/10.1093/jmcb/mjz091

Yeldag, G., Rice, A., & Hernández, A. del R. (2018). Chemoresistance and the self-maintaining tumor microenvironment. In *Cancers* (Vol. 10, Issue 12). MDPI AG. https://doi.org/10.3390/cancers10120471

Yeung, T. M., Gandhi, S. C., Wilding, J. L., Muschel, R., & Bodmer, W. F. (2010). Cancer stem cells from colorectal cancer-derived cell lines. *Proceedings of the National Academy of Sciences of the United States of America*, *107*(8), 3722–3727. https://doi.org/10.1073/pnas.0915135107

Yi, Y. W., You, K. S., Park, J. S., Lee, S. G., & Seong, Y. S. (2022). Ribosomal protein S6: A potential therapeutic target against cancer? In *International Journal of Molecular Sciences* (Vol. 23, Issue 1). MDPI. https://doi.org/10.3390/ijms23010048

Yoo, H. C., Yu, Y. C., Sung, Y., & Han, J. M. (2020). Glutamine reliance in cell metabolism. In *Experimental and Molecular Medicine* (Vol. 52, Issue 9, pp. 1496–1516). Springer Nature. https://doi.org/10.1038/s12276-020-00504-8

You, M., Xie, Z., Zhang, N., Zhang, Y., Xiao, D., Liu, S., Zhuang, W., Li, L., & Tao, Y. (2023). Signaling pathways in cancer metabolism: mechanisms and therapeutic targets. In *Signal Transduction and Targeted Therapy* (Vol. 8, Issue 1). Springer Nature. https://doi.org/10.1038/s41392-023-01442-3

Yuan, H. X., Xiong, Y., & Guan, K. L. (2013). Nutrient Sensing, Metabolism, and Cell Growth Control. In *Molecular Cell* (Vol. 49, Issue 3, pp. 379–387). https://doi.org/10.1016/j.molcel.2013.01.019

Yuan, J., Dong, X., Yap, J., & Hu, J. (2020). The MAPK and AMPK signalings: Interplay and implication in targeted cancer therapy. In *Journal of Hematology*

and Oncology (Vol. 13, Issue 1). BioMed Central Ltd. https://doi.org/10.1186/s13045-020-00949-4

Zhai, Z., Vaddi, P. K., Samson, J. M., Takegami, T., & Fujita, M. (2021). Nlrp1 functions downstream of the mapk/erk signaling via atf4 and contributes to acquired targeted therapy resistance in human metastatic melanoma. *Pharmaceuticals*, *14*(1), 1–15. https://doi.org/10.3390/ph14010023

Zhang, N., Yin, Y., Xu, S. J., & Chen, W. S. (2008). 5-Fluorouracil: Mechanisms of resistance and reversal strategies. In *Molecules* (Vol. 13, Issue 8, pp. 1551–1569). https://doi.org/10.3390/molecules13081551

Zhang, Y., Xu, L., Ren, Z., Liu, X., Song, J., Zhang, P., Zhang, C., Gong, S., Wu, N., Zhang, X., Xie, C., Lu, Z., Ma, M., Zhang, Y., Chen, Y., & Lin, C. (2023). LINC01615 maintains cell survival in adaptation to nutrient starvation through the pentose phosphate pathway and modulates chemosensitivity in colorectal cancer. *Cellular and Molecular Life Sciences*, *80*(1). https://doi.org/10.1007/s00018-022-04675-7

Zhao, L., Teng, B., Wen, L., Feng, Q., Wang, H., Li, N., Wang, Y., & Liang, Z. (2014). mTOR inhibitor AZD8055 inhibits proliferation and induces apoptosis in laryngeal carcinoma. In *Int J Clin Exp Med* (Vol. 7, Issue 2). www.ijcem.com/

Zhu, J., & Thompson, C. B. (2019). Metabolic regulation of cell growth and proliferation. In *Nature Reviews Molecular Cell Biology* (Vol. 20, Issue 7, pp. 436–450). Nature Publishing Group. https://doi.org/10.1038/s41580-019-0123-5

APPENDICES

A. Western Blot Buffer Components Used in This Study

Table A.1 Compositions of buffers used in Western Blot experiment

4% SDS-PAGE STACKING GEL	**12% SDS-PAGE SEPARATING GEL**
3.1 mL distilled autoclaved H_2O	3.4 mL distilled autoclaved H_2O
1.25 mL Stacking Buffer (0.5M Tris-HCl, pH 6.8)	2.5 mL Stacking Buffer (1.5M Tris-HCl, pH 8.8)
650 µL Acrylamide/Bis Solution (SERVA, Germany)	4 mL Acrylamide/Bis Solution (SERVA, Germany)
50 µL 10% APS	100 µL 10% APS
5 µL TEMED (SERVA, Germany)	10 µL TEMED (SERVA, Germany)
6X SDS-PAGE SAMPLE LOADING DYE	**10X SDS-PAGE RUNNING BUFFER**
12% SDS	25 mM Tris-HCl
30% β-mercaptoethanol	192 mM Glycine
30% Glycerol	0.1% SDS
0.012% Bromophenol Blue	**1X SDS-PAGE RUNNING BUFFER**
0.375 M Tris-HCl pH 6.8	100 mL 10X Running Buffer and 900 mL distilled H_2O
10X TRANSFER BUFFER	**1X TRANSFER BUFFER**
0.25 M Tris-HCl	100 mL 10X Transfer Buffer
1.92 M Glycine	200 mL Methanol
pH 8.3 in 1 L distilled H_2O	Complete remaining to 1L with distilled H_2O

Table A.1 (cont'd) Compositions of buffers used in Western Blot experiment

20X TBS (pH 7.4 in 1 L dH_2O)	**1X TBS-T**
50 mM Tris-HCl	50 mL 20X TBS
300 mM NaCl	950 mL distilled H_2O
4mM KCl	1 mL Tween 20
MILD STRIPPING BUFFER (pH 2.2 in 1L dH_2O)	
15 g Glycine	
1 g SDS	
10 mL Tween-20	

B. STR Analysis Report of HCT-116 Cell Line

The DNA samples from the specimens HCT-116 were amplified using the AmpFℓSTR Identifiler Plus PCR kit and analysed on the 3130XL Genetic Analyzer sequencing device (with Sanger sequencing). The data were analysed using the GeneMapper program, and the results are presented in the outcome Figure B1.

Marker	HCT-116	
	Alel A	Alel B
D8S1179	12	14
D21S11	29	30
D7S820	11	12
CSF1PO	7	10
D3S1358	12	19
TH01	8	9
D13S317	10	12
D16S539	11	13
D2S1338	16	16
D19S433	12	13
vWA	17	22
TPOX	8	8
D18S51	17	17
Amelogenin	X	X
D5S818	10	11
FGA	18	23

Figure B1 The STR analysis of the HCT-116 cell line with indicated markers

C. Fold Change Graphs for Figure 3.9

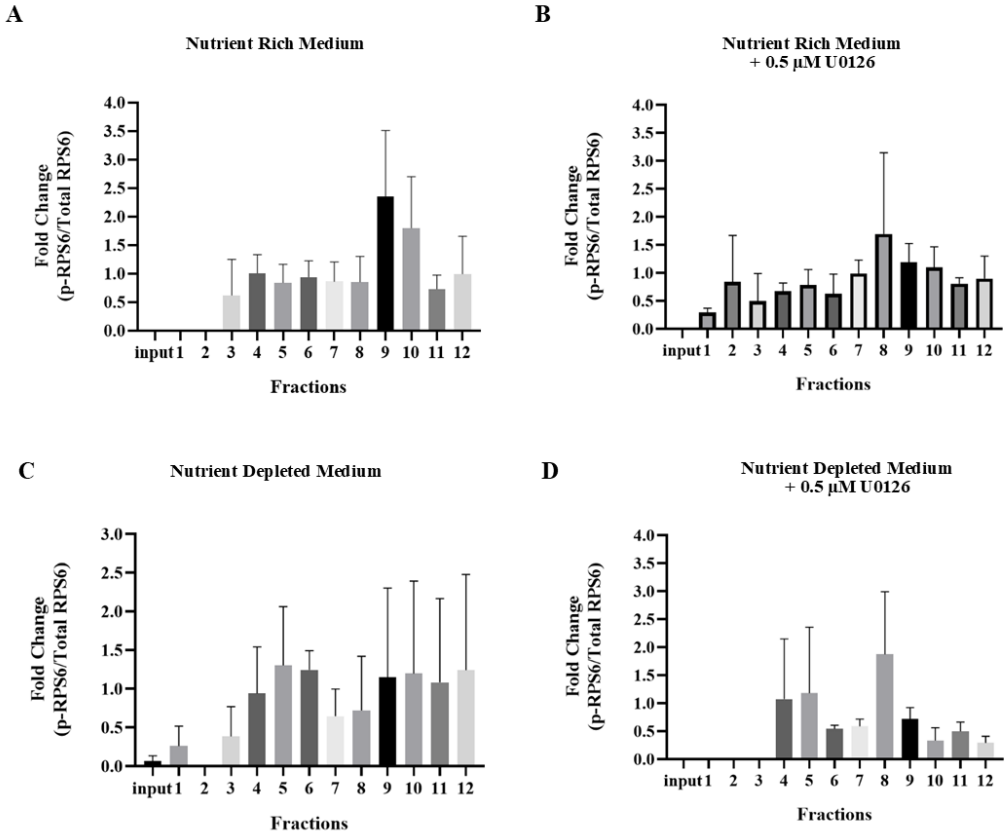

Figure C1 Fold change graphs of p-RPS6 (Ser 235/236) with respect to fractions in polysome Profiling

D. Full Blot Image of Figure 3.10

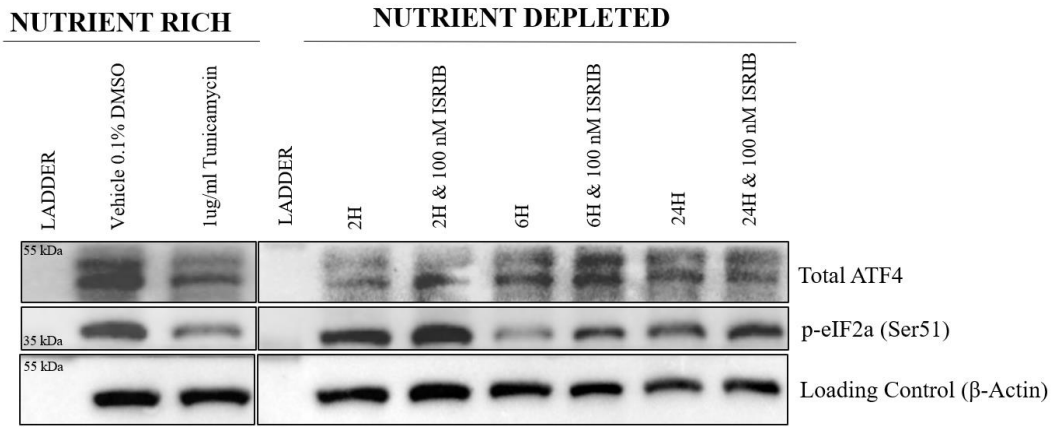

Figure D1 The evaluation of the ISR activation in response to nutrient depletion in HCT-116 colorectal cancer cells

E. Determination of ISRIB Concentration

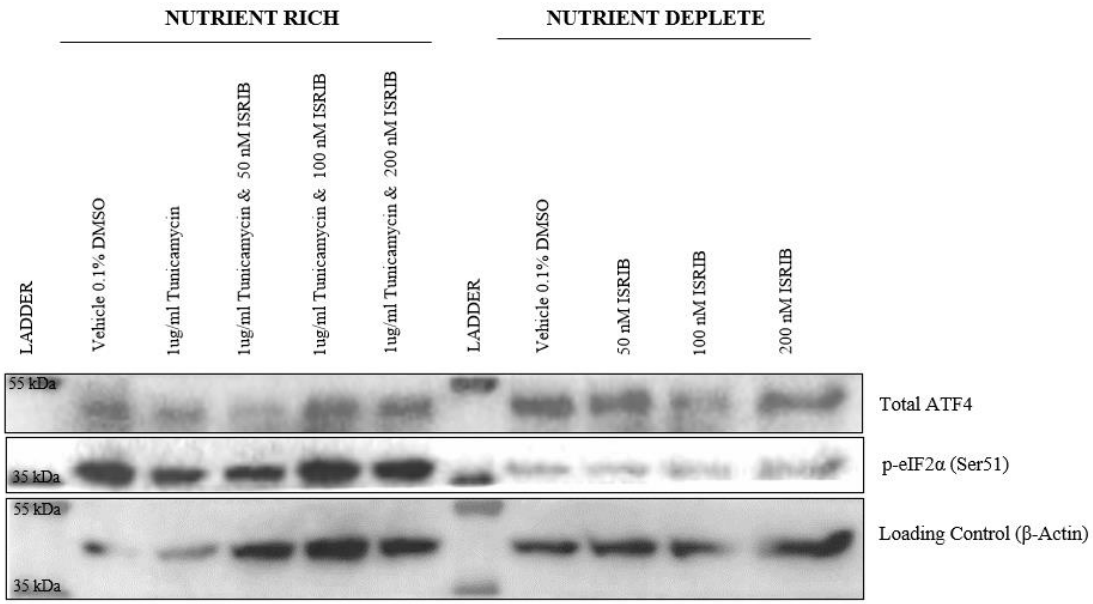

Figure E1 Determination of ISRIB concentration in HCT-116 cells with respect to ATF4 levels